

MASTER THESIS

Uncertainty Modelling in Life Cycle Costing Analysis for Rail Level Crossing Systems

Y. Shang

MSc Construction Management & Engineering

Uncertainty Modelling in Life Cycle Costing Analysis for Rail Level Crossing Systems

By
Y. (Yue) Shang

in partial fulfilment of the requirements for the degree of

Master of Science

in Construction Management and Engineering

at the Delft University of Technology

to be defended publicly on Friday August 31, 2018 at 14:30.

Committee

Chairman	Prof.dr.ir. A.R.M. (Rogier) Wolfert	TU Delft
Supervisor	Ir. M. (Martine) van den Boomen	TU Delft
Supervisor	Dr. M.T.J. (Matthijs) Spaan	TU Delft
Company Supervisor	Dr.ir. A.P. (Amy) de Man	edilon)(sedra
Company Supervisor	R. (Rik) Monteban	edilon)(sedra

Acknowledgements

This thesis is the result of graduation research regarding life cycle costing analysis for an innovative track structure, embedded rail system. It started in November 2017. The subject is a combination of infrastructure asset management and economic analysis. I felt motivated when I first saw the topic, which came from the interest in lectures Financial Engineering. Once I got started I immediately realized it might be a tough work for me. The subject ‘uncertainty modelling’ manifests itself as a journey with an unknown destination, while I was not even familiar with the knowns at that stage. As a newcomer in the railway industry, I would like to express my sincere gratitude to Amy for offering me the intern opportunity and guiding me on track to railway engineering. And many thanks to Rik, for providing me access to practitioners and helping me out with input gathering for the thesis. Thank you for the working experience in edilon)(sedra.

The result of this research would not be possible without the contribution of ProRail, Strukton and ASSET Rail. All these people who provided me with practical insight into the field of track maintenance and made it possible for me to graduate, thank you for the willingness to cooperate.

Doing a research is not only about gaining knowledge but about molding one’s character for the future challenge. I have been made frustrated and stressed when I had made great efforts but saw little progress. I also experienced how the enjoyable and rewarding involvement could be. Now I realize how essential patience is for one person and his life. I would like to give special thanks to Martine, to whom I could always come for questions. Thank you for your patience, encouragement and all your support. And, Prof. Wolfert, thank you for chairing the graduation committee and your critical contributions to my work. Also, I would like to thank Matthijs for giving me valuable suggestions and comments. It was a valuable experience to study at the Delft University of Technology, which gives me the confidence to move on with my own career.

Yue Shang

Delft, August 2018

Abstract

Over the past decades, many railway infrastructure management organizations have shifted from separate investment management and maintenance interventions to an integral asset management approach by looking into the life cycle cost (LCC) of the assets. The asset degradation and maintenance strategies are driving factors that cause the variation in the LCC. The output of case-specific LCC evaluation may become less reliable when it comes to the general condition. The impact of uncertainty regarding rail degradation and maintenance strategies have been analyzed by several researchers, but the emphasis was laid on traditional ballasted tracks. Another type of track structure, embedded rail system (ERS), has not received much attention to date.

The research screens the problem to embedded rail level crossings (Harmelen level crossing system (LCS) as in use in the Dutch national railway network), one of the applications of ERS, and proposes a reliability-based LCC model for this type of railway assets.

With gained knowledge about the system characteristics and maintenance interventions, the research narrows down the scope to the rails in Harmelen LCS and describes the development of the reliability-based LCC model, which integrates the life distribution, age replacement model and several LCC techniques. The life distribution, as a common way being applied in the reliability engineering, quantifies the rail reliability condition, which accounts for the variation in the time to failure of the rails. The age replacement model, as a general maintenance optimization model, provides an estimate for optimized preventive replacement intervals from the LCC point of view. Given the limitation of the fundamental age replacement model, where only a tradeoff between the preventive and corrective replacement cost is made, the research extends it in order to incorporate the operating costs (rail grinding cost, ultrasonic and visual inspection cost) into the preventive replacement optimization. The LCC techniques are combined to account for the time value of money and cope with the common limitation in the literature with regard to the maintenance optimization for the railway assets. With the integration of the theory from railway engineering, reliability engineering and engineering economics, the model captures the interaction among LCC, rail degradation (in Harmelen LCS) and maintenance interventions.

The proposed model is executed using Microsoft Excel and partly validated by field data. With the rail break data, it proves that the 2-parameter Weibull probability distribution is a reasonable fit to model the rail failures (by corrosion) in the Harmelen LCS. The model output is able to answer two practical questions: ‘when would be the most cost efficient to preventively replace the rails in the Harmelen LCS’ and ‘how much money does one asset manager have to save to own the asset in the optimized lifecycle’. Furthermore, sensitivity analysis is performed to facilitate better understandings about connections between input variables and outcomes, associated with suggestions for more cost-efficient asset management. Recommendations regarding the model application are provided both for the Harmelen LCS and other types of railway assets.

Table of Contents

Acknowledgements	i
Abstract	ii
List of Tables	v
List of Figures	vi
List of Abbreviations	vi
1. Introduction	1
1.1 Slab track structures.....	1
1.2 edilon)(sedra & embedded rail system.....	2
1.3 Problem statement.....	2
1.4 Research objective & scope.....	4
1.4.1 Research objective.....	4
1.4.2 Research scope.....	4
1.5 Research questions.....	5
1.6 Research framework & thesis outline.....	5
2. Theoretical Background	7
2.1 Harmelen LCS & its degradation.....	7
2.1.1 Rail.....	7
2.1.2 ERS.....	10
2.1.3 Slab.....	11
2.2 Inspection & maintenance.....	11
2.2.1 Inspection practices.....	11
2.2.2 Maintenance.....	13
2.3 Conclusion.....	16
3. Model Development	18
3.1 Starting point.....	18
3.2 Degradation modelling.....	20
3.2.1 Failure data gathering (step 1).....	20
3.2.2 Reliability model selection (step 2).....	20
3.2.3 Parameter estimation (step 3).....	26
3.3 Effect of maintenance interventions.....	28
3.3.1 Impact of grinding (step 4).....	28
3.3.2 Reliability evaluation (step 5).....	30
3.4 Integration.....	30
3.4.1 Extension of age replacement model (step 6).....	30
3.4.2 Cost discounting (step 7).....	33
3.5 Conclusion.....	37
4. Application & Validation	39
4.1 Data gathering (step 1).....	39
4.2 Probability plotting (step 2).....	41

4.2.1	Corrosion failure mode.....	41
4.2.2	RCF failure mode.....	43
4.3	Maximum likelihood estimation (MLE) (step 3).....	45
4.4	Reliability evaluation (step 4 & 5).....	47
4.5	Cost optimization (step 6 & 7).....	48
5.	Discussion.....	51
5.1	Impact of economic factors.....	51
5.1.1	Operating cost.....	51
5.1.2	Preventive replacement cost.....	54
5.1.3	Discount rate.....	56
5.2	Policy impact.....	59
5.2.1	Grinding frequency.....	59
5.2.2	PGO contractors.....	62
6.	Conclusions & Recommendations	65
6.1	Conclusions.....	65
6.1.1	Failure mode & failure data.....	65
6.1.2	Maintenance interventions & extension of age replacement model	65
6.1.3	Uncertainty exploration in age replacement optimization.....	66
6.2	Recommendations	67
6.2.1	Model application in the Harmelen LCS	67
6.2.2	Applicability for other railway assets.....	68
6.2.3	Future improvement	70
	Bibliography.....	71
	Appendices	74
	Appendix A Interview transcript.....	74
	Interview I.....	74
	Interview II.....	76
	Interview III	78
	Interview IV	81
	Appendix B Overview inspection & maintenance for Harmelen LCS.....	84
	Appendix C Rail break record in Harmelen LCS (2015-2018) (ProRail, 2018a).....	85
	Appendix D Ultrasonic inspection reports.....	86
	Appendix E Exponential distribution & probability plotting.....	87

List of Tables

Table 1 An overview of types of slab track structures (adapted from Esveld (2001, p. 234)).....	1
Table 2 LS regression in Excel (corrosion failure; exact failure times; field data)	41
Table 3 Result of regression statistics.....	43
Table 4 Ultrasonic inspection report (squats in Harmelen LCS).....	43
Table 5 LS regression in Excel (RCF failure, interval data; assumed data).....	44
Table 6 Weibull MLE for corrosion failure data (starting estimates from LS regression)	45
Table 7 Weibull MLE for corrosion failure data (after Solver).....	46
Table 8 Weibull MLE for RCF failure data (after Solver).....	47
Table 9 Comparison of LS estimates and MLEs.....	47
Table 10 Input cost data (ProRail).....	48
Table 11 Comparison of total EMC (the 179 th – 192 nd month)	53
Table 12 Impact of PR cost on age replacement optimization & total LCC over the optimized replacement cycle	55
Table 13 Impact of discount rate on age replacement optimization & total LCC over the optimized replacement cycle	58
Table 14 Cost components of total EMC under different annual discount rate	58
Table 15 Impact of grinding intervals on age replacement optimization & total LCC (when grinding cost is €2000)	61
Table 16 Impact of grinding intervals on age replacement optimization & total LCC (when grinding cost is €500)	62
Table 17 Input cost data (PGO contractors).....	63

List of Figures

Figure 1 Cover picture (Christophi & Mazarrasa, 2015)	1
Figure 2 Ballasted track structure (Esveld, 2001, p. 203)	1
Figure 3 Schematic diagram of ERS in a concrete/steel channel (edilon)(sedra, 2017).....	2
Figure 4 Rail level crossing (adapted from ProRail (2018a))	2
Figure 5 Interaction among cash flows (LCC), asset degradation and maintenance interventions	3
Figure 6 Research framework	6
Figure 7 (Left) Installation of embedded rail LCS (pouring Corkelast®) (edilon)(sedra, 2018b); (right) Schematic diagram of ERS in a concrete/steel channel (edilon)(sedra, 2017).....	7
Figure 8 Crack development process (Cannon et al., 2003).....	7
Figure 9 (a) Appearance of squats; (b) Rail fracture resulting from squats; (c) Cross section of the broken rail (UIC, 2002).....	8
Figure 10 (a) Initial horizontal crack at the rail web; (b) Rail fracture resulting from horizontal cracks at the web (UIC, 2002)	8
Figure 11 The end of Harmelen LCS / connecting area to the ballasted track (location: IJsseldijk 92.673; time: 17/09/2015) (ProRail, 2018a).....	9
Figure 12 Rail break near the end of Harmelen LCS (ASSETRail, 2018).....	9
Figure 13 Wooden sleepers in the transition and pollution at the rail ends (ProRail, 2018a).....	9
Figure 14 Reduced profiles in rail foot at the end of LCS caused by corrosion (ProRail, 2017).....	10
Figure 15 Corkelast® not completely attached to the channel wall & possibly corroded area (location: Almelosestraat, 19.373; time: 01/08/2016) (ProRail, 2018a).....	10
Figure 16 Unreliable measurement of defect depths using ultrasonic inspection (Popović et al., 2013)	12
Figure 17 Grinding machine GWM 250 (Esveld, 2001, p. 352; PlasserAmerican, 2018).....	14
Figure 18 Grinding machine with rotating stones (adapted from Esveld (2001, p. 353)).....	14
Figure 19 (a) Positions of rotating stones; (b) Illustration of grinding path in the contact area (Zhi et al., 2014).....	14
Figure 20 Asymmetric ground rail profile (location: Woeziksestraat Ht-Nm, 59.026; time: 23/08/2016) (ProRail, 2018a)	15
Figure 21 Removal of Corkelast® resin in the rail replacement (edilon)(sedra, 2018b).....	16
Figure 22 Replacement cycles: age-based replacement policy (Fernández & Márquez, 2012, p. 222).....	18
Figure 23 Relation between $f(t)$, $F(t)$ and $R(t)$	22
Figure 24 Example of regression line (adapted from Tobias & Trindade (2011, p. 155)).....	24
Figure 25 Comparison of the (real) hazard rate and adjusted hazard rate (adapted from (Coria et al., 2015)).....	29
Figure 26 Relation between preventive and corrective cycle under one age replacement policy (adapted from Jardine & Tsang (2013, p. 50))	31
Figure 27 The incurrence of operating costs under the age replacement policy	32
Figure 28 Diagrams for P, F and A (Sullivan et al., 2012, p. 56).....	34

Figure 29 Flowchart of the reliability-based LCC model	38
Figure 30 Specification of DB for preventive grinding program in the mainline (heavy rail) of the DB network (rails in curves with radii from 500 to 5000 m) (NeTIRail, 2015).....	40
Figure 31 Weibull probability plotting (corrosion failure data)	42
Figure 32 Exponential probability plotting (corrosion failure data).....	42
Figure 33 Weibull probability plotting (RCF failure data)	44
Figure 34 Solver entries for MLE.....	46
Figure 35 Output of age replacement optimization (reference case: 12-month grinding interval).....	49
Figure 36 Impact of operating cost on age replacement optimization (excl. investment cost)	51
Figure 37 The balance between preventive and corrective cycle cost in the age replacement optimization	52
Figure 38 (Left) reliability $R(t)$; (right) CDF $F(t)$	52
Figure 39 Impact of PR cost on age replacement optimization.....	54
Figure 40 Impact of annual discount rate on age replacement optimization.....	57
Figure 41 Impact of grinding interval on age replacement optimization (grinding cost €2000).....	59
Figure 42 Impact of grinding operations on rail reliability (T_0 is assumed to be 12 months).....	60
Figure 43 Impact of grinding interval on age replacement optimization (grinding cost €500 versus €2000).....	61
Figure 44 Age replacement optimization (PGOs)	64

List of Abbreviations

CBM – condition-based maintenance
CDF – cumulative distribution function
CM – corrective maintenance
CR – corrective replacement
CW – capitalized equivalent worth
EAC – equivalent annual cost
EMC – equivalent monthly cost
ERS – embedded rail system
HPP – Homogeneous Poisson Process
i.i.d. – independent and identically distributed
LCC – life cycle cost
LCCA – life cycle costing analysis
LCS – level crossing system
LIK - likelihood
Log LIK – Log likelihood
LS – least squares
MLE – maximum likelihood estimation
MLEs – maximum likelihood estimators
MTTF – mean time to failure
NDT – non-destructive testing
NHPP – Non-homogeneous Poisson Process
PDF – probability distribution function
PGO – Prestatiegericht onderhoud (Performance focused maintenance)
PM – preventive maintenance
PR – preventive replacement
PV – present value
RCF – rolling contact fatigue
TBM – time-based maintenance
UIC – Union Internationale des Chemins (International Union of Railways)

1. Introduction

1.1 Slab track structures

Traditional ballasted tracks consist of a flat framework made up of rails, sleepers and fasteners which is supported by ballast (Esveld, 2001, p. 203). The ballast lays on the sub-ballast which forms a transition layer between the track superstructure and subgrade (Esveld, 2001, p. 203), as shown in Figure 2. During the past decades, various types of slab (or sometimes called ballastless) track structures have been developed and put into service around the world (Gailienė & Laurinavičius, 2017; Gautier, 2015). In comparison to the ballasted tracks, the slab tracks replace the traditional combination of ballast and sleepers by a rigid concrete slab which transfers the load (Esveld, 2001, p. 231). The decision to design and lay this type of structures is more often made with high-speed railway lines (Gailienė & Laurinavičius, 2017), as it can provide far higher structural and geometric stability, given a good slab foundation (Esveld, 2001, p. 232).

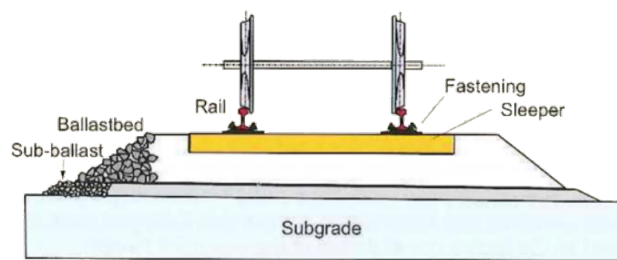


Figure 2 Ballasted track structure (Esveld, 2001, p. 203)

There are a variety of designs of slab tracks, each with distinct features (Esveld, 2001, p. 233). As presented in Table 1, the slab structures can be categorized into two major types according to how the rails are supported, i.e., discrete rail support and continuous rail support (Esveld, 2001, p. 234). Initial designs of the slab structures replace the ballast with a concrete slab and keep the sleepers resting on the concrete or asphalt layers (Gautier, 2015). With an evolution of the technology, the sleepers or blocks are progressively embedded into the slab. More radically the sleepers are suppressed and the rail is directly fastened to the slab through baseplates (Gautier, 2015). Another radical option is embedded rail structure, in which the rail is completely embedded in the slab (concrete or steel channels) and fixated by means of an elastic poured compound which surrounds almost the entire profile of the rails except for the rail head (Esveld, 2001, p. 253). The distinct feature of the embedded rail structure is, due to the elastic compound, it combines the track ballast, rail fastening and the concrete slab into one structural monolithic unit and is able to provide a continuous elastic support along the full length of the rails, comparable to the three former types with discrete rail support.

Table 1 An overview of types of slab track structures (adapted from Esveld (2001, p. 234))

Slab track structures			
Discrete rail support		Continuous rail support	
With sleepers/blocks		Without sleepers/blocks	Embedded rail
Sleepers/blocks on top of concrete/asphalt layer	Sleepers/blocks embedded in slab	Rail directly fastened to the slab through baseplates	Rail embedded in slab

1.2 edilon)(sedra & embedded rail system

edilon)(sedra is an international supplier of rail track systems with a broad field of application in the railway industry - rail tracks on/in the civil structures (e.g., bridges and tunnels), level crossings, stations, etc. It is specialized in providing innovative track solutions and one of the track designs is embedded rail system (ERS). The ERS, as stated above, belongs to the slab track structures. As shown in Figure 3, it is a rail fastening system composed of edilon)(sedra Corkelast® (a polymer embedding compound with hardness), resilient ERS strip (provides elasticity and deflection control) and material saving items (reduce the use of embedded compound; e.g., filler blocks, tubes, etc.) (edilon)(sedra, 2018b).

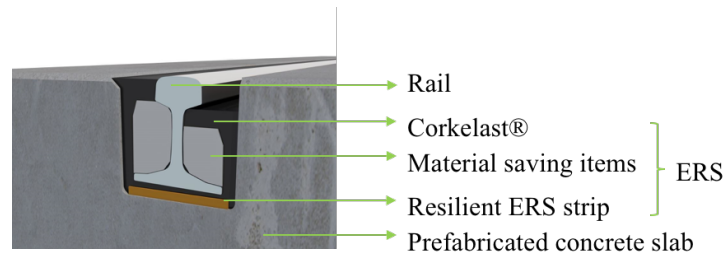


Figure 3 Schematic diagram of ERS in a concrete/steel channel (edilon)(sedra, 2017)

The ERS rail fastening system is characterized by continuous rail support and elimination of all forms of traditional hardware components (e.g., sleepers, fasteners), in which forces are more evenly distributed and a better rail fatigue and wear performance is expected due to the reduction of high dynamic forces¹ in rails (edilon)(sedra, 2018a; Esveld, 2001, p. 254; Zoeteman & Esveld, 1999, p. 254). One of its application is in rail level crossings, in which the system product is edilon)(sedra Corkelast® Level Crossing System (LCS). A rail level crossing is an intersection where a railway line and a road cross at the same level (Esveld, 2001, p. 226). It is a special object compared to the normal railway lines. As demonstrated in Figure 4, a level crossing consists of two zones, i.e., level crossing zone (the area where both trains and motor vehicles pass over) and transition zone (the area from the ballasted track onto the slab and from the slab onto the ballasted track). The edilon)(sedra LCS is applicable in the level crossing zone and the structure in the transition zone is the conventional ballasted track which makes a connection to the normal railway lines.

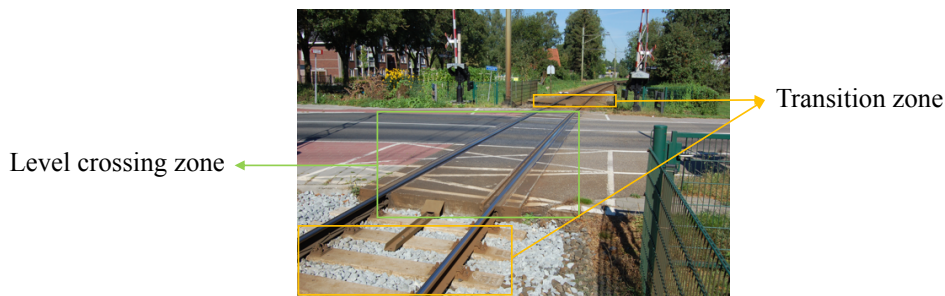


Figure 4 Rail level crossing (adapted from ProRail (2018a))

1.3 Problem statement

Life cycle costing analysis (LCCA) is an economic evaluation technique that seeks to optimize the cost of acquiring, operating and maintaining infrastructure assets by taking into account all cost elements throughout the life cycle of the alternatives being considered (Ammar, Zayed, & Moselhi, 2012;

¹ The dynamic forces are caused by secondary bending between discrete rail supports (Esveld, 2001, p. 254).

Lindholm & Suomala, 2007). A few studies have evaluated the LCC of embedded rail LCS (Gailienė & Laurinavičius, 2017; Zoeteman & Esveld, 1999), but they are more case-specific – based on deterministic cost data of particular cases. The degradation of the railway assets and maintenance interventions vary from case to case, which may cause variation in LCC. The LCC output on one specific asset may become less reliable when it comes to the general condition.

To clearly demonstrate the interaction among LCC, asset degradation and maintenance interventions, Figure 5 presents one possible scenario for the incurrence of cash flows during the lifecycle of one railway asset. The reliability index is a general term that measures the asset reliability. Starting from the initial reliability, in the absence of interventions the degradation of the asset could be indicated by the dotted line; if a series of interventions are carried out in its lifecycle, the reliability level of the asset can be retained to some extent, depending on the type of interventions. Small preventive maintenance actions can only recover a small portion of the asset reliability, so do minor repair actions (like removing small defects). Once the reliability level reduces to zero (failure), possibly only the replacement can be performed, implying the lifecycle of this system terminates. With different time frames of the interventions, the timing of cash flows varies, associated with different degradation patterns, which in turn influences the lifespan of the asset and total LCC (the sum of cash flows indicated).

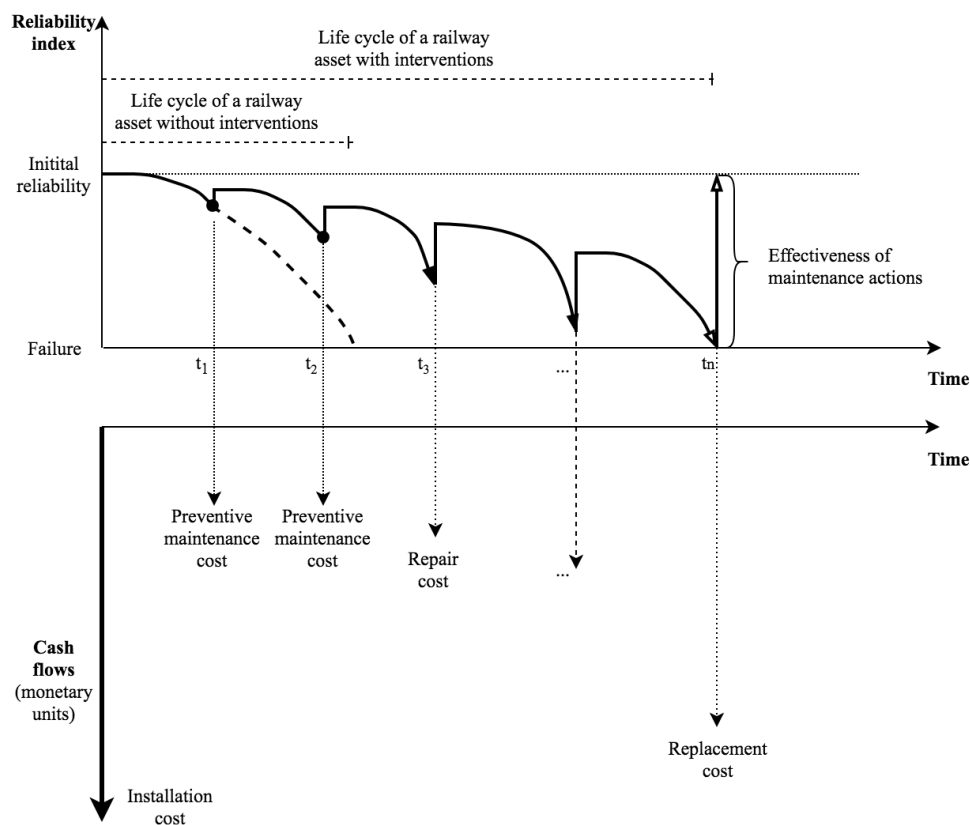


Figure 5 Interaction among cash flows (LCC), asset degradation and maintenance interventions

Several researchers have put effort in analyzing the impact of uncertainty regarding rail degradation and maintenance strategies on LCC (Patra, Söderholm, & Kumar, 2009; Rahman & Chattopadhyay, 2010; Vandoorne & Gräbe, 2018; J. Zhao, Chan, Roberts, & Madelin, 2007). The common problem in their cost calculation is neglecting cost discounting. The cost discounting accounts for the time value of money (van den Boomen, Schoenmaker, & Wolfert, 2018). The rail assets often have long lifespans and a series of cash flows may occur in different years, as an example presented in Figure 5. Ignoring the time value of money may lead to a wrong calculation of cash flows and a biased LCC (van den Boomen, Schoenmaker, Verlaan, & Wolfert, 2017). Moreover, they focused on the ballasted tracks and the mathematical models they developed are not applicable to the embedded rail LCS, considering the

different degradation mechanisms and maintenance interventions applied over the lifecycle of the systems. Another critical problem is the misuse of mathematical tools. In their papers (Vandoorne & Gräbe, 2018; J. Zhao, Chan, Roberts, & Stirling, 2006), the arrivals of rail defects were assumed to follow a Non-homogeneous Poisson Process (NHPP)² (power law model) with an intensity function given by the hazard rate of Weibull probability distribution. Although the power law intensity function and Weibull hazard rate have similar forms, a distinction should be made between the life distribution³ model – Weibull distribution and the stochastic process – NHPP. The former is applicable for the lifetime of non-repairable systems (time to failure) whereas the latter focuses on the interarrival times of failures (time between failure) for repairable systems. The procedures applicable to the Weibull distribution is not correct for the NHPP (Tobias & Trindade, 2011, p. 490).

edilon)(sedra wants to gain more insight into the lifecycle performance of the embedded rail LCS, both from financial (LCC) and technical perspectives, in order to improve the system production and obtain a positive feedback loop in the lifecycle management of the system. Limited literature has been found that evaluates the LCC of embedded rail LCS based on its degradation and maintenance interventions. It is still not very clear how the system degrades in practice, what maintenance interventions are followed to retain its reliability, which cost elements are important contributors to total LCC of the system and how the system degradation and maintenance interventions influence its LCC.

1.4 Research objective & scope

1.4.1 Research objective

In order to tackle the practical problems and add values to the literature, the research is aimed at developing a reliability-based LCC model for the embedded rail level crossings, considering the interaction between LCC and uncertainties involved in the asset degradation and maintenance interventions during the lifetime of the systems in an effort to optimize maintenance interventions and achieve a cost-effective life cycle management of the embedded rail LCS.

1.4.2 Research scope

Basically there are three types of edilon)(sedra embedded rail LCS:

- The heavy-duty level crossings for mainline (heavy rail) traffic as in use in the network of ProRail (Dutch rail infrastructure manager) and some other national railway infrastructure;
- The standard level crossings for mainline (heavy rail) traffic as in use in the network of some other national railway infrastructure organizations and industrial areas;
- The light rail level crossings for tram/urban rail (light rail) traffic as in use in some local networks.

The information about degradation mechanisms and maintenance policies of the embedded rail LCS (edilon)(sedra LCS) is collected from ProRail, Strukton and ASSET Rail (maintenance contractors of ProRail) so that the research focuses on the first type, heavy-duty level crossings (in Dutch ‘Harmelen’, named after the town of Harmelen) (edilon)(sedra, 2018a), for mainline traffic as in use in the Dutch railway network.

² NHPP is a stochastic process which permits a nonstationary events by allowing the constant repair rate at time t to be a function of t (Tobias & Trindade, 2011, p. 488). See more illustration in section 3.2.2.

³ Life distribution model is defined as *the theoretical distribution used to describe the lifetime of a component/system* (Tobias & Trindade, 2011, p. 29), in which the time t should be positive, i.e., $t \geq 0$. More details in section 3.2.2.

1.5 Research questions

In line with the research objective, the research question for this thesis is defined as:

How can uncertainty associated with the degradation of Harmelen LCS and maintenance strategies be incorporated in the LCC analysis in order to capture the interaction between the uncertainties and LCC of the systems and optimize maintenance strategies from the LCC point of view?

To guide the research and give an answer to the main question, a set of sub-questions are formulated.

- What are the main degradation mechanisms of the Harmelen LCS?
- How are the Harmelen LCS maintained during their lifetime?
- How can the degradation of the Harmelen LCS be modelled?
- How can the effect of maintenance interventions on the asset degradation be evaluated?
- How can results of degradation modelling (incl. the impact of maintenance interventions) be integrated into cost estimation?

1.6 Research framework & thesis outline

Follow the above sub-questions, the research framework is formulated as shown in Figure 6.

The research consists of eight steps. At first, the necessity for the research and formulation of the research objective and questions are addressed in Chapter 1. With knowledge gained from the literature review (general railway assets) and interviews with practitioners (specific to the Harmelen LCS), Chapter 2 covers step 2 & 3, which presents the characteristics of the Harmelen LCS, its dominant degradation mechanisms and maintenance interventions that are adopted during the lifetime of the systems. It provides a theoretical background for model formulation and gives answers to sub-question 1 & 2.

Then, step 4 is going to perform the reliability analysis to model the system degradation. With the reliability model, step 5 incorporates the impact of interventions and step 6 integrates the output of step 4 & 5 to cost (LCC) modelling and maintenance optimization, which give answers to sub-question 3, 4, and 5, respectively. The three steps guide the model development and all are addressed in Chapter 3. Combine the output of the sub-questions, the reliability-based LCC model for the Harmelen LCS will be developed, where the interaction among the system degradation, maintenance interventions and LCC is expected to be captured.

Step 7 considers the model application and validation, which is addressed in Chapter 4. Initial modelling results are also presented in the end. Step 8, addressed in Chapter 5, takes more different settings into account and performs sensitivity analysis to identify connections between input variables and model output in order to test the robustness of the model and facilitate better understandings about how the model works in reality. Chapter 6 concludes the key outcomes of the previous chapters and, in response to the observations made in Chapter 5, deals with the model generalization in regard to the applicability to other systems and for different stakeholders. And suggestions for future improvement are addressed in the end.

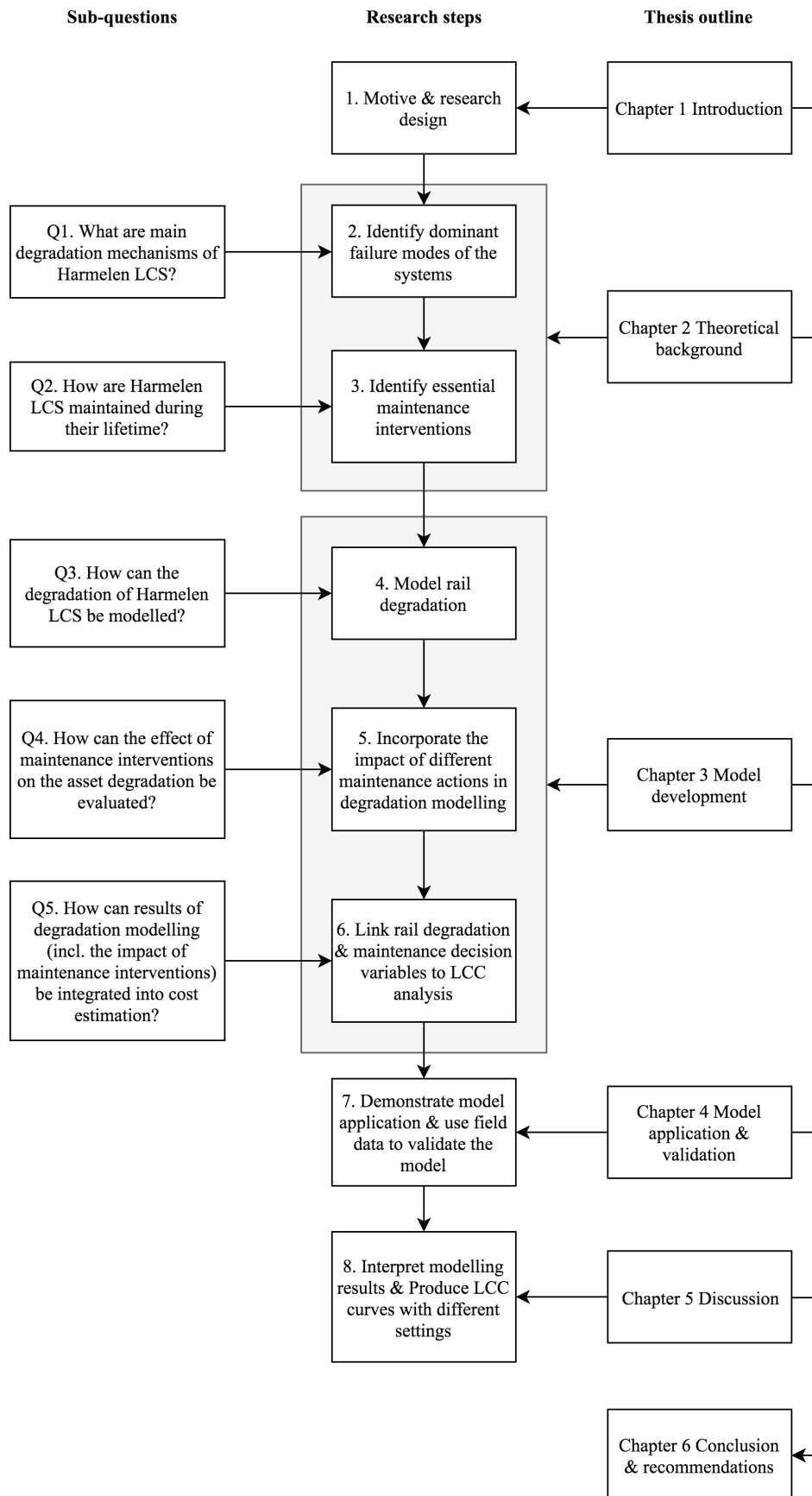


Figure 6 Research framework

2. Theoretical Background

This chapter deals with the theoretical background of this thesis, based on the literature review and interviews with practitioners. It covers two topics, section 2.1 discusses the features of the main components of the Harmelen LCS and the dominant degradation mechanisms during their lifetime. Section 2.2 presents the inspection and maintenance interventions that are applied in practice to keep the systems safe and serviceable.

2.1 Harmelen LCS & its degradation

Basically one Harmelen LCS consists of three components, namely rail, ERS and slab, as shown in Figure 7 (right), and the left indicates the installation of the LCS: the embedding work is applied by manual pouring from buckets (edilon)(sedra, 2018b). General descriptions about the degradation of the Harmelen LCS are presented below, based on asset management guideline (RLN00104) of ProRail (ProRail, 2010), in combination with interviews and literature review.

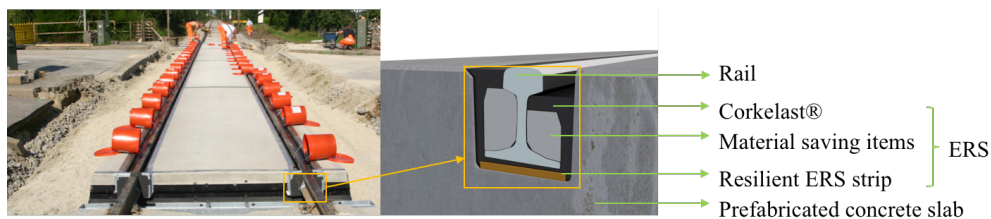


Figure 7 (Left) Installation of embedded rail LCS (pouring Corkelast®) (edilon)(sedra, 2018b); (right) Schematic diagram of ERS in a concrete/steel channel (edilon)(sedra, 2017)

2.1.1 Rail

The main functions of the rails are: 1) to accommodate the wheel loads and transmit the forces to the track bed; 2) to guide vehicles together with the wheel tread and flange (Cannon, Edel, Grassie, & Sawley, 2003; Esveld, 2001, p. 206). It has little redundancy and its failure may pose a threat to the safe operation of the railway, at worst leading to derailment of vehicles (Cannon et al., 2003). It is therefore a safety-critical component in the railway systems. In the thesis, only rail defects that are closely related to the Harmelen LCS are presented. More details of classification and description of rail defects refer to UIC code 712R: rail defects (UIC, 2002).

- Rolling contact fatigue (RCF)

Like many metallic components, the rail, subjected to repeated loading cycles, is susceptible to metal fatigue (Cannon et al., 2003). With increasing traffic loading and train speed the rail deterioration tends towards rolling contact fatigue (RCF) damage (Vandoorne & Gräbe, 2018). Cannon et al. (2003) described the development of rail RCF damage in three basic phases, as shown in Figure 8. A fatigue crack initiates when repeated stress with sufficient magnitude is applied to a rail section; it goes on propagating with the accumulation of loading cycles over time. Without any intervention to control the end result of the crack development process is rail break (Cannon et al., 2003; Kumar, 2006).

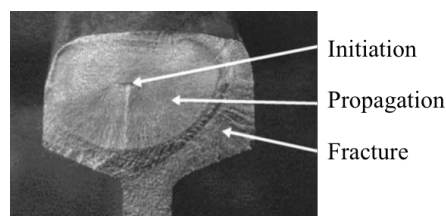


Figure 8 Crack development process (Cannon et al., 2003)

The rail defects which occur due to RCF can be categorized into surface-initiated and subsurface-initiated (or internal) RCF defects (Kumar, 2006). One of the typical surface-initiated RCF defects is

squats, which are mostly caused by contact stresses between the rail and wheel (Cannon et al., 2003). It became clear from interviews that the squat defect is one of the common RCF defects that occur in the Harmelen LCS, which may pose a threat to safety issues (rail breakage) (refer to Appendix A, Interview III & IV). UIC code for squats is 227: the first digit indicates the *situation* of the rails (2: zone away from rail ends); the second digit represents the *location* of the rails (2: surface of rail head); the third digit means the *pattern* of defects (7: cracking & local substance of the surface) (UIC, 2002). Figure 9 (a) clearly displays the characteristics of squats. Its cause manifests itself as a localized depression on the rail running surface; (b) in the absence of control, the cracks may propagate inside the rail head and when the depths reach 3-5 mm, their downward-turning crack development may lead to the final rail break (UIC, 2002). Figure 9 (c) presents the cross section of a broken rail caused by squats (UIC, 2002).



Figure 9 (a) Appearance of squats; (b) Rail fracture resulting from squats; (c) Cross section of the broken rail (UIC, 2002)

The internal RCF defects are mainly caused by non-metallic imperfections originating from the manufacturing process which then propagate with loading cycles (Cannon et al., 2003). One of the common internal RCF defects occur in the Harmelen LCS is the *horizontal crack at the web-head fillet radius* (UIC, 2002). UIC code for this defect is 2321, 2 (situation): zone away from rail ends; 3: (location) web; 2: (pattern) horizontal; 1: (additional features) web-head fillet radius (UIC, 2002). As shown in Figure 10 (a), a crack initiates in the rail, parallel to the web-head fillet radius; with its progression, the crack can turn upward and/or downward (UIC, 2002). According to UIC code 712 (UIC, 2002), this type of cracks finally results in rail fragmentation (Figure 10 (b)).

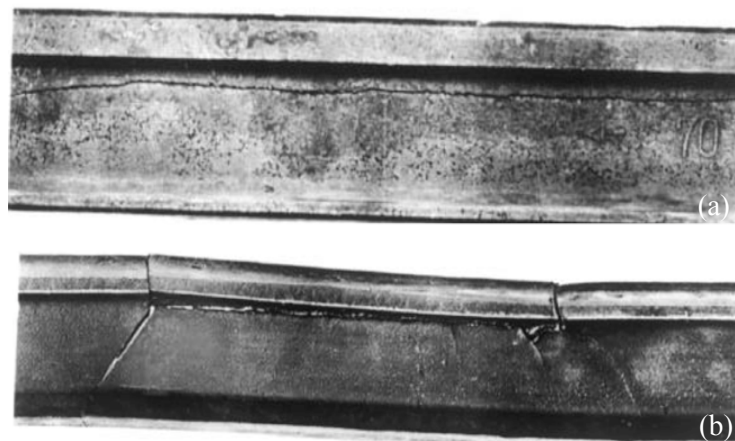


Figure 10 (a) Initial horizontal crack at the rail web; (b) Rail fracture resulting from horizontal cracks at the web (UIC, 2002)

- Corrosion

In addition to the RCF defects, rail corrosion is another dominant factor that influences the rail degradation of the Harmelen LCS. The corrosion can occur anywhere in the rail. A point of attention is the rail sticking out of the slabs where the ballasted track continues, in which the rail ends must be protected from corrosion by anti-corrosive coating, as shown in Figure 11. The rail is in good condition

in this figure but it can be observed the rail at the end of the Harmelen LCS is more susceptible to moisture.



Figure 11 The end of Harmelen LCS / connecting area to the ballasted track (location: IJsseldijk 92.673; time: 17/09/2015) (ProRail, 2018a)

In addition to moisture, a combination of other factors like road debris, de-icing salt, limited ventilation and lack of sunlight plays a role in accelerating the corrosion process (Valkenburg, 2015). All these are external factors, while the nature of the rail corrosion occurs in the Harmelen LCS is the local settlement (track geometry) in the transition zone and debonding of Corkelast® (ERS). The settlement in the connecting area originates from different bearing capacity: the slab in the embedded rail LCS is a rigid and durable concrete structure and can hardly be exposed to bending forces, comparable to the lower bearing strength of ballast bed in the transition area. The ballast bed is composed of loose and coarse-grained materials, in which internal friction between the grains provides the strength of the ballast bed and support the track superstructure (Esveld, 2001, p. 205). With the accumulation of traffic loading, the ballast material will gradually deteriorate and cause geometric unevenness. When a train goes from a ballasted track onto the LCS, dynamic impact (a bump) would occur due to the local settlement, which will in turn cause rotation of the rail (may lead to the rail fracture as shown in Figure 12) and debonding of the elastic compound near the end of LCS. Once there is a fissure between the elastic compound and rails, dirt combined with water (and other external factors act together) will flow into the gaps and the rail corrosion starts. The geometric problem becomes more severe when wooden sleepers are used in the transition area, as shown in Figure 13, since the wooden sleepers have lower capacity, compared to concrete sleepers, and are more vulnerable to geometric unevenness. Figure 13 also indicates that the rail ends sticking out of LCS are more likely to suffer from dirt.

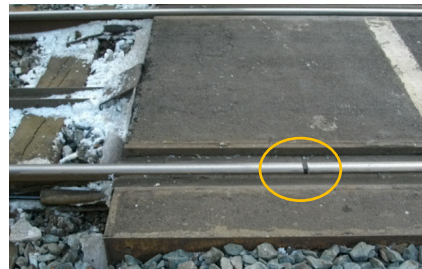


Figure 12 Rail break near the end of Harmelen LCS (ASSETRail, 2018)



Figure 13 Wooden sleepers in the transition and pollution at the rail ends (ProRail, 2018a)

The problem of corrosion is in the long term a deterioration of bearing capacity of the rail, caused by volume reduction of the rail foot (Valkenburg, 2015), as presented in Figure 14. At worst it may lead

to rail breakage. From the interviews it became clear approximately 50% of the rail foot corrosion causes rail breakage (Appendix A, Interview III), and this type of failure is very unpredictable, compared to the RCF-initiated breaks, as there are relatively well-developed inspection techniques for RCF defects and crack propagation can be controlled once they are detected.

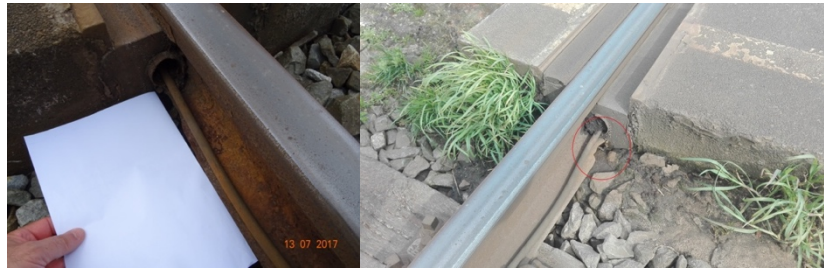


Figure 14 Reduced profiles in rail foot at the end of LCS caused by corrosion (ProRail, 2017)

According to ProRail’s policy, the expected lifecycle of the rails in the Harmelen LCS is 20 years, which is defined based on the past experience. In the conventional ballasted tracks, rail breaks can be repaired by cutting out the section of the failed rail and welding in a new segment, while, for the Harmelen LCS, rail replacement must be performed in case of rail breaks as it is not allowed to have welds in the level crossings with ERS (ProRail, 2010), implicating that the rail life terminates when a rail break occurs in the Harmelen LCS.

2.1.2 ERS

For the Harmelen LCS, the rails are embedded in Corkelast® resin (ERS). According to the management guideline (ProRail, 2010), the casting compound must be repaired when less than 75% casting materials stick to channel walls. It is also prescribed that the compound must be attached to the rail along the entire length of the level crossings, except 30 cm at the ends (ProRail, 2010). As shown in Figure 15, a tape measure combined with a knife is used to check the distance of the debonding of Corkelast® resin. The debonding of the compound is closely related to the rail foot corrosion at the end of LCS. It can be observed in Figure 15 the rail web and foot are ponded with water. A combination of debonding, moisture, limited ventilation, lack of sunlight and other substances plays as a breeding ground for the corrosion.



Figure 15 Corkelast® not completely attached to the channel wall & possibly corroded area (location: Almelosestraat, 19.373; time: 01/08/2016) (ProRail, 2018a)

In practice the lifespan of ERS has not been observed as ERS has a longer life than the rails but the former has to be removed completely from the channels when rail replacement is conducted. After cleaning and preparation of the channels, the new rails can be primed, installed and poured back in with Corkelast® resin (new ERS). In most cases the lifespan of ERS depends on the rail degradation, due to the full replacement. It is therefore assumed that the degradation of ERS only has *cost impact*: in the cost modelling, replacement costs of the ERS is implicitly included in the rail replacement costs.

2.1.3 Slab

In principle, there are few maintenance needs for the track geometry in concrete plates during their lifetime (ProRail, 2010), as the concrete plates are robust structures. In exceptional circumstances, if settlement occurs a technically simple and proven technology of injection methods can restore the geometric condition (ProRail, 2010). It is also possible that the slabs suffer from other failures like cracking, horizontal movement, etc. The cracks with a depth large than 0.2mm must be injected with a low-viscous and moisture-insensitive injection resin (ProRail, 2010). Horizontal correction of the plates is far-reaching and expensive; however, by careful implementation at construction, horizontal correction at a later stage can be prevented (ProRail, 2010).

Due to the nature of the concrete slabs, they have a longer technical lifespan than the rails that are used. According to the policy of ProRail, the expected lifespan of the concrete slabs is 40 years, compared with the lifespan of the rails, 20 years. Therefore once, twice or sometimes even three times the rails will be replaced caused by various factors without removing the concrete slabs. Considering the following reasons, the degradation modelling and cost modelling in this research focus on the rails (with the cost impact of the ERS).

- The slab has a much longer lifespan than the rail;
- The slab has fewer maintenance needs during its lifecycle;
- The costs used to maintain the slab (e.g., injection) are lower than that used for rail maintenance (rail replacement cost is a major cost contributor to LCC of the Harmelen LCS);
- The inspection and maintenance of the slab are generally separated from the rail and ERS.

2.2 Inspection & maintenance

2.2.1 Inspection practices

For any preventive maintenance program, inspection is always a necessary activity, since it provides information on the condition of the railway assets and facilitates the decisions and execution of repair and/or replacement (Wang, 2012). The inspection policies considered in the research are determined from interviews (ProRail, Strukton and ASSET Rail, refers to Appendix A).

- *Inspection for RCF defects*

An optimal inspection method for the RCF defects should provide early detection of rail defects and reliable data in regard to their position, depths and lengths, etc., while this kind of method does not exist so far (Popović, Radović, Lazarević, Vukadinović, & Tepić, 2013). A combination of rail inspection methods is therefore used in order to increase the accuracy of inspection, namely non-destructive testing (NDT) cars (ultrasonic inspection and eddy-current inspection, etc.), visual inspection and track circuit detection by signals (part of central traffic control system) for detection of possible rail defects (Kumar, 2006).

Visual inspection is a traditional track inspection method, its accuracy is influenced by the knowledge and skills of inspectors and possibly other external factors (Popović et al., 2013). The NDT techniques allow maintenance personnel to check the internal structure of the rails. It measures internal discontinuities in the rails that are not visible from the outside, while ultrasonic inspection cannot provide accurate measurement when it comes to the detection of surface fissures at small angles towards the rail head surface (Popović et al., 2013). As shown in Figure 16, some of deeper cracks are left undetected through ultrasonic inspection.

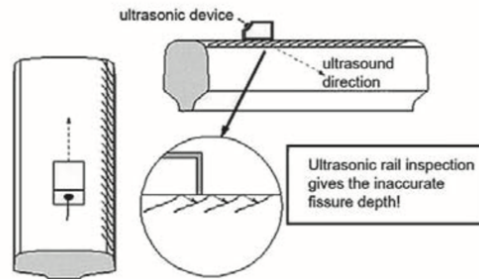


Figure 16 Unreliable measurement of defect depths using ultrasonic inspection (Popović et al., 2013)

Eddy current inspection, however, has great sensitivity to small defects. It can early detect initial fissures below the rail running surface (Popović et al., 2013; Rajamäki, Vippola, Nurmikolu, & Viitala, 2018). But the drawback is it has a limit of penetration depth. Cracks which are over this limit cannot be detected and measured reliably (Rajamäki et al., 2018). The statement has been verified by experts via interviews (Appendix A, Interview III): eddy-current inspection has better accuracy than ultrasonic equipment but the former can only detect 4 mm in the rails from the top. The combination of ultrasonic inspection and eddy current inspection will increase the probability of early detection of RCF defects.

Ultrasonic inspection is the dominant one used for detecting the rail defects in the Harmelen LCS. It is performed by ProRail within a national programme for the whole railway network that is owned by ProRail (out of the scope of PGO contracts⁴). It is carried out twice a year. Ultrasonic inspection trains give a first indication of the possible defects. If a certain spot is suspicious, ProRail will send the inspection reports to the PGO contractors. The contractors will send manual crews and they will do validation of the weak points (with hand-held ultrasonic equipment): classify the numbers of rail defects based on RLN00036 catalogue⁵ (ProRail, 2012) and severity levels⁶ of the defects and finally write the ultrasonic inspection report with decisions in regard to interventions. If the defects are not identified through inspection, they may lead to rail breaks, which could be detected through the signaling system or visual inspection.

- *Inspection for rail corrosion*

Inspection techniques used for detecting the rail corrosion in Harmelen LCS are mainly ultrasonic inspection, visual inspection and G-scan equipment (not extensively applied). The strength of ultrasonic inspection compared to eddy current inspection is it can inspect more about the rail condition: in addition to RCF defects, it can give an indication about the rail foot corrosion by measuring the difference in height (the loss of the rail profile caused by corrosion). Although the result is not reliable, it provides information and supports replacement decisions.

⁴ Track maintenance contract (Performance Focused Maintenance; in Dutch: Prestatiegericht onderhoud): with the aim of improving the availability and quality of the track, ProRail wants to make a switch to performance-oriented maintenance, in which the effort one contractor has to make (traditional maintenance contracts) is no longer prescribed, but the desired performance. The PGO contracts are publicly tendered. Note that the new PGO contracts have a duration of 10 years, comparable to 5 years of old PGO contract (ProRail, 2018b).

⁵ RLN00036 has the same rail defect coding system as UIC code 712R (UIC, 2002).

⁶ There are four categories which classify the severity of rail defects in the ultrasonic inspection report: category 1 – replace the rail within 24 hours; category 2 – replace the rail within 4 weeks; category 3 – replace the rail within 3 months; category 4 – replace the rail within 6 months. The old category slightly differs from the new: category 3 is to replace the rail within 6 months and category 4 is to keep monitoring. The attached ultrasonic inspection report (squats) in Appendix D adopts the old regime of classification.

Visual inspection is conducted with the focus on the rail corrosion at the end of LCS: sometimes inspect visually and sometimes check the corrosion with instruments (measure the difference in rail profiles between the corroded and standard rails). The visual inspection is also a check of the general condition of Harmelen LCS. It covers the embedded rails, Corkelast[®], slabs and adjacent tracks (transition zone). The frequency of visual inspection varies depending on the asset managers. For ProRail, visual inspection at the rail ends specifically for Harmelen LCS is performed every four years; and once a year for the general visual inspection in ProRail by inspectors who are responsible for certain areas.

2.2.2 Maintenance

Maintenance is defined as *a set of activities used to restore a system to a level where it can perform designated functions* (Ahmad & Kamaruddin, 2012; Sánchez-Silva & Klutke, 2016, p. 271). It can be classified into *preventive maintenance* (PM) and *corrective maintenance* (CM) (Ahmad & Kamaruddin, 2012; Sánchez-Silva & Klutke, 2016, p. 272). PM indicates the maintenance activities that are performed prior to the system failure while CM, known as the run-to-failure action or reactive action, is a strategy to repair an asset and restore it to designated functions after its failure (Ahmad & Kamaruddin, 2012). Nowadays railway asset managers tend towards PM as this strategy contributes to reducing failure risks of railway tracks and preventing downtime loss. Within the regime of PM, it can be further classified into time-based maintenance (TBM) and condition-based maintenance (CBM) (Ahmad & Kamaruddin, 2012). TBM is a traditional maintenance technique, in which maintenance actions are performed at a fixed interval, determined based on analysis of failure time data (Ahmad & Kamaruddin, 2012), and therefore it is also known as periodic-based maintenance. CBM is a more modern maintenance program, known as predictive maintenance (Ahmad & Kamaruddin, 2012), in which the core is the reliability of condition monitoring techniques: the asset condition is monitored continuously or periodically with well-defined indicators and intervention thresholds (Campos, 2009). Maintenance decisions are made based on the information collected from the monitoring process and the interventions are carried out only when needed or just before a failure occurs (Ahmad & Kamaruddin, 2012).

According to the effectiveness, maintenance actions may also be classified into three cases: perfect, minimal and imperfect (Blischke & Murthy, 2000, pp. 187, 188). In a perfect maintenance, the operation restores a system to be *as good as new*; a minimal maintenance is assumed to restore a system to be *as bad as old*, the same as just before the maintenance is performed; and an imperfect maintenance restores a system to a state between *as good as new* and *as bad as old* (Wu & Zuo, 2010). The effect of the maintenance interventions on the asset reliability has been visualized in Figure 5, where only the perfect and imperfect actions are mentioned: the PM and repair action are imperfect, i.e., only restore a small portion of asset reliability and replacement is considered as a perfect maintenance. i.e., retain the asset back to the initial quality. Both CM and PM, depending on situations, can be perfect, minimal or imperfect maintenance actions. Most PM actions in practice are imperfect (Coria, Maximov, Rivas-Dávalos, Melchor, & Guardado, 2015).

- Rail grinding

The RCF-initiated cracks are contributors to rail degradation, although not all of them impose the risk of rail fracture (Cannon et al., 2003; Popović et al., 2013). Some cracks are removed by wear process during their early development, while most of them should be removed by grinding measures. The cracks can be controlled to a certain extent by grinding the rail running surface to remove fatigue-damaged materials and form an improved rail head profile, which is an important condition for smooth running and noise reduction (Cannon et al., 2003; Esveld, 2001, p. 352). Generally two principles are applied for rail grinding: longitudinally oscillating stones or rotating stones (Esveld, 2001, p. 352). In the first type of grinding, taking grinding machine GWM 250 as an example, the stones are placed in a 2.5 m long frame, as shown in Figure 17, which oscillates longitudinally with the movement of the machine and smooths the rail head profile.



Figure 17 Grinding machine GWM 250 (Esveld, 2001, p. 352; PlasserAmerican, 2018)

Figure 18 presents a grinder with rotating stones, which is more effective than the other as the grinding action can be concentrated on a specific area (Esveld, 2001, p. 352), as depicted in Figure 19 (a). The stones (flat part) are placed on the rail contact surface and rotated driven by motors with speed ω . The machine moves with speed v and combined with the rotation speed, the grinding trace is like a spiral line, depicted by the dotted line in Figure 19 (b) (Zhi, Li, & Zarembski, 2014).

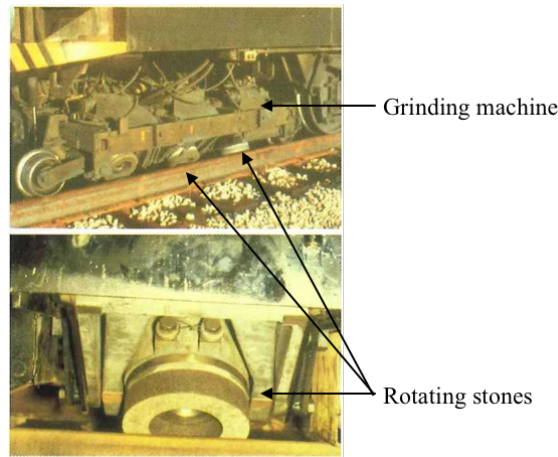


Figure 18 Grinding machine with rotating stones (adapted from Esveld (2001, p. 353))

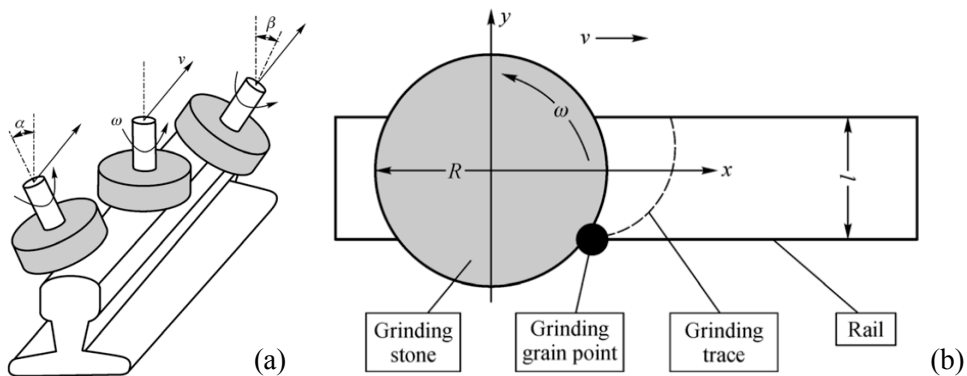


Figure 19 (a) Positions of rotating stones; (b) Illustration of grinding path in the contact area (Zhi et al., 2014)

Figure 20 presents an improved rail profile in one Harmelen LCS after grinding, which can remove the small surface defects, reduce contact stresses between the wheel and rail and control the subsequent

formation of the rail fatigue defects. Note that grinding operations only have an impact on controlling the occurrence and propagation of surface-initiated RCF defects⁷.



Figure 20 Asymmetric ground rail profile (location: Woeziksestraat Ht-Nm, 59.026; time: 23/08/2016) (ProRail, 2018a)

The same as the ultrasonic inspection, grinding operations are carried out by ProRail, within the national programmes. Both preventive and corrective grinding are performed in practice, while there is hardly any corrective grinding that was performed (once or twice in the lifecycle of the rails in Harmelen LCS). The corrective grinding deals with RCF separate defects, which is location specific. If preventive grinding performs well, most of the defects are under control and there is no need to do corrective (Appendix A, Interview IV).

ProRail adopts preventive cyclic grinding policy (TBM), which was introduced in 2004 (pilot phase) and 2005 (national rollout) (Zoeteman, Dollevoet, & Li, 2014). Until 2008, the preventive cyclic grinding regime has been fully employed over the Dutch national railway network (Zoeteman et al., 2014). The grinding cycles are planned based on the local tonnage (MGT) with different curvatures (Appendix A, Interview III). The rails in the level crossings are ground every 15 MGT with each 0.2 mm-depth metal removal. Small grinders are used on the level crossings. The acceptable wear levels (total depth of metal removal) vary depending on the profile type and local speed. In most cases the maximum wear allowed is 17 mm.

An alternative to grinding is milling. Milling can take away of more steel in one pass. If there are deeper cracks, grinding will not help and milling will be a better solution for the long term. ProRail is shifting from rail grinding to milling. In the new PGO contract (starting from 2018), grinding/milling is no longer within the national programme and PGO contractors are responsible for it (whether to use grinding or milling is in the hand of PGO contractors) (Appendix A, Interview IV).

- *Rail replacement*

Only the grinding/milling exists for repairing the defects that are detected in the Harmelen LCS and these operations can only control surface defects, like squats. But for now, there are no possible repairs for corrosion-initiated defects. Only pre-coating measures are available to control the initiation and progression of corrosion (details refer to Valkenburg (2015)). Both RCF- and corrosion-initiated defects make contributions to rail breakage. Once a rail break occurs, an immediate action should be followed, in which the broken rail should be replaced within 24 hours, implicating that the rail life terminates when a rail break occurs in the Harmelen LCS. The replacement in this case is corrective, while it is possible to preventively replace the rails. The decision on the preventive replacement is in the hand of asset managers: in most cases it depends on the local situation (results of ultrasonic inspection (for RCF defects) and visual inspection (for corrosion)) (Appendix A, Interview I & III). Some indicators to

⁷ Rail grinding is also effective in controlling other types of rail surface defects, e.g., corrugation (Esveld, 2001, p. 232), while the dominant failure modes of the rails in Harmelen LCS are corrosion and RCF defects so that the other modes are not mentioned.

support the decision are like the severity of rail corrosion at the end of LCS, bonding of Corkelast®, cracks in the rail (ultrasonic inspection reports) and the age of the rails, etc.

When replacing the rails in Harmelen LCS, either corrective or preventive, Corkelast® bonding materials need to be completely removed from the channels by means of a so-called ‘Pizza knife’, as shown in Figure 21. After cleaning and preparation of the channels, the new rails can be primed, installed and poured back in with new Corkelast®. Mostly both rails are replaced in the preventive replacement, and in case of rail breaks, a single rail is replaced (corrective replacement) (refers to Appendix A, Interview III).



Figure 21 Removal of Corkelast® resin in the rail replacement (edilon)(sedra, 2018b)

The corrective replacement in the Harmelen LCS normally takes 12 hours. Apart from replacement activities, maintenance personnel have to work with traffic management companies to deal with the road traffic: deviate the routes and put signs and barriers. Asset managers especially ProRail prefer preventive to corrective replacement, as in case of the latter they have to mobilize all the necessary personnel and resources within a very limited time period and in the Netherlands the normal possession time for the railway tracks is in the night of 4 hours, which means the corrective replacement will definitely influence the track availability. Fortunately, in most cases there is no risk of derailment when a rail break occurs in the Harmelen LCS, as the rails are fixated in the elastic compound (as shown in Figure 12). A point of attention is the train protection system, which is a railway technical installation in the whole railway network, connected by the rails, to continuously provide information to trains regarding their relative locations to other trains. The signals will disappear once a rail break occurs, which may pose a threat to safe operations of trains. In this case, use a copper leash to connect two ends and make the connection again (Appendix A, Interview IV). This temporary measure requires the lower speed of trains so that it may have an impact on train availability.

2.3 Conclusion

This chapter gives all the necessary information to conclude the following sub-questions:

Q1: What are main degradation mechanisms of the Harmelen LCS?

The main track components in the Harmelen LCS are rails, ERS and slabs. Both corrosion and RCF defects are contributors to rail degradation in the Harmelen LCS, where rail foot corrosion near the end of LCS caused by local settlement (at the transition zone) and debonding of Corkelast®, in combination with some external factors, is a dominant failure mode in Harmelen LCS, distinguished from other types of track structures. If there is no problem in the geometric condition of the transition zone, probably the bonding of Corkelast® can stay longer; substances with water will not flow into the gaps and the rails will somewhat not suffer from corrosion. The corrosion may lead to rail breaks, which may suddenly occur without any notice. Asset managers are normally risk-averse so that they prefer replacing the rails once they consider the corrosion becomes severe during the inspections. The dominant RCF defects that occur in the Harmelen LCS are squats and horizontal cracks in the rail web, where squats may cause safety issues (rail breaks).

Q2: How are the Harmelen LCS maintained during their lifetime?

The common practice for detecting RCF defects is ultrasonic inspection (ultrasonic inspection trains for a sketch and hand-held ultrasonic equipment for verification and decision making). Rail grinding, either preventive or corrective, is effective in RCF surface defects. Normally the potential rail breaks caused by RCF defects can be prevented by planned rail replacement, while, unfortunately, excluding pre-coating measures carried out in the beginning for protecting the rails from corrosion, no mature and reliable technique (by now) is available for detecting and remedying corrosion-related defects in the rails of Harmelen LCS. Visual inspection is the dominant inspection activity for identifying the debonding of elastic compound and rail corrosion defects; however, there are still some areas that are not visible and left undetected, especially the rail foot, which may lead to the instant breaks without any notice and in this case only immediate replacement (within 24 hours) can deal with it. It is therefore concluded that the essential maintenance interventions involved in maintaining the Harmelen LCS are grinding (mostly preventive) and replacement (preventive and corrective).

Appendix A presents minutes of four important interviews that were carried out in the research process, which facilitated the understanding about the system failure behaviors and the improved view of maintenance strategies with relevance to different stakeholders. The information with regard to the degradation mechanisms and maintenance policies of the Harmelen LCS collected from the interviews is organized and presented in Appendix B, overview inspection & maintenance for Harmelen LCS.

3. Model Development

The previous chapter described the dominant rail defects in the Harmelen LCS and maintenance interventions that are applied in practice. An approach to model the degradation process and predict the rail failures is addressed in this chapter. In accordance with the research framework (Figure 6), this chapter contains three parts: 1) model rail degradation; 2) incorporate the effect of maintenance interventions in the degradation modelling; 3) link the degradation and maintenance interventions to LCC analysis, which give answers to sub-questions 3, 4, and 5, respectively. The output of this chapter is an LCC model that integrates the uncertainties in rail degradation and maintenance strategies in cost estimation, which is considered as the main outcome of this research.

3.1 Starting point

Although the Harmelen LCS require less routine maintenance, its rail replacement cost is costly as the Corkelast® bonding materials need to be removed when rail replacement is carried out even if it is in good condition. Another reason is that rail breaks occurring in Harmelen LCS prompts a corrective replacement and partial rail replacement by welding is not possible (ProRail, 2010).

Rail replacement cost is considered as the most important cost contributor to the LCC of the Harmelen LCS. When rail breaks occur, it is not unreasonable to assume that the corrective rail replacement is more costly than the preventive replacement (Stapelberg, 2009, p. 378). For the preventive rail replacement, activities are planned for it to be carried out without unnecessary delays (Stapelberg, 2009, p. 378), while the corrective rail replacement is conducted after the unexpected failures have occurred and costs for repair may be higher due to emergency situations, possible safety issues and the economic impact on train availability.

Due to the substantial contribution to LCC, rail replacement strategies significantly influence the cost development of the Harmelen LCS in their lifecycle. As stated in Chapter 2, corrective replacement is conducted upon instant rail breaks, while the decision about performing the preventive replacement is more complicated, depending on situations and asset managers, which leads to a set of questions: how does preventive replacement decision influence the LCC of Harmelen LCS? Is it possible to determine an interval for preventively replacing the rails in Harmelen LCS in order to minimize the LCC of the systems and in the meanwhile the system reliability can be somewhat ensured? In this case, the *age replacement model* is considered.

The age replacement model, as a generic maintenance optimization model, has broad applicability for practitioners to set up a long-term asset planning due to its ease and ability to provide a quick estimate for optimized preventive replacement intervals (van den Boomen et al., 2018). In an age replacement model, *an asset is replaced preventively when it reaches a predefined replacement interval or correctively upon failure, whichever comes first* (Sánchez-Silva & Klutke, 2016, p. 282; van den Boomen et al., 2018). To be specific, as presented in Figure 22, preventive replacement (PR) is performed after an asset reaches a predefined operating time, t_p . In case of a failure, a corrective replacement (CR) is conducted and the next preventive replacement is scheduled after t_p units of time (Fernández & Márquez, 2012, p. 222).

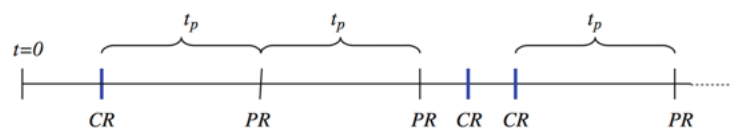


Figure 22 Replacement cycles: age-based replacement policy (Fernández & Márquez, 2012, p. 222)

Normally when applying the age replacement model, the focus is on one replacement cycle and assuming identical and repeating cycles to infinity (van den Boomen et al., 2018; van Noortwijk, 2003), as the replacement is a maintenance action that bring an asset back into its original condition or ‘good as new state’. When it is performed, the lifetime of the asset terminates and after each replacement the

cycle (in a statistical sense) starts all over again (van Noortwijk, 2003). In this case, it is defined that one lifecycle of the rails in Harmelen LCS begins with a replacement and ends with the next replacement.

The basic form of the fundamental age replacement model is as follows (Fernández & Márquez, 2012, p. 222; Jardine & Tsang, 2013, p. 51),

$$C(t_p) = \frac{\text{Total expected replacement cost over a cycle } [0, t_p]}{\text{Expected cycle length } E(L)} = \frac{C_p R(t_p) + C_c F(t_p)}{t_p R(t_p) + M(t_p) F(t_p)} \quad (1)$$

where

$C(t_p)$ = total expected replacement costs *per unit time* for interval $[0, t_p]$ [currency/unit time]

t_p = preventive replacement interval [unit time]

$R(t_p)$ = probability that the component/system is still surviving at least at time t_p

$F(t_p)$ = probability that a failure occurs before time t_p , which equals to $1 - R(t_p)$

C_p = preventive replacement cost [currency]

C_c = corrective replacement cost [currency]

$M(t_p)$ = expected length of the failure cycle/mean time to failure when preventive replacement takes place at age t_p [unit time]

As shown in the denominator of Eq.1, there are two possible cycles of operation, given a predefined preventive replacement interval t_p : 1) one cycle being determined by the component/system reaching predefined preventive replacement age (t_p), with a probability $R(t_p)$, in which the incurred cost is C_p ; 2) the other cycle being determined by the component/system ceasing to operate due to a failure occurring before t_p , with a probability $1 - R(t_p)$ or $F(t_p)$, in which the incurred cost is C_c and the cycle length is the expected failure cycle $M(t_p)$ (Jardine & Tsang, 2013, p. 51). $M(t_p)$ is estimated by calculating the expected value of the failure distribution (i.e., mean time to failure) truncated at t_p ⁸, given by (Fernández & Márquez, 2012, p. 222; Jardine & Tsang, 2013, p. 51),

$$M(t) = \int_0^{t_p} \frac{t f(t) dt}{F(t_p)} \quad (2)$$

where $f(t)$ = failure probability density function and $\int_0^t f(t) dt = F(t)$ ⁹

The age replacement model is aimed at determining the optimal preventive replacement interval t_p for one asset to minimize the total expected replacement costs per unit time $C(t_p)$. As it can be observed in Eq.1 and Eq.2, the optimization is made based on a tradeoff between preventive and corrective replacement cost, in consideration of the reliability condition of the asset, i.e., $R(t_p)$ and $F(t_p)$. It therefore leads to a question for the modelling: how can the reliability condition of the rails in the Harmelen LCS be evaluated?

⁸ The mean time to failure of a life distribution is calculated by $\int_0^{\infty} t f(t) dt$. The reason why a truncation is needed here refers to Jardine & Tsang (2013, p. 51).

⁹ See section 3.2.2 for more details.

3.2 Degradation modelling

Several papers, based on field data, has addressed that the prediction of occurrence of rail failure is governed by Weibull distribution (Caetano & Teixeira, 2015; Cannon et al., 2003; Esveld, 2001, p. 331; Liu, Lovett, Dick, Rapik Saat, & Barkan, 2014; Olofsson & Nilsson, 2002; Rahman & Chattopadhyay, 2010; Vandoorne & Gräbe, 2018; J. Zhao et al., 2006; J. Zhao, Chan, A. H. C., & Stirling, A. B., 2006), while note that the Weibull law is found in the conventional ballasted tracks. The research focuses on the rail level crossings with the special track structure, embedded rail system. Compared to the normal track lines, the LCS is more open and interactive: the rail failure in the LCS may be influenced by road vehicles and some other external factors. For instance, road traffic may deposit small stones around the rails and trains may take them away into small defects on the rail running surface, developing into squats or other surface defects. Besides, limited literature has been found that analyzes the degradation of the embedded rail structure. It is unknown whether the Weibull distribution model is applicable for the Harmelen LCS. Therefore, following the basic procedure of reliability analysis, the model starts with ‘looking’ at the data: gathering failure data from a sample¹⁰ of the Harmelen LCS.

3.2.1 Failure data gathering (step 1)

Sources of failure data are generally either field data reflecting the normal use of a component/system or failures observed from reliability testing (Ebeling, 2005, p. 306). This research only considers field data, which reflects the actual operating environment of the Harmelen LCS. There may be two forms of failure data, namely exact times of failures and interval data¹¹. The interval data originates from the situation where the exact failure times of one system cannot be observed and only an interval (where failures occurred) is observed and recorded.

Two dominant failure modes are involved in the Harmelen LCS, corrosion and RCF. Both are contributors to rail breakage. Each mode of failure may have different degradation patterns (i.e., follow different life distributions or different parameter values for the same life distribution) so that when gathering the failure data, it is desirable to separate the data based on the failure modes.

3.2.2 Reliability model selection (step 2)

The second step is to select a model from a set of reliability model candidates which fits the given dataset. Basic reliability models are life distributions and stochastic process models.

- Overview of reliability models

In the case of non-repairable systems, every failure leads to a replacement of the failed systems by a new one and only the time to first failure is of interest (Blischke & Murthy, 2000, p. 93). Therefore, an important measure of the reliability for this kind of systems are *time to failure*, which is treated as a random variable, evaluated by various life distributions. The definition of the life distribution model refers to note 3. The theoretical distributions¹² that are widely used in the reliability engineering are for

¹⁰ Sample in statistics is defined as *a subset of data taken from a population* (Tobias & Trindade, 2011, p. 2). Population is defined as *the entire set of measurements of interest* (Tobias & Trindade, 2011, p. 1). For example, the population in this research considers all possible failure times of the Harmelen LCS used in the Dutch national railway network (owned by ProRail), while the sample can be the failure times of 20 Harmelen LCS that have been observed in practice. The objective of the reliability analysis in this research is to extract useful information from a sample and make inferences about the population, i.e., evaluate the reliability of the population, in which the nature is inferential statistics, comparable to descriptive statistics.

¹¹ Further illustration of types of reliability data refers to Tobias & Trindade (2011, p. 41).

¹² Probability distributions fall into two categories: continuous or discrete. The examples listed are continuous. Continuous probability distributions are extensively used to model the time to failure of non-repairable systems.

example exponential distribution, Weibull distribution, normal and lognormal distribution, etc. The working assumption in such distribution models is that the *time to failure is sample of independent and identically distributed (i.i.d.) observations from a population* (Tobias & Trindade, 2011, p. 417). In this case, the sample data in regard to the rail failure times, e.g., collected from 20 Harmelen LCS (as stated in note 10), does not have a trend or occurrence order of failures (*independent*) and follows the same probability distribution (*identically distributed*). With the i.i.d. assumption, the individual failure times can be combined and analyzed by the lifetime distributions.

When a repairable system fails, it can be either repaired or replaced and restored to the satisfactory operation. The analysis of time to first failure is not enough and attention should be paid to subsequent failures, as the subsequent failures depend on the type of actions taken for rectifying the previous failures (Blischke & Murthy, 2000, p. 169), and there may be a trend (dependency) in the failure times data. In this sense, the life distribution models are not applicable (given the *i.i.d.* assumption) for modelling the failure times of the repairable systems, except for special cases like *renewal process* (see next paragraph) (Tobias & Trindade, 2011, p. 417). An important measure of the reliability for repairable systems is the cumulative number of failures occurring in the system by time t (normally denoted as $N(t)$), which is considered as a random variable, evaluated by stochastic process¹³ models (Tobias & Trindade, 2011, p. 419). A *counting process* is a stochastic process $\{N(t), t \geq 0\}$ with values that are integer and non-decreasing, normally used to model the total number of events (like failures), $N(t)$, that have occurred until time t (Blischke & Murthy, 2000, p. 738). The commonly used stochastic counting processes in reliability analysis are for example Homogeneous Poisson Process (HPP), Non-homogeneous Poisson Process (NHPP) (see note 2), etc.

A renewal process would be expected if repair could restore the system to ‘as good as new’ condition, for instance, for one single-component system, the failed component is replaced by a new one from the same population (Tobias & Trindade, 2011, p. 418). Here the arguments on ‘replaced by a new one’ and ‘from the same population’ implicitly and respectively address the original and replaced items fail *independently* and follow the *common distribution*, which means the i.i.d. assumption retains in the renewal process. The HPP holds if a renewal process is exponentially distributed (i.e., failure times are independent and follow the exponential distribution) (Tobias & Trindade, 2011, p. 441). The renewal process is actually the generalization of HPP: the former allows the distribution to be arbitrary and not necessarily to be the exponential distribution.

For a multi-component system, however, renewal process may not be assured, as the replacement of one item does not influence the other items of the system and the system may not return to the ‘like new’ condition. In this case, the frequency of failures in one system may increase or decrease with age (a trend). An increased trend implies the degradation and a decrease indicates an improvement of the system over time. The renewal process which assumes no trend in the failure data may become invalid. And the NHPP would be recommended to model the trend in the frequency of failures.

As the renewal process and life distributions have the same assumption (i.i.d.), some theoretical simplifications are possible under the renewal process: the life distribution models are applicable to characterize the *independent* time between failures (Tobias & Trindade, 2011, p. 418) and some analysis procedures of the life distribution models are also applicable. It is noted however this simplification is only valid under the assumption of renewal process.

The failure times are also called lifetime of the systems so that the life distribution models normally refer to lifetime distributions or failure distributions.

¹³ The *stochastic process* is defined as *a collection of random variables that describes the evolution in time of a process* (Tobias & Trindade, 2011, p. 419).

Based on the features of rail degradation and interventions, it is observed that the Harmelen LCS are non-repairable systems and for modelling the rail failures in the Harmelen LCS the time to failure is of great importance. There are two ways to analyze the time to failure data (Ebeling, 2005, p. 388): parametric method and non-parametric (empirical) method. The first method is to fit a theoretical distribution (e.g., Weibull, exponential, normal, lognormal distribution, etc.) to failure data; the second is to derive a (empirical) distribution directly from the failure data (Ebeling, 2005, p. 388). Generally it is preferred to use the first approach, as the empirical distribution is derived based on sample data and the small sample size may provide limited information regarding the failure process, while if the sample is connected to a theoretical distribution and proves that the distribution model fits well to the data, much stronger results, which may be beyond the range of the sample data, based on the properties of the theoretical distributions are expected (Ebeling, 2005, p. 389; Meeker & Escobar, 2014, p. 21). Therefore the first approach is adopted in this research.

- *Basics of life distribution & Weibull distribution*

Five basic mathematical forms are generally used to represent one life distribution and describe the reliability of a system: the *cumulative distribution function* (CDF, denoted as $F(t)$), the *reliability function* (or *survival function*, denoted as $R(t)$), the *probability distribution function* (PDF, denoted as $f(t)$), the *hazard rate* (or *failure rate*, denoted as $h(t)$), and the *cumulative hazard function* (denoted as $H(t)$) (Ebeling, 2005, p. 23; Tobias & Trindade, 2011, p. 29).

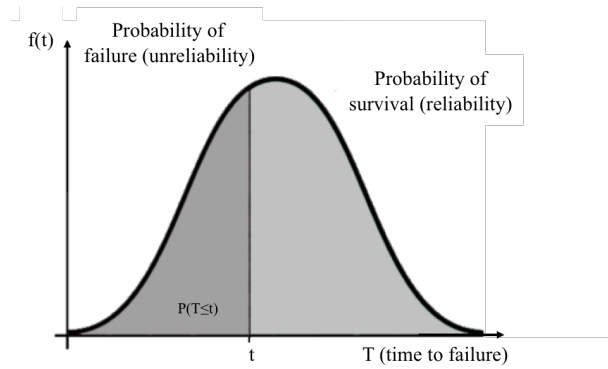


Figure 23 Relation between $f(t)$, $F(t)$ and $R(t)$

To express the above functions mathematically, define a continuous random variable T , evaluated at t , as *time to failure* of a population. Then CDF $F(t)$ can be expressed as (Ebeling, 2005, p. 23),

$$F(t) = P(T \leq t) \quad (3)$$

Eq.3 can be interpreted as CDF $F(t)$ is *the probability that a failure occurs before time t* (Ebeling, 2005, p. 24). In this text, the CDF represents the probability that a rail failure (break) occurs in the Harmelen LCS before time t .

PDF $f(t)$ is the derivative of $F(t)$ and $R(t)$ represents the probability that a system is still surviving at least at time t (Tobias & Trindade, 2011, p. 30) or would not fail before it reaches time t (Blischke & Murthy, 2000, p. 96). Figure 23 presents an arbitrary PDF graph. Pictorially, the CDF is the area under the PDF to the left of time t , as shown in the dark grey region of Figure 23. The probability of failure approaches one when the time t reaches infinity and the total area under the PDF is unity. The light grey area indicates the probability of survival $R(t)$ and the sum of $F(t)$ and $R(t)$ is unity.

The hazard rate, $h(t)$, represents the *conditional probability* of a failure in the time interval from t to $t + \Delta t$, given the system has survived to time t (Ebeling, 2005, p. 29). Let Δt approach zero, $h(t)$ can be expressed as follows.

$$h(t) = \frac{F(t+\Delta t) - F(t)}{R(t)} = \frac{f(t)}{R(t)} \quad (4)$$

The hazard rate is a fundamental quantity for reliability analysis (Elmahdy, 2015) and the well-known *Bathtub curve*¹⁴ is plotted based on the appearance of the hazard rate. Like the PDF $f(t)$ can be integrated to obtain the CDF $F(t)$, the hazard rate $h(t)$ can be integrated to the cumulative hazard function $H(t)$ (Tobias & Trindade, 2011, p. 33). The cumulative hazard can be interpreted as the (mathematically) expected number of failures that would be observed over a given period (Cleves, Gould, Gould, Gutierrez, & Marchenko, 2008, p. 13).

At first the 2-parameter Weibull distribution is selected as its hazard rate (Eq.4) has been used by many researchers to model and predict the rail failures in the ballasted tracks and has proven to be a successful model for many failure mechanisms of infrastructure assets. As one of the most useful distribution model for reliability analysis, its strength lies in its flexible shape to fit different types of failure data (Tobias & Trindade, 2011, pp. 87, 90).

The relevant functions of the 2-parameter Weibull distribution are expressed as follows¹⁵ (Tobias & Trindade, 2011, pp. 87, 88), and with any one of them, all of the other functions can be derived.

$$\text{Hazard function: } h(t) = \frac{\beta}{\alpha} \left(\frac{t}{\alpha}\right)^{\beta-1} \quad (5)$$

$$\text{Cumulative hazard function: } H(t) = \left(\frac{t}{\alpha}\right)^{\beta} \quad (6)$$

$$\text{Probability density function: } f(t) = \frac{\beta}{\alpha} \left(\frac{t}{\alpha}\right)^{\beta-1} e^{-\left(\frac{t}{\alpha}\right)^{\beta}} = h(t) \cdot e^{-H(t)} \quad (7)$$

$$\text{Cumulative distribution function: } F(t) = 1 - e^{-\left(\frac{t}{\alpha}\right)^{\beta}} = 1 - e^{-H(t)} \quad (8.1)$$

$$\text{Reliability function: } R(t) = e^{-\left(\frac{t}{\alpha}\right)^{\beta}} = e^{-H(t)} \quad (9)$$

in which the parameter α is a *scale parameter*, known as the *characteristic life*¹⁶ and the parameter β is a *shape parameter*. Both α and β must be larger than zero (Tobias & Trindade, 2011, p. 88).

- *Probability plotting (least squares fit)*

Probability plotting is a method to graphically analyze the failure data. It allows checking the applicability of the assumed distribution model and a side benefit is to provide estimates of parameters of the distribution being fitted from the plots (Blischke & Murthy, 2000, p. 376; Tobias & Trindade, 2011, p. 153). The underlying technique for the probability plotting is *least squares fit* (or often called *regression analysis* (Draper & Smith, 1998, p. 17))¹⁷. As shown in Figure 24, assume in a given set of data points (indicated by dots), y is a dependent variable (or prediction variable) and x is an independent variable (or predictor variable). There is a relation between x and y and it is expected to predict the value of y given the value of x . The least squares fit strives for a 'best fit' line for the given dataset,

¹⁴ Details about the Bathtub curve refer to Tobias & Trindade (2011, p. 36) and Ebeling (2005, p. 31).

¹⁵ There is no consistent convention in the literature to represent relative functions of the Weibull distribution and name the Weibull parameters. The Weibull equations here refer to Tobias & Trindade (2011, p. 88).

¹⁶ A distinction should be made between *characteristic life* and *mean life*. The former fixes the 63.2 percentile of CDF, i.e., $F(t = \alpha) = 0.632$, in which the point is called *characteristic life point* (Tobias & Trindade, 2011, p. 92). The mean life is known as the *mean time to failure* or MTTF for non-repairable systems, see note 8 about the equation for calculating mean time to failure.

¹⁷ Basics of LS fit refer to Tobias & Trindade (2011, p. 155). The LS technique falls into two categories: linear or non-linear LS. The thesis directly goes to one of the applications of LS fit: probability plotting, which is the application of the first type.

where the sum of the squares of the deviations of the predicted y values from the actual observed y values is a minimum (Tobias & Trindade, 2011, p. 155). This best fit line is called a LS or regression line (Tobias & Trindade, 2011, p. 155).

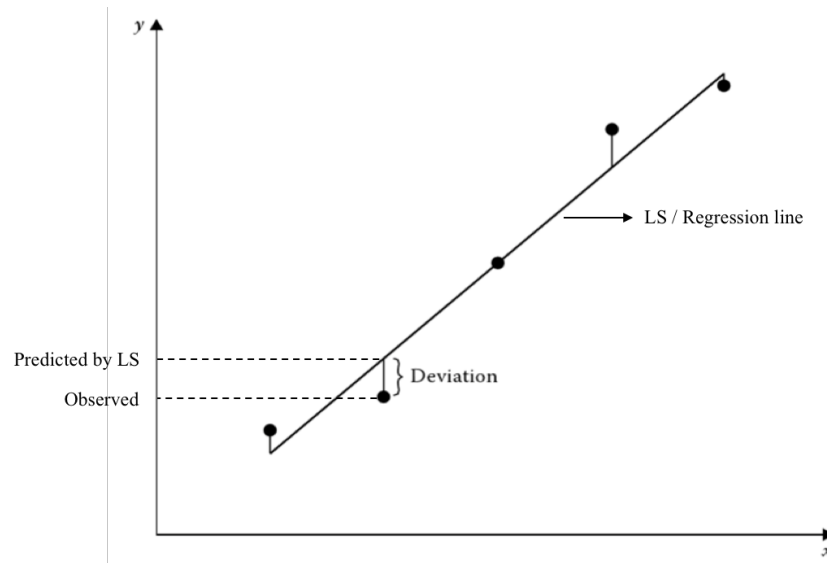


Figure 24 Example of regression line (adapted from Tobias & Trindade (2011, p. 155))

The principle of the probability plotting is to rectify the failure data (time to failure t_i and CDF $\hat{F}(t_i)$, where $i = 1, 2, \dots, n$) in such a way that plotted points (CDF estimates versus time to failure) can approximately fall on a straight line, if an assumed distribution fits the data (Tobias & Trindade, 2011, p. 161). The CDF $\hat{F}(t_i)$ is empirical or distribution free, as no distribution is assumed and it holds for any life distribution (Tobias & Trindade, 2011, p. 163). The rectification is called *linear rectification*, which varies depending on the selection of life distributions. Based on the transformed data points, a nonlinear plot is an indication that given the sample dataset the assumption regarding the distribution is incorrect and other distributions may be tried (Blischke & Murthy, 2000, p. 378).

The probability plotting is actually an alternative graphical plotting to analyzing the failure data, other plots like hazard plots are also applicable (Blischke & Murthy, 2000, p. 382), while the former is the most widely applied method. Their difference lies in the rectification of different mathematical forms: the former linearizes the CDF of the selected distribution (e.g., Eq.8.1), while the latter, as the term implies, rectifies the hazard function (e.g., Eq.5).

To transform the Weibull CDF, rewrite Eq.8.1 in such a way that

$$1 - F(t) = e^{-\left(\frac{t}{a}\right)^\beta} \quad (8.2)$$

Take natural logarithms of both sides twice and get,

$$\ln\{-\ln[1 - F(t)]\} = \beta \ln t - \beta \ln a \quad (10)$$

$$Y = \beta X + b \quad (11)$$

Eq.10 is the linear rectification form of the 2-parameter Weibull distribution, comparable to the form of a straight line¹⁸ (Eq.11). If the Weibull distribution holds, the plot of $\ln\{-\ln[1 - F(t)]\}$ on a linear

¹⁸ Eq.11 presents an alternative expression for a straight line, in which b is called the intercept of a straight line, which can be obtained by setting x equal to zero, then $Y = b$.

y-axis versus $\ln t$ on a linear x-axis should result in data points that approximately fall on a straight line with slope β and intercept b (i.e., $-\beta \ln \alpha$) (Tobias & Trindade, 2011, pp. 110,175). The Weibull shape parameter is estimated directly from the slope of the LS. The value of the scale parameter α is estimated by $e^{\left(-\frac{\text{intercept}}{\beta}\right)}$, derived from the slope and intercept of the LS.

One of the main tasks in probability plotting is to estimate $Y (= \ln\{-\ln[1 - \hat{F}(t)]\})$, where $\hat{F}(t)$ has to be estimated. For different types of failure data, exact failure times or interval data, the methods to derive $\hat{F}(t)$ are different. Normally *median rank estimate* is used for exact failure times (Tobias & Trindade, 2011, p. 163) and *binomial estimate* is used for interval data (Tobias & Trindade, 2011, p. 171)¹⁹.

The concept of median rank estimates is based on *ordered statistics* (Tobias & Trindade, 2011, p. 163). The *ordered* sample of failure times is obtained by arranging the times to failure in ascending order, which can be represented by t_1, t_2, \dots, t_n , where t_i indicates the time to the i^{th} failure and $t_i \leq t_{i-1}$. t_1 is the *first-order statistic* and t_2 is the *second-order statistic* and so on. As time to the i^{th} (ordered) failure varies from sample to sample, each order statistic has its own distribution (denoted as CDF $F_i(t)$). The median of t_i (time to the i^{th} failure), which makes its own CDF $F_i(t)$ equal to 0.5, is called a *median rank*, denoted as $\hat{F}_{M_i}(t)$ ²⁰ (Tobias & Trindade, 2011, p. 164). The median rank at the i^{th} failure is a good property for representing its CDF $F_i(t)$. The median position of each order statistic is a function of both the order (i^{th}) and sample size (denoted as n_1), which has to be computed numerically (Ebeling, 2005, p. 309). In this case, an approximation of the median rank is often used (Benard & Bos-Levenbach, 1955),

$$\hat{F}_{M_i}(t) \cong \frac{i-0.3}{n_1+0.4} \quad i = 1,2,3, \dots \quad (12)$$

where n_1 = the sample size (the number of failure times that are observed).

The method for estimating CDF $\hat{F}(t)$ for interval (grouped) data refers to Tobias & Trindade (2011, p.171). Like the estimation of CDF for the exact failure time data, the sample of failure times needs to be sorted to ascending magnitude. Let T_i ($i = 1,2,3 \dots$) denote a *fixed* time interval and d_i be the number of failures in the i^{th} interval, i.e., (T_{i-1}, T_i) . The CDF at the k^{th} interval is estimated by (Tobias & Trindade, 2011, p. 171),

$$\hat{F}(T_k) = \frac{\sum_{i=1}^k d_i}{n_2} \quad i = 1,2,3, \dots \quad (13)$$

where n_2 = the sample size (the number of failure times in the interval data); $\sum_{i=1}^k d_i$ denotes the cumulative failure times at the k^{th} interval. The CDF $\hat{F}(t)$ for the interval data is estimated at the end of each interval by the cumulative failure times divided by the total number of failure times – binomial

¹⁹ Alternative estimators for $\hat{F}(t)$ refer to Ebeling (2005, pp. 308, 309) and Tobias & Trindade (2011, p. 163).

²⁰ Distinctions among $\hat{F}(t)$, $F_i(t)$ and $\hat{F}_{M_i}(t)$: the first is an empirical CDF derived from sample data (as stated in note 17). In the probability plotting it is used to test the model fit. $F_i(t)$ is the CDF of i^{th} ordered time to failure, which is unknown and varies from sample to sample. $\hat{F}_{M_i}(t)$ is a point which fixes $F_i(t)$ equal to 0.5. The idea is using $F_i(t)$ (ordered statistics) to represent $\hat{F}(t)$. As the median rank estimate $\hat{F}_{M_i}(t)$ is a good indicator to represent the property of $F_i(t)$, $\hat{F}_{M_i}(t)$ in this case is used to estimate $\hat{F}(t)$. When the $\hat{F}(t)$ is derived, substitute it in the linear rectification formula (Eq.10) and plot the transformed data points to observe whether the plot appears to be linear.

estimate. Both the median rank estimate and binomial estimate are based on the theory of ordered statistics.

After deriving the CDFs for exact times of failure (Eq.12) and interval data (Eq.13), the data points ($\ln t, \ln\{-\ln[1 - F(t)]\}$) can be plotted and the model fit can be evaluated visually (based on whether the plot appears to be linear).

Apart from the visual test, regression statistics can provide numeric assessment and relatively reliable evidence on the model fit, in which one of the measures, R-squared value (or the *coefficient of determination*), is used in the research, as it can be derived directly from the regression analysis and is useful to compare the fit of competing distribution models. The R-squared value, denoted as R^2 , is calculated as follows (Elmahdy, 2015),

$$R^2 = 1 - \frac{SS_{res}}{SS_{tot}} \quad (14)$$

where

$$SS_{res} = \text{sum of squares of residuals}^{21} = \sum_j (y_j - \hat{y}_j)^2$$

$$SS_{tot} = \text{total sum of squares (measure of deviations of the observations around the overall mean)} \\ = \sum_j (y_j - \bar{y})^2$$

y_j = observed value of the dependent variable

\hat{y}_j = predicted value of the dependent variable by the regression line

$$\bar{y} = \text{mean of the observed data} = \frac{\sum_{j=1}^n y_j}{n} \quad (\text{n is the sample size})$$

As noted before, there would be some deviations of the y values predicted by the regression line from the actual observed y values. The coefficient of determination *gives the percentage of the variation in the dependent variable (Y) that is explained by the regression line* (Wilson, Keating, Beal-Hodges, & Business Expert, 2012, p. 50) and, therefore, it evaluates the explanatory or predictive power of the model (Blischke & Murthy, 2000, p. 417; Wilson et al., 2012, p. 49). The coefficient of determination is an index number, ranging from zero to one, which is unit free: if $R^2=1$, the best possible regression model which explains all of the variations in the dependent variable around its mean is expected; if $R^2=0$, the model cannot explain any variation in the dependent variable around its mean (Wilson et al., 2012, p. 50).

Provided that the Weibull distribution is a reasonable fit to the given dataset based on the probability plotting, the next step is to determine the statistical properties of the model – parameter estimation.

3.2.3 Parameter estimation (step 3)

Although the least squares (LS) fit is able to provide quick estimates of parameters for the fitted model, another approach, *maximum likelihood estimation* (MLE), is applied in this research to provide more accurate parameter estimates, which is the recommended method for estimating Weibull parameters in most reliability analysis references (e.g., (Ebeling, 2005, pp. 409, 427; Tobias & Trindade, 2011, p. 98). The LS estimates will be used as starting guess of the shape and scale parameters for Weibull MLE.

Given a dataset, MLE attempts to find the parameter values that maximize the *likelihood (LIK) function*. A loose but useful definition of the LIK function is *a product containing the data points (sample) and*

²¹ Sometimes called residual sum of squares; the term ‘residual’ implies the deviation of the value, for each data point, predicted by the regression line from the actual observed value (Draper & Smith, 1998, p. 29).

unknown parameters (Tobias & Trindade, 2011, p. 99). The LIK function differs depending on the type of failure data.

- *Exact failure times*

The observations that have exact failure times (t_i) contribute to the form $f(t_i)$ to the LIK function. In this case, the LIK is written by multiplying the PDF $f(t_i)$ evaluated at each data point, considering n times of failures are observed, as presented in Eq.15 (Tobias & Trindade, 2011, p. 101).

$$\text{LIK}(\alpha, \beta) = \prod_{i=1}^n f(t_i) = \prod_{i=1}^n \frac{\beta}{t_i} \left(\frac{t_i}{\alpha}\right)^{\beta} e^{-\left(\frac{t_i}{\alpha}\right)^{\beta}} \quad (15)$$

where

n = the total number of exact failures
 $f(t_i)$ = Weibull PDF at time t_i (Eq.7)

- *Interval data*

The observations that indicate one component/system failed somewhere in an interval, say $(T_{i-start}, T_{i-end})$, contribute a term of the form $[F(T_{i-end}) - F(T_{i-start})]$ in the LIK equation. The term, $F(T_{i-end}) - F(T_{i-start})$, can be interpreted as the probability that the component/system survives to time $T_{i-start}$ but fails before time $F(T_{i-end})$. In this case, the LIK for the interval $(T_{i-start}, T_{i-end})$ is written as follows.

$$\text{LIK}(\alpha, \beta) = \prod_{i=1}^r [F(t_{i-end}) - F(t_{i-start})] = \prod_{i=1}^r \left\{ \left[1 - e^{-\left(\frac{t_{i-end}}{\alpha}\right)^{\beta}} \right] - \left[1 - e^{-\left(\frac{t_{i-start}}{\alpha}\right)^{\beta}} \right] \right\} \quad (16)$$

where

r = the number of failures in an interval $(T_{i-start}, T_{i-end})$
 $F(t)$ = Weibull CDF at time t (Eq.8.1)

To obtain the ‘most likely’ values that maximize the LIK function, the standard way is to take partial derivatives regarding each parameter, set them as zero and finally yield the equations to obtain MLEs (Tobias & Trindade, 2011, p. 99). However, considering the complexity of the LIK functions, a simplified way (also commonly used) is to firstly take natural logarithm of the LIK function (log likelihood), take partial derivatives of the negative log LIK and finally solve for a minimum (Tobias & Trindade, 2011, p. 99). The parameter values that minimize the negative log likelihood also maximize the LIK function.

Follow the idea of the simplified method, take natural logarithms to Eq.15 and obtain log LIK,

$$\ln(\text{LIK}) = n \cdot \ln\beta - n\beta \cdot \ln\alpha + \sum_{i=1}^n [(\beta - 1) \cdot \ln t_i] - \sum_{i=1}^n \left(\frac{t_i}{\alpha}\right)^{\beta} \quad (17)$$

Apply natural logarithms to Eq.16 and get,

$$\ln(\text{LIK}) = r \cdot \ln \left\{ \left[1 - e^{-\left(\frac{t_{i-end}}{\alpha}\right)^{\beta}} \right] - \left[1 - e^{-\left(\frac{t_{i-start}}{\alpha}\right)^{\beta}} \right] \right\} \quad (18)$$

The Weibull MLE must be computed numerically (Ebeling, 2005, p. 409) so that in this chapter only the LIK and log LIK functions for exact failure times and interval data are derived. The next chapter will demonstrate the application of Weibull MLE in Microsoft Excel.

3.3 Effect of maintenance interventions

3.3.1 Impact of grinding (step 4)

As stated above, rail grinding is an effective tool to remove shallow cracks produced by RCF and control the development of the small cracks into significant defects (Cannon et al., 2003). Preventive grinding is able to eliminate the accumulated rail degradation, which can be considered as a periodic lifetime-extending maintenance and its impact on controlling RCF defects cannot be ignored.

There are several researchers who have modelled the impact of rail grinding on the occurrence and propagation of rail RCF defects. For instance, Rahman & Chattopadhyay (2010) included the impact of grinding on RCF by an age reduction factor: there is an effective age reduction after undertaking a rail grinding and the hazard rate continues to be a function of the effective age (adjusted time t) (Coria et al., 2015; Rahman & Chattopadhyay, 2010). Zhao et al. (2006) considered the effect of rail grinding on RCF by failure rate reduction, i.e., multiplying the original hazard rate of RCF defects (without grinding) by a reduction factor. The drawbacks of these models however are the adjustment factors are determined by subjective opinions. It is hard to make decisions about these unknown reduction factors (Coria et al., 2015) and it provides limited insight into the interaction among maintenance decisions (grinding interval) and degradation.

Coria et al. (2015) proposed a PM optimization model with a more general relation between the PM interval and hazard function. The adjusted hazard function (which includes the impact of PM) is formulated as a function of the current PM interval T_0 and optimal PM interval T^* (Coria et al., 2015). The PM considered in this model is periodic PM policy (TPM). It considers the current interval has already influenced the system failure behaviors (reflected in the failure data) and optimal PM interval is a PM decision variable, to be optimized from the cost perspective. It was found the model is suitable for modelling the impact of preventive grinding operations on rail degradation, as it introduces the PM intervals in the modelling and creates a basis for evaluating the impact of the grinding decision variable (interval) on the rail degradation (and, in turn, the LCC).

Assume that the grinding is performed at fixed intervals T_{pm} (T_{pm} = grinding interval) and the time of the k^{th} grinding is $t_k = kT_{pm}$, $k=1, 2, \dots, N$, where N is the number of rail grinding within one replacement cycle T and $t_{N+1}=T$. Suppose that the hazard rate of RCF-initiated failures is $\lambda_k(t)$ at time t after the k^{th} rail grinding, where $0 \leq t < T_{pm}$. As stated in section 3.2.2, the integration of hazard function, i.e., cumulative hazard function, in a mathematical sense can be interpreted as the expected number of failures for a given time. Therefore, here, for one replacement cycle ($T = N \cdot T_{pm}$), the expected number of failures is given by (Coria et al., 2015),

$$E(N(T)) = \sum_{k=1}^N \int_0^{T_{pm}} \lambda_k(t) dt \quad (19)$$

According to Coria et al. (2015), the following equation holds,

$$\sum_{k=1}^N \int_0^{T_{pm}} \lambda_k(t) dt = \int_0^T h(t, T_{pm}) dt \quad (20)$$

which implies that the area under both functions, i.e., the original hazard rate at time t after the k^{th} grinding $\lambda_k(t)$ and the adjusted hazard rate $h(t, T_{pm})$, defines the same expected number of fatigue failures for one replacement cycle T , as visualized in Figure 25. The adjusted hazard rate (including the grinding impact) smooths the original function by using the grinding interval T_{pm} as one parameter, i.e., $h(t, T_{pm})$.

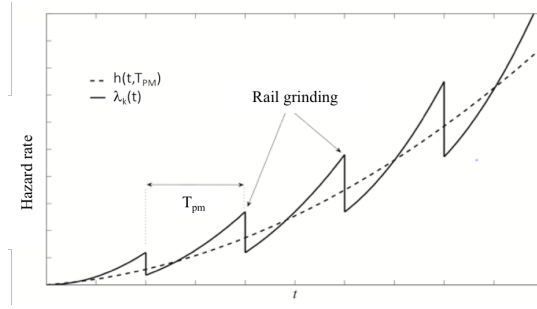


Figure 25 Comparison of the (real) hazard rate and adjusted hazard rate (adapted from (Coria et al., 2015))

Recall the Weibull hazard function in Eq.5, where β influences the shape of the hazard rate (the value of β determines what type of failures is being modelled, e.g., the hazard rate is increasing when $\beta > 1$, which is used for modelling wear-out failures) and α is a scale parameter which shrinks or stretches the hazard function to describe the level of aging (when $\beta > 1$) (Coria et al., 2015). Besides, as stated above, α represents the characteristic life of a population, which means approximately 63.2% of the population fails by the characteristic life point (see note 16). The grinding can be considered as a life-extending measure and its impact can be reflected in the extended characteristic life.

According to Coria et al. (2015), the hazard rate can be a function of grinding interval, T_{pm} , only through the scale parameter, α . When grinding frequency is increased (reduced T_{pm}), its impact on the time of RCF-initiated rail failure can be reflected in a stretched appearance of the hazard rate, i.e., an increased α parameter and a reduced hazard rate, and vice versa. Therefore, α can be expressed as a function of T_{pm} , i.e., $\alpha(T_{pm})$. The function must satisfy the following boundary conditions (Coria et al., 2015):

- There is an inverse relationship between T_{pm} and α ;
- When the system is not maintained, $\alpha = \alpha_\infty$;
- When $T_{pm} \rightarrow 0$, $\alpha(T_{pm}) \rightarrow +\infty$, i.e., the system is continuously maintained and no failure occurs.

To satisfy the above conditions, Coria et al. (2015) proposed a function $\alpha(T_{pm})$, which is expressed as,

$$\alpha(T_{pm}) = \alpha_\infty + \frac{\gamma}{T_{pm}}, \text{ with } \gamma > 0 \quad (21)$$

To estimate the parameters α_∞ and γ , an important assumption in this function is $\alpha_\infty \ll \frac{\gamma}{T_0}$, where T_0 is the current grinding interval. As the current grinding interval is determined based on long-term experience and expert opinions, it is reasonable to expect that compared to not performing any maintenance actions, the rail will degrade much slower and the RCF-initiated failures are less likely to occur with the current grinding policy. Therefore, the term α_∞ can be neglected and it follows that (Coria et al., 2015),

$$\alpha(T_{pm}) = \frac{\gamma}{T_{pm}} \quad (22)$$

Note that the current grinding interval T_0 has affected the times of RCF-initiated rail breaks: the α is estimated by MLE (section 3.2.3), where the grinding interval is T_0 . Therefore, the parameter γ can be estimated from Eq.22 in the form $\gamma = \alpha T_0$.

Substitute γ into Eq.22 and obtain,

$$\alpha(T_{PM}) = \frac{\gamma}{T_{pm}} = \alpha \cdot \frac{T_0}{T_{pm}} \quad (23)$$

Substitute the scale parameter (Eq.23) into the original hazard rate (Eq.5) and obtain the adjusted hazard rate as,

$$h(t, T_{pm}) = \left(\frac{T_{pm}}{T_0}\right)^\beta \frac{\beta}{\alpha} \left(\frac{t}{\alpha}\right)^{\beta-1} \quad (24)$$

where T_0 = current grinding interval; T_{pm} = grinding interval variable to be optimized.

Considering the dominant failure modes of the rails in Harmelen LCS, the grinding can only control the surface RCF defects and the adjustment is made on the hazard rate of rail failures caused by the surface RCF defects, like squats.

3.3.2 Reliability evaluation (step 5)

Given the answer to the first sub-question: both corrosion and fatigue take place and contribute to the rail failure in the Harmelen LCS. In this case, they can be interpreted as the *competing risk*, which occurs when *a population has several failure modes and the entire population is at risk from either failure mode* (Elmahdy, 2015). To estimate the probability of failure for the component with two (or more) failure modes, the *series system model* is applicable, in which an important notion, is: *a single component with several independent failure modes is analogous to a system with several independent components* (Tobias & Trindade, 2011, p. 346). The application of the *series system model* in this case is called *the competing risk model* (Tobias & Trindade, 2011, p. 346).

Follow the series system probability argument, the system hazard rate is calculated as follow (Tobias & Trindade, 2011, p. 346),

$$h_s(t) = \sum_{i=1}^n h_i(t) = h_1(t) + h_2(t) + \dots + h_n(t) \quad (25)$$

where $h_i(t)$ = hazard rate of failure caused by i^{th} failure mode; n = the number of failure modes that are of interest.

Recall the hazard rate of the corrosion-initiated failure (Eq.5) and the adjusted hazard rate (account for grinding) of RCF surface defects (Eq.24), the total hazard rate of the rails in the Harmelen LCS is expressed as,

$$h_s(t) = h_1(t) + h_2(t) = \frac{\beta_1}{\alpha_1} \left(\frac{t}{\alpha_1}\right)^{\beta_1-1} + \left(\frac{T_{pm}}{T_0}\right)^\beta \frac{\beta_2}{\alpha_2} \left(\frac{t}{\alpha_2}\right)^{\beta_2-1} \quad (26)$$

Integrate the total hazard rate, $h_s(t)$, to the cumulative hazard function and follow Eq.7, Eq.8.1, Eq.9, the total CDF, PDF, and reliability function can be derived.

3.4 Integration

3.4.1 Extension of age replacement model (step 6)

Recall that the age replacement model searches for the economic optimum of a preventive replacement interval, given the reliability condition of the assets and replacement costs (preventive & corrective), which is obtained by minimizing the cost function $C(t_p)$ (Eq.1). The fundamental age replacement model only considers a tradeoff between corrective and preventive replacement costs. The expenditures used at the operation stage for routine maintenance directed at lifetime extension/risk reduction, e.g., the preventive grinding, is not considered, while it influences the rail reliability and failure cycle length. Besides, from the cost point of view, it is unknown whether and how the operating cost (the sum of grinding and inspection cost in this case) influences the LCC of the systems. Therefore an extended age replacement model that allows for the inclusion of the operating cost (see Eq. 27 the cost elements)

needs to be developed. Here the operating cost incurred in a preventive replacement interval $[0, t_p]$, denoted as $C_o(t_p)$, is calculated as²²,

$$C_o(t_p) = \text{preventive grinding cost} + \text{inspection cost} = C_{pm} \cdot \left\lfloor \frac{t_p}{T_{pm}} \right\rfloor + C_i \cdot \left\lfloor \frac{t_p}{T_i} \right\rfloor \quad (27)$$

where

C_{pm} = cost of one-time preventive grinding operation [currency]

T_{pm} = grinding interval [unit time]

t_p = preventive replacement interval [unit time]

C_i = cost of one-time inspection activity [currency]

T_i = inspection interval [unit time]

As stated in section 3.1, there are two possible cycles of operation in the fundamental age replacement model: one preventive cycle length with a probability $R(t_p)$ and one corrective cycle length with a probability $1 - R(t_p)$ or $F(t_p)$. Pictorially, recall Figure 23 and define the time t as the preventive replacement interval t_p , as depicted in Figure 26: under the age replacement policy (one asset is either preventively replaced when it reaches the age t_p or correctly replaced upon failure), the probability of preventive cycle is equivalent to the probability that a failure occurs after time t_p (the shaded area) and the probability of corrective cycle is determined by the probability that a failure occurs before time t_p (the unshaded).

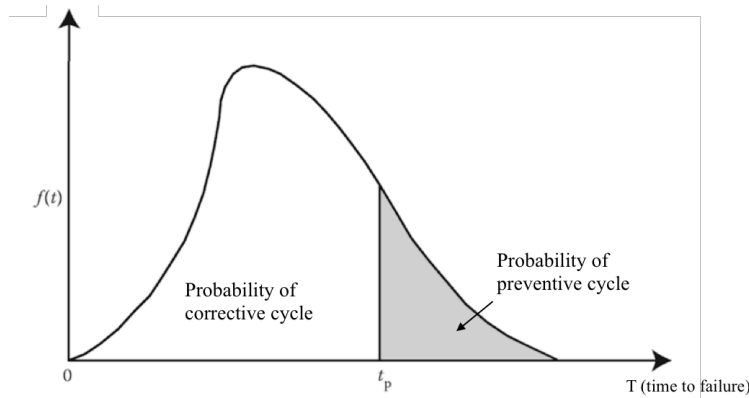


Figure 26 Relation between preventive and corrective cycle under one age replacement policy (adapted from Jardine & Tsang (2013, p. 50))

In consistency with the notion, the incurrence of operating costs under the age replacement policy is influenced by the occurrence of failure. It has two conditions as demonstrated in Figure 27: 1) in case of a failure occurring before the planned replacement age t_p , say, t , with a probability $F(t)$, derived by $\int_0^t f(t)dt$, the cumulative operating expenditures occur over the period $[0, t]$; 2) in case that no failure

²² [] means round down the values calculated to the nearest integer in Eq.27 to count the number of grinding and inspection activities that are performed by time t_p .

occurs in the preventive replacement interval $[0, t_p]$, with a probability $R(t_p)$, the cumulative operating expenditures occur in $[0, t_p]$.

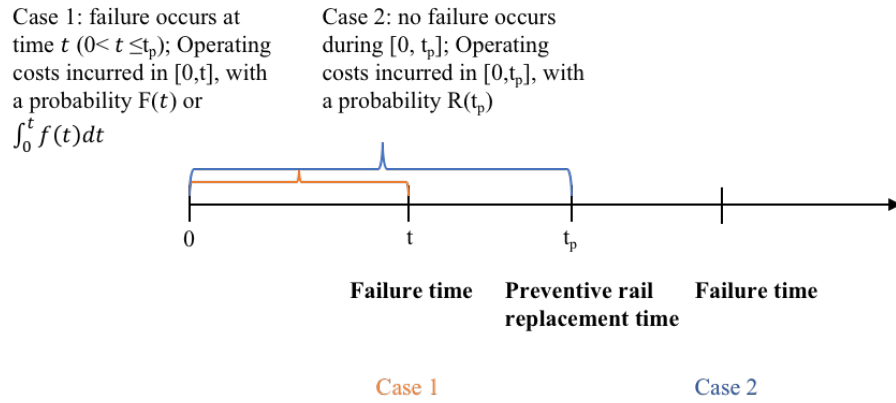


Figure 27 The incurrence of operating costs under the age replacement policy

The total weighted average operating cost under the age replacement policy is a product of probabilities of the two possible replacement cycles with the associated operating costs, which is expressed as,

$$E[C_o(t_p)] = \int_0^{t_p} C_o(t) \cdot f(t) dt + C_o(t_p) \cdot R(t_p) \quad (28)$$

where

$E[C_o(t_p)]$ = total weighted average cumulative operating cost in $[0, t_p]$; [currency]

$C_o(t)$ = (case 1) operating cost incurred in the interval $[0, t]$, where $t < t_p$; it is a variable associated with the event of rail break; [currency]

$C_o(t_p)$ = (case 2) operating costs incurred in the interval $[0, t_p]$, see Eq.27; [currency]

$f(t)$ = PDF of one failure distribution; $\int_0^t f(t) dt = F(t) = 1 - R(t)$

$R(t_p)$ = probability that one rail is still surviving at time t_p / a failure occurs after time t_p

The equation for calculating the expected cycle length remains unchanged, as mentioned in Eq.1, since the inclusion of operating costs has no influence on it. Excluding the initial investment, the mathematical equation of the extended age replacement model (without discounting) that considers the operating costs is expressed as follows (combining Eq.1 and Eq.28),

$$C(t_p) = \frac{\text{total expected cost over a cycle } [0, t_p]}{\text{expected cycle length } E(L)} = \frac{C_c \cdot F(t_p) + C_p \cdot R(t_p) + \int_0^{t_p} C_o(t) \cdot f(t) dt + C_o(t_p) \cdot R(t_p)}{t_p R(t_p) + M(t_p) F(t_p)} \quad (29)$$

where

$C(t_p)$ = total expected costs per unit time for interval $[0, t_p]$ [currency/unit time]

C_c = cost of corrective replacement [currency]

C_p = cost of preventive replacement [currency]

t_p = preventive replacement interval [unit time]

$R(t_p)$ = probability that the rail is still surviving at time t_p

$F(t_p)$ =probability that a failure occurs before time t_p , which equals to $1-R(t_p)$

$f(t)$ = PDF of one failure distribution; $\int_0^t f(t)dt = F(t) = 1 - R(t)$

$C_o(t)$ = cumulative operating cost incurred in $[0, t]$, where $0 < t \leq t_p$ (case 1); [currency]

$C_o(t_p)$ =cumulative operating costs incurred in $[0, t_p]$ (case 2); [currency]

$M(t_p)$ =expected length of the failure cycle (Eq. 2)

3.4.2 Cost discounting (step 7)

Money has a time value. The principle that €1 today is worth more than €1 tomorrow is called *time value of money* (Brealey, Myers, Allen, & Mohanty, 2012, p. 21; Sullivan, Wicks, Koelling, Kumar, & Kumar, 2012, p. 4). Discounting accounts for the time value of money (van den Boomen et al., 2018), which gains in importance when long-lived assets are being considered. As stated above, the expected lifecycle of the rails in the Harmelen LCS is 20 years. Future costs in this case should be converted to present values in order to fairly compare the LCC of different maintenance strategies and obtain more reliable LCCA output.

van den Boomen et al. (2018) has proposed a LCC approach for inclusion of the time value of money in the fundamental age replacement model, in which three LCC techniques, namely the present worth, the annuity factor and the capitalized equivalent worth (van den Boomen et al., 2018), are combined and used in the discounting. The research applies the stepwise LCC methodology for discounting in the proposed extended age replacement model. Before illustrating the three LCC techniques, five engineering economy elements need to be defined, i.e., t, i, P, F and A (Sullivan et al., 2012, p. 56). Given four of the five variables, the fifth value can be solved.

- t : number of periods
- i : interest rate per period ²³
- P : present value that are equivalent to a cash flow series
- F : future value at the end of period t equivalent to a cash flow series
- A : (often called an annuity) uniform periodic cash flow at the end of every period from 1 to t that is equivalent to a cash flow series

Figure 28 presents simple cash flow diagrams to illustrate the P, F and A , where the real cash flow series is not presented for simplicity. t equals to 5 units of time, which could be month, quarter or year, etc. The interest rate in this case should be consistent to the time unit. The P is a time-0 cash flow that is equivalent to later cash flows (Sullivan et al., 2012, p. 54). Time 0 is the beginning of period 1. The F is the end-of-period cash flow and the A is a uniform constant amount distributed for periods 1 through

²³ Interest rate is the *return on capital*; capital is the invested money (Sullivan et al., 2012, p. 31). Discount rate is the interest rate used to find the present value of the future cash flows (Brealey et al., 2012, p. 23).

The interest rate may vary over time, influenced by many factors, e.g., inflation, regulations. Inflation is defined as *a decrease in the buying power of money*, i.e., *the increase in the general level of prices*; deflation is the rarer opposite situation (Sullivan et al., 2012, p. 407). The inflation rate would result in a lower real interest rate for the time value of money (Sullivan et al., 2012, p. 32).

In most engineering economic analysis, the inflation is implicitly addressed, as most costs have prices that increase at the same inflation rate as the general economy condition. It is instead addressed by stating the costs in real values (inflation free) and using the real interest rate (inflation free). If using a market interest rate (incl. inflation rate), cash flows should also be stated in inflated terms, which would complicate the cost estimation. Therefore, the interest rate used in this research is real interest rate and all the costs are expressed in real terms. And the interest rate is assumed to be constant, which is also a common practice of engineering economic analysis (Sullivan et al., 2012, p. 32).

t. In sum, the P, F, and A are three alternatives to represent the economic value of one cash flow series. The conversion among the P, F and A is governed by various engineering economic factors. Examples are the three LCC techniques as mentioned above.

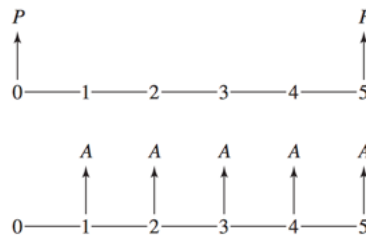


Figure 28 Diagrams for P, F and A (Sullivan et al., 2012, p. 56)

The present worth factor is used for converting a future value F to its present value P. It is denoted as $(P/F, i, t)$, which indicates: find the present value P, given the future value F, the (monthly) discount rate i and the time of occurrence t (Sullivan et al., 2012, p. 58; van den Boomen et al., 2018). It is given by (Sullivan et al., 2012, pp. 58, 62),

$$(P/F, i, t) = \frac{1}{(1+i)^t} \quad (30)$$

where

i = monthly interest rate²⁴ or monthly discount rate = $(1 + r)^{\frac{1}{12}} - 1$

r = yearly interest rate

t = time of occurrence (in months)

The present worth factor is used for standard discrete discounting (van den Boomen et al., 2018; van Noortwijk, 2003), comparable to the continuous cost discounting, like exponential discounting (J. Van der Weide & van Noortwijk, 2008; J. A. Van der Weide, Pandey, & van Noortwijk, 2010), which is an alternative used for including the time value of money in the maintenance optimization models (van den Boomen et al., 2018). The discounting in this research considers the discrete discounting on a *monthly* basis and it is assumed that only the initial investment occur at time 0, i.e., the beginning of period 1, and all other cash flows occur at the end of each month.

The annuity factor or capital recovery factor, denoted as $(A/P, r, t)$, converts a present value P to *equivalent annual cost* (EAC) over a time period t. The denotation reads as: find A (annuity or EAC), given the present value P, the (annual) discount rate r and the time units t (Sullivan et al., 2012, p. 58). The annuity factor is given by (Sullivan et al., 2012, p. 65),

$$(A/P, r, t) = \frac{r(1+r)^t}{(1+r)^t - 1} \quad (31.1)$$

The capital recovery factor is named by asking ‘*how much must be saved in each period (A) to recover the capital cost of the initial expenditure (P)?*’ (Sullivan et al., 2012, p. 65)’. As the monthly discounting is used in this research, the EAC should be interpreted as the *equivalent monthly cost* (EMC), so that Eq.31.1 is revised to (the same parameters as defined in Eq.30),

²⁴ Interest is compounded at the end of each period. If the interest rate is 5% per year but periods are counted in months, the monthly interest rate is not equal to $\frac{5\%}{12}$, due to the impact of monthly compounding. The relation between the annual and monthly interest rate is instead expressed as $1 + r = (1 + i)^{12}$ (Sullivan et al., 2012, p. 45).

$$(A/P, i, t) = \frac{i(1+i)^t}{(1+i)^t - 1} \quad (32)$$

The third LCC technique is the capitalized equivalent worth (CW) factor (van den Boomen et al., 2018). It is necessary to address the concept of *perpetual annuity* before illustrating the CW factor. As presented in Eq.31.1, when t approaches infinity, the limit of (A/P, r, t) is r^{25} , which is mathematically expressed as,

$$(A/P, r, \infty) = r \quad (31.2)$$

Assuming t approaches infinity means assuming perpetual life (Sullivan et al., 2012, p. 156). An annuity in this case is called a perpetual annuity. The assumption of infinity is useful when it comes to the economic analysis of infrastructure assets (Sullivan et al., 2012, p. 156), as they often have long lifespans that are approximately perpetual in an economic sense (impact of cost discounting). Back to the Harmelen LCS, the rails have an expected lifespan of 20 years, with a few cases that they are still in service more than 30 years. It would be reasonable to assume the infinite timespan in this case.

With an assumption of perpetual life, repeated replacement and perpetual annuities are consistently assumed (Sullivan et al., 2012, p. 161). A point of attention is that the perpetual annuity is constant regardless of timespans, i.e., the perpetual annuity over one lifecycle (or more) or infinity are the same. Recall the assumption when applying the age replacement model (section 3.1): focus on one replacement cycle and assume identical and repeated cycles to infinity, which is to some extent consistent with the assumption of infinity and perpetual annuities. It is believed that the nature of both assumptions is the *i.i.d.* premise, i.e.,

- replacement is made with identical assets and failure behaviors of assets are identical (failure times of asset 2 (and 3, 4, ...) follow the same probability distribution as asset 1);
- failure times of the assets are independent;
- incurred costs are identical: asset 2 (and 3, 4, ...) has the same installment and maintenance costs as asset 1.

Back to the capitalized equivalent worth, it is named from the definition of *capitalized cost*. The capitalized cost is *the present value of constant annual costs that are assumed to be incurred in perpetuity* (Sullivan et al., 2012, p. 130). Therefore the factor is used to convert the EAC of one life cycle²⁶ to the present value of an infinite number of cycles (van den Boomen et al., 2018). Recall Eq. 31.2, the CW factor is expressed as (Sullivan et al., 2012, p. 130),

$$CW = \frac{EAC}{r} \quad (33)$$

where r is an annual discount rate. Due to the monthly discounting, Eq.33 is revised to (the same parameters as defined in Eq.30),

$$CW = \frac{EMC}{i} \quad (34)$$

Combining the three LCC techniques, cost discounting in the extended age replacement model is presented below, which contains four steps:

²⁵ Derivation of the limit refers to Sullivan et al., (2012, p. 156).

²⁶ As addressed above, in the case of perpetual life (infinity), an annuity becomes a constant cash flow that are assumed to occur in perpetuity, in which $EAC_{one\ cycle} = EAC_{\infty}$.

- Calculate the PV of maintenance costs ²⁷ over one life cycle t_p
- Calculate the EMC of maintenance costs over the expected cycle length $E(L)$
Under the assumption of repeating and identical replacement cycles: $EMC_{E(L)} = EMC_{\infty}$
- Calculate the EMC of initial investment over infinity
- Calculate the Total EMC over infinity

1) PV of maintenance costs over one life cycle

Recall that the total maintenance cost incurred during $[0, t_p]$ without discounting is expressed as the numerator of Eq.29, the present value of maintenance costs over one life cycle, denoted as PV_m , is calculated as ²⁸,

$$PV_m = C_p R(t_p) \alpha(t_p) + \sum_{t=1}^{t_p} C_c f(t) \alpha(t) + PV_o \quad (35)$$

where

$\alpha(t)$ = present worth factor (Eq.30) at time t

$\alpha(t_p)$ = present worth factor (Eq.30) at time t_p

PV_o = discounted total operating costs, calculated as follows ²⁹

$$\begin{aligned} PV_o &= \sum_{t=1}^{t_p} C_o(t) \cdot F(t) + C_o(t_p) \cdot R(t_p) \\ &= \{C(1)\alpha(1)F(1) + [C(1)\alpha(1) + C(2)\alpha(2)]F(2) + \dots \\ &\quad + [C(1)\alpha(1) + C(2)\alpha(2) + \dots + C(t_p)\alpha(t_p)]F(t_p)\} \\ &\quad + [C(1)\alpha(1) + C(2)\alpha(2) + \dots + C(t_p)\alpha(t_p)]R(t_p) \end{aligned} \quad (36)$$

where

$C_o(t)$ = discounted cumulative operating cost incurred in $[0, t]$

$C(t)$ = monthly operating cost in time t without discounting

2) EMC of maintenance costs over the expected cycle length $E(L)$

The expected cycle length is calculated according to Eq.2. Convert the PV_m (Eq.35) by the annuity factor $(A/P, i, t)$ (Eq.32, where t equals to $E(L)$), the EMC over the expected cycle length $E(L)$ can be found.

²⁷ The maintenance cost considers the (corrective and preventive) replacement cost, preventive grinding cost and (ultrasonic and visual) inspection cost.

²⁸ Because of the need for discrete discounting, the corrective replacement cost is distributed over $[0, t_p]$ by means of the discrete probability distribution function $f(t)$ and $\sum_{t=0}^{t_p} f(t) = F(t_p) = 1 - R(t_p)$ (van den Boomen et al., 2018). $f(0)$ is assumed to be zero.

²⁹ Eq.36 changes the continuous probability distribution (in Eq.28) to discrete distribution due to the need for discrete discounting.

$$EMC_{E(L)} = PV_m \cdot (A/P, i, E(L)) \quad (37)$$

Assuming the identical and repeated replacement cycles over infinity results in $EMC_{E(L)} = EMC_{\infty}$.

3) EMC of initial investment over infinity

By using the capitalized equivalent worth, as presented in Eq.34, the initial investment cost (C_{in}) is equally distributed over infinity and the EMC of the investment cost is calculated as,

$$EMC_{in} = C_{in} \cdot i \quad (38)$$

4) Total EMC over infinity (objective function)

Combining Eq.37 and Eq.38, the total EMC over infinity can be obtained,

$$EMC_{total} = EMC_{E(L)} + EMC_{in} \quad (39)$$

It is the objective function that links the rail degradation (measured by CDF $F(t)$, PDF $f(t)$, or reliability function $R(t)$) and maintenance strategies (preventive replacement interval, grinding interval and inspection interval) to LCC. The minimum of the cost function provides an economic optimum for preventive replacement interval (time-based). Further sensitivity analysis can be performed to steer values of input parameters (that are of interest) and observe their impact on the optimum and LCC.

Eq.39 uses the total EMC as the cost criterion to find the optimized preventive replacement interval, it is also possible to convert the EMC to total PV over infinity by the capitalized equivalent worth (Eq.34 in the case of monthly discounting). The two criteria yield the same age replacement optimization result.

3.5 Conclusion

This chapter presents the detailed procedures of the model from the data gathering to the derivation of the objective cost function, which gives answers to sub-questions 3-5.

Q3: How can the degradation of the Harmelen LCS be modelled?

Chapter 2 narrowed down the scope of degradation modelling to the rails and in this chapter the life distribution is used to model the rail degradation (time to failure) in the Harmelen LCS as the system is non-repairable. Following the basic procedures of reliability analysis, the degradation modelling has three steps: data gathering -> preliminary model selection -> parameter estimation. It is firstly assumed that the rail failures in the Harmelen LCS follow the 2-parameter Weibull distribution. Probability plotting (least squares fit) is used to test the model fit and give initial estimates of parameters. If the plotted points cannot approximately fall one straight line (visual test), other distribution models may be tried. Once it is verified that the model fits the data well, MLE is used to estimate the parameters of the fitted distribution. Once MLEs are solved, the specified life distribution model can be used to account for the variability of time to failures of the rails in a population of the Harmelen LCS.

Q4: How can the effect of maintenance interventions on the asset degradation be evaluated?

The preventive grinding is effective in controlling the initiation and propagation of the RCF surface defects. Possibly it could extend the rail's lifespan in the Harmelen LCS. Its impact is evaluated by adjusting the hazard rate of the rail failure caused by RCF defects (while the hazard rate of corrosion-initiated failures remains unchanged). The adjustment is based on an existing PM optimization model (Coria et al., 2015), which includes the PM interval as a variable so that it provides an insight into the interaction between the maintenance decision variable (the grinding interval as considered in this research) and rail degradation. The total hazard rate of the rails is estimated based on the notion of competing risk model, with the assumption of independence between the two failure modes.

Q5: How can results of degradation modelling (incl. the impact of maintenance interventions) be integrated into cost estimation?

The degradation modelling provides five alternative measures to account for the variability of rail failures (time to failure) in the Harmelen LCS, namely hazard rate, CDF, PDF, reliability function, cumulative hazard function. The age replacement model is used to link the degradation modelling

results to cost estimation. Due to the limitation of the fundamental age replacement model, this research extends the age replacement model to incorporate the grinding cost and inspection cost in the LCC calculation and replacement optimization. As these cost elements incorporate the maintenance decision variables (grinding interval and inspection interval), the extension creates extra dimensions of optimization in the age replacement model and provides a basis to investigate the impact of these decision variables on the replacement optimization and LCC.

Combining the above conclusions, the reliability-based LCC model for the Harmelen LCS that considers the interaction between LCC and uncertainties involved in the rail degradation and maintenance interventions is developed. The theoretical model is demonstrated as shown in Figure 29. It contains three major parts, model degradation -> incorporate the effect of maintenance in degradation modelling -> integrate degradation and maintenance interventions to LCC analysis. Each part gives answers to sub-questions 3-5, respectively.

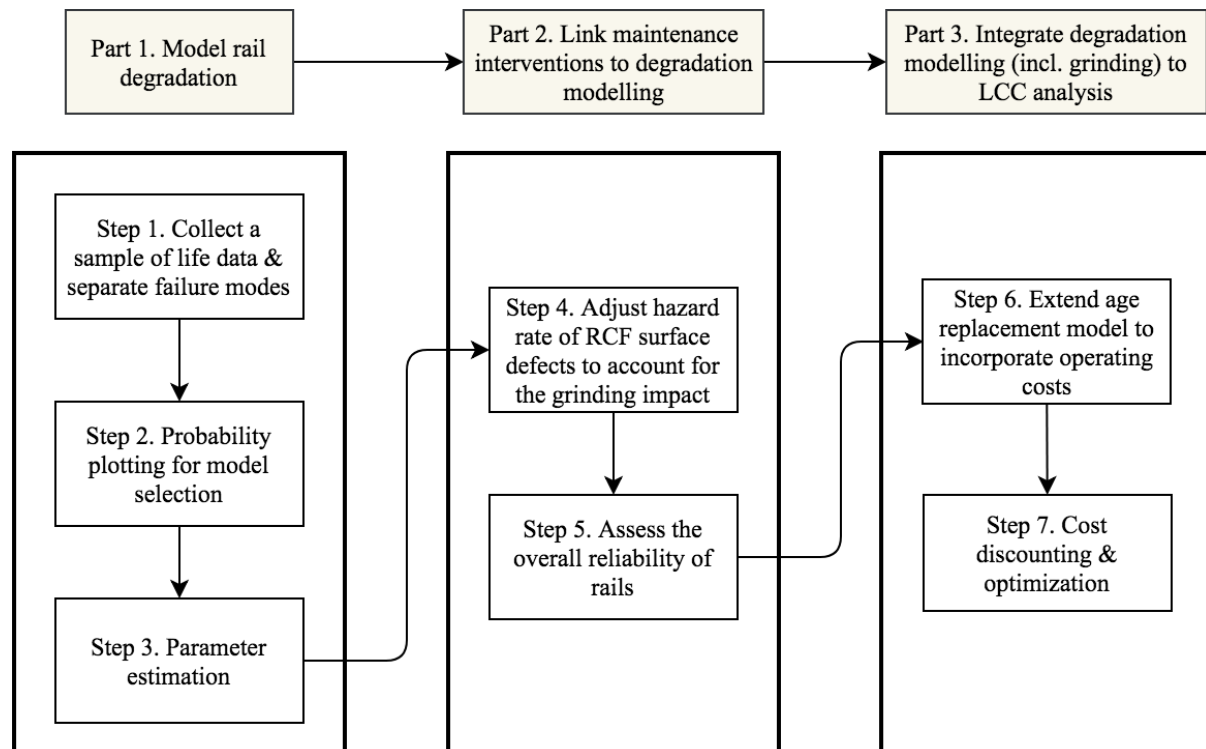


Figure 29 Flowchart of the reliability-based LCC model

4. Application & Validation

In this chapter, the proposed model is executed using Microsoft Excel and validated by field data. The application of the model follows the modelling procedures as proposed in Figure 29.

4.1 Data gathering (step 1)

A rail break record (occurred in the Harmelen LCS) was collected from ProRail (Appendix C). In total 21 rail breaks have occurred during the period from 2015 to 2018 in the Harmelen LCS (Dutch national railway network), in which 19 rail breaks occurred in the level crossing zone and 2 failures in the transition zone. The installation dates of all the systems are missing (only mentioned in years) and it is not possible to retrieve the exact dates of the installation. Therefore it is assumed that all the systems were installed in the middle of the years (1st of July). Besides, the installation years of two systems (of 21) are missing so that only 19 rail breaks are used in modelling.

An important observation in the failure record is that almost³⁰ all the breaks were caused by corrosion and it was indicated in the failure mode analysis that corrosion breakage has no relationship with squats. The statement verifies the assumption made in Chapter 3: corrosion and RCF failure modes are independent and therefore the competing risk model is applicable.

Recall that there are two rail replacement scenarios involved in the Harmelen LCS. Corrective replacement is done upon instant breaks (in which the exact failure times of the rails can be observed), and preventive replacement is conducted before real failures occur. The underlying reason that nearly all the recorded rail breaks are related to corrosion is that: potential rail breaks caused by RCF defects can be identified through more reliable inspection techniques and avoided through the preventive replacement. In practice, 90% rail replacement in the Harmelen LCS are preventive and the rest are corrective (Appendix A, Interview III). The rail break record only indicates the cases of corrective replacement and it is unknown how the rest 90% looks like. Both corrosion and RCF defects pose threats to rail breakage and it is necessary to incorporate the contribution of RCF defects (to rail breakage) into the modelling and obtain a more reliable calculation of probability (of rail breakage). Therefore, in addition to the rail break record, which indicates the exact times of corrosion-initiated breaks, the ultrasonic inspection reports need to be gathered, in which the inspection time, the diagnosis of RCF-related defects and (replacement) decisions on how and when to deal with the identified defects are recorded. With expert judgment on the question,

‘Starting from the inspection date (when the identified defect is defined to severity level 1 (or other levels) in the ultrasonic inspection report), how long can the rail stand before it breaks, considering ‘do nothing’ scenario?’

For instance, if the answer is ‘one year’ (from level 2 to the occurrence time of the potential failures) and the age of the rail when it was inspected is 20 years (240 months), it is possible to infer that the potential rail break caused by the recorded RCF defect may occur during the 240th -252nd month. When the sample size is large enough, it can be used for reliability analysis. This kind of failure data refers to interval data or grouped data, and the methods of probability plotting (LS) and parameter estimation (MLE) have been described in chapter 3.

In total 7 ultrasonic inspection reports have been gathered, in which two types of RCF defects are involved, namely squats (surface RCF) and horizontal cracks in the rail web (internal RCF). 4 cases are related to the horizontal cracks, while it was understood from the interviews that in practice the horizontal cracks occurring in the Harmelen LCS may not directly pose threats to rail break (Appendix

³⁰ The failure mode of one rail break is missing; One rail break was caused by weld defects (with a question mark).

A, Interview III & IV), which means only the inspection records with regard to the squats are of interest in assessing the reliability of the rails (i.e., calculating the probability of rail breaks). The 3 cases for squats are not sufficient to support modelling. The ultrasonic inspection is performed within the national programme and the PGO contractors only have a few ultrasonic reports (specific to Harmelen LCS) in their PGO regions. ProRail has an enormous database for ultrasonic inspection records, while the data is recorded based on the types of rails, switches, etc. and it is not possible to retrieve the ultrasonic inspection records specific to the Harmelen LCS. Although assuming data may cause noises in data and lead to biased results, neglecting one failure mode may significantly influence the reliability evaluation. To demonstrate the model application, the research assumes the time intervals when the squat-initiated rail breaks may occur, based on one³¹ ultrasonic inspection report and the 20-year expected life cycle of the rails that is defined by ProRail.

Another barrier confronted in the data gathering is ‘grinding policy’. The grinding decisions in ProRail are made based on traffic loading and curvatures. The current practice of preventive grinding is one-time 0.2mm metal removal at a fixed interval 15 MGT for the level crossings, as stated in section 2.2.2. However, the gathered failure data (21 Harmelen LCS) was recorded in time and their respective traffic conditions were not mentioned. Furthermore, the traffic demand varies depending on track lines. It is unknown how ProRail determines the accumulative traffic tonnage as 15 MGT to facilitate the grinding operations on all the level crossings in the entire network. The preventive grinding practices of Deutsche Bahn AG (abbreviated as DB, German railway infrastructure manager) found in the literature (NeTIRail, 2015) support the decision in this research to convert the unit of MGT to time with regard to the grinding interval to overcome the challenge of the insufficient data.

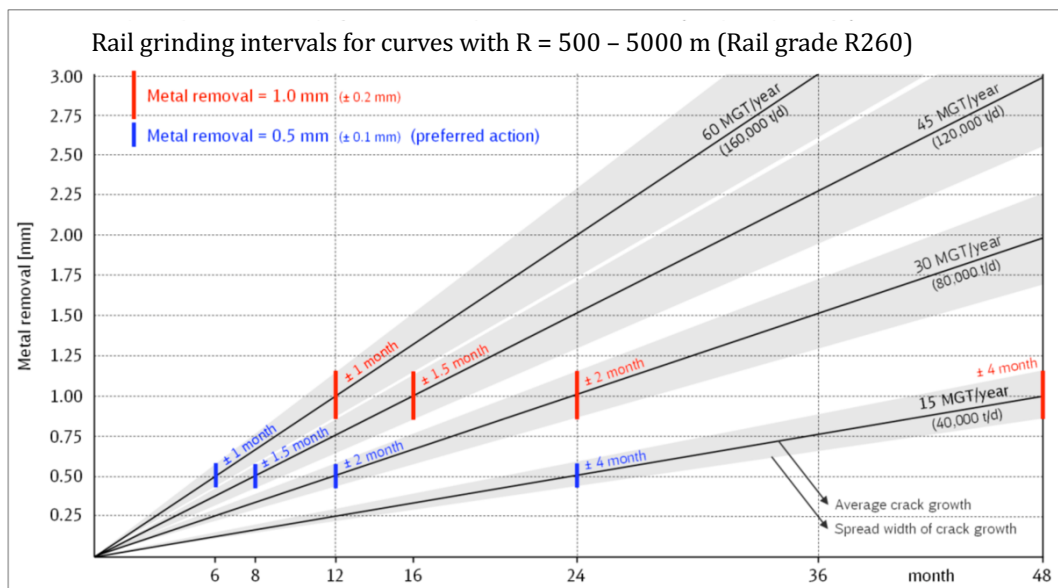


Figure 30 Specification of DB for preventive grinding program in the mainline (heavy rail) of the DB network (rails in curves with radii from 500 to 5000 m) (NeTIRail, 2015)

As shown in Figure 30, the grinding practices in DB also depend on traffic tonnage. DB integrates the annual tonnage, time frequency (in months) and metal removal and uses time to inform the implementation of grinding operations. The time interval varies from 0.5 to 2 years. For example, in case that the annual tonnage is 15 MGT/year and the grinding cycle is once per 12 months, one-time

³¹ One not three because only one inspection report finally decided to do preventive replacement.

mental removal is 0.25 mm. If the grinding operations are early performed or delayed (measured in months), less or more mental removal (in mm) should be consistently considered, as indicated in red and blue lines. It is considered that the grinding specifications in ProRail may differ (but not much) from the practices of DB. Therefore, the research sets 15 MGT equal to 12 months of train operation as an average to incorporate the impact of cyclic preventive grinding in rail degradation modelling and to further explore how the grinding policy influences the LCC. Furthermore, as addressed in section 2.2.2, in most cases the maximum wear on the rail head is 17 mm. Consider a 30-year time horizon, the preventive grinding is performed once a year with each 0.25mm mental removal. The total wear depth is 7.5 mm, much smaller than the 17 mm limit. Hence, the total depth limit of preventive grinding is neglected in this research.

4.2 Probability plotting (step 2)

The step 2 is to perform probability plotting in order to test the model fit and provide initial parameter estimates. Considering the corrosion and surface RCF are two distinct failure modes, the data plotting is addressed in separate sections.

4.2.1 Corrosion failure mode

As presented in Table 2, enter the dates of installation and rail breaks, time to failure is given by Excel 'DAYS360' function. Then sort the 'time to failure' in ascending order by Excel 'Order' function. According to Eq.10, linear rectification formula of the 2-parameter Weibull distribution, enter the equations $x=\ln t$ and $y=\ln\{-\ln[1-F(t)]\}$. To solve y , median rank $\hat{F}(t)$ is calculated by Eq.12 (for exact times of failure). Use Excel 'Slope' function and 'Intercept' function, the slope and intercept of the regression line can be derived, respectively. The slope represents the value of β , and the value of the scale parameter α is estimated by $e^{\left(\frac{-intercept}{\beta}\right)}$.

Table 2 LS regression in Excel (corrosion failure; exact failure times; field data)

Installation date	Date rail break	Time to failure (in months)	Failure count i	Ordered failure time ti (in months)	$x_i=\ln(t_i)$	Median rank $F(t_i)$	$y_i=\ln(-\ln(1-F(t_i)))$
		222	1	163	5,09	0,04	-3,30
	Note: not available for confidentiality reasons	163	2	163	5,09	0,09	-2,39
		237	3	187	5,23	0,14	-1,90
		365	4	222	5,40	0,19	-1,55
		281	5	224	5,41	0,24	-1,28
		268	6	224	5,41	0,29	-1,06
		224	7	237	5,47	0,35	-0,86
		224	8	268	5,59	0,40	-0,68
		187	9	281	5,64	0,45	-0,52
		339	10	296	5,69	0,50	-0,37
		296	11	300	5,70	0,55	-0,22
		379	12	300	5,70	0,60	-0,08
		163	13	308	5,73	0,65	0,06
		308	14	320	5,77	0,71	0,20
		440	15	331	5,80	0,76	0,35
		320	16	339	5,83	0,81	0,50
		331	17	365	5,90	0,86	0,68
		300	18	379	5,94	0,91	0,89
		300	19	440	6,09	0,96	1,20
			β	4,14	=slope		
			$-\beta \ln(\alpha)$	-23,73	=intercept		
			α (months)	309,85	=exp(-intercept/ β)		

Apply Excel add-ins 'Data analysis toolkit' and solve for 'regression analysis', the Weibull plotting for corrosion failure data can be given, as presented in Figure 31.

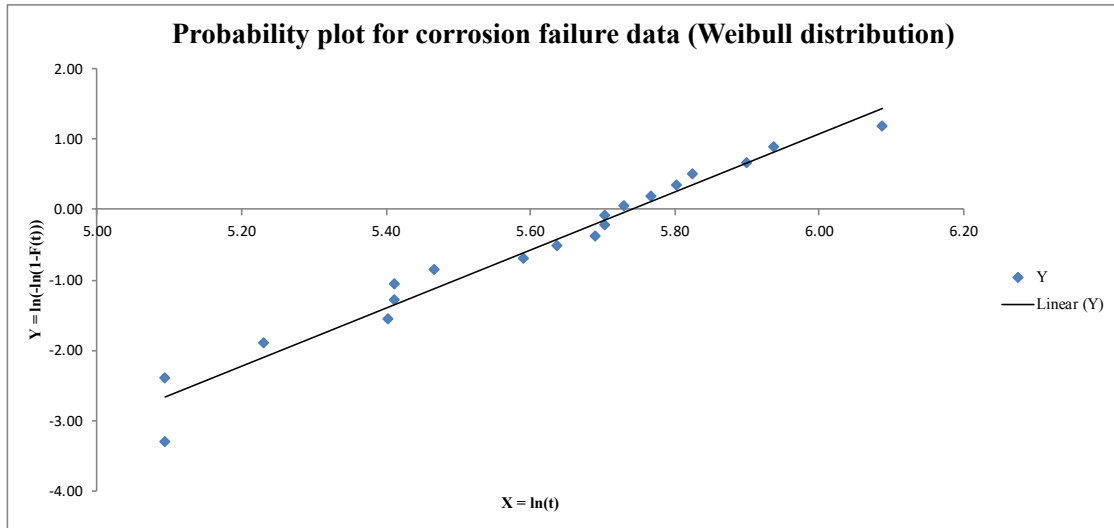


Figure 31 Weibull probability plotting (corrosion failure data)

The blue dots represent the observed value (sample data) of the dependent variable (y_j). It can be observed that most of the data points (observed data) fall on the straight line, indicating the Weibull distribution fits the data well.

Apart from the visual test, the ‘regression analysis’ tool in Excel provides the results of regression statistics, in which goodness-of-fit measures are automatically calculated and presented, as shown in Table 3, which provides numeric assessment of how well the model fits the sample data. R-squared value is equal to 0.965, indicating that 96.5% of the variation of y-values around the mean can be explained by the regression line.

The strength of R^2 is it provides a basis to compare the fit of alternative models. The closer to 1 the R^2 is, the more appropriate the model is for the given dataset. To demonstrate this notion, another life distribution, exponential distribution, is tested as a reference to the R^2 given by the 2-parameter Weibull distribution. The exponential distribution is another extensively used distribution in the reliability analysis. Its basic formula and linear rectification form for probability plotting are presented in Appendix E. Given the corrosion failure data, the exponential plotting is presented in Figure 32.

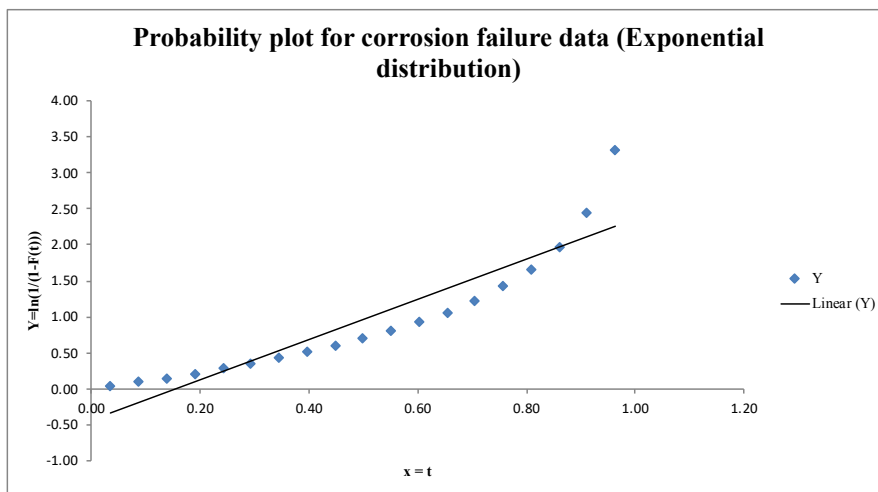


Figure 32 Exponential probability plotting (corrosion failure data)

It is obvious in Figure 32 that the exponential distribution provides a poor fit to the given sample data, where the obvious trend in the data is not well explained. Then look into the regression statistic: R-

squared value is approximately equal to 0.844, which proves it is not a good fit compared to the 2-parameter Weibull distribution with the R-squared value equal to 0.965.

Table 3 Result of regression statistics

Regression Statistics	Weibull	Exponential
R Square	0.96467947	0.84427617

The output of the regression analysis is:

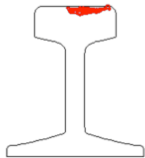
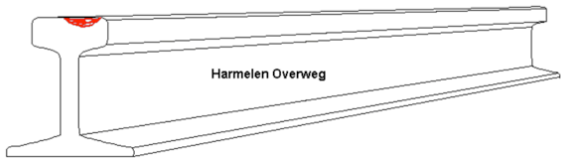
- Weibull distribution is a good fit to the given dataset
- Linear regression equation with Weibull probability plotting: $y = 4.14x - 23.73$
- Weibull shape and scale parameters are $\hat{\beta} = 4.14$ and $\hat{\alpha} = 309.85 \text{ months}$ (approximately 25.82 years), respectively.

Recall that α represents the characteristic life of a population, which means, due to the corrosion, roughly 63.2% of the rails in the Harmelen LCS fails by 25.82 years.

4.2.2 RCF failure mode

Then look into the RCF failure mode. Table 4 presents one ultrasonic inspection report (part) for the Harmelen LCS (Appendix D). It indicates the rail was manufactured³² in May, 2000. The defect identified by the ultrasonic inspection is squats (UIC code 227). The decision is to replace the rail within 4 weeks (severity level 2), made on September 4, 2016.

Table 4 Ultrasonic inspection report (squats in Harmelen LCS)

Detailtekening:			
			
Plaats v/h gebrek:		<ul style="list-style-type: none"> ▪ Overweg, Spoorstaaf ▪ Dwarsfout van 0 mm tot 12 mm diep 	
Soort spoor:		Bogen:	
Spoorconstructie:		Op/aanlassing: Geen	
Walsteken(s):			
profiel links	54E1	profiel rechts	54E1
merk	DO (Voest-Alpine)	merk	DO (Voest-Alpine)
datum	05-2000	datum	05-2000
kwaliteit	E1	kwaliteit	E1
UIC foutcode:		227	
Foutclassificatie / Advies:		2 / Uitwisselen binnen 4 weken	
Datum rapport ontvangen:		04-09-2016	
Datum advies herstel:		02-10-2016	

As the potential rail breaks caused by squats cannot be observed, it is assumed the time frame from the time when a squat is defined as level-2 defect to its potential failure (do nothing) is 12 months, which

³² There may be time delay from new production to installation. It is recommended to take it into account when collecting field data. It is not considered in this research as the RCF-related failure data is assumed.

means the rail break caused by the squat may occur between September 4, 2016 to September 4, 2017. Its time to failure is around 196-208 months. Similarly, assume 6-month, 18-month, 24-month time frame for level-1, level-3 and level-4 defect, respectively.

Due to the inadequacy of data (ultrasonic inspection reports), the research assumes 17 rail failures caused by squats to illustrate the model application, as shown in Table 5, in which only the time intervals where the failures occur are known. Column F, CDF $\hat{F}(t)$, is calculated by binomial estimate (Eq.13), distinguished from the median rank estimate. Note that the last failure, occurring in the interval 340-360 months, is neglected because if it is included in estimating $\hat{F}(t)$, the $\hat{F}(t)$ at the end of the interval will be 100%. It is unrealistic to expect that the 17 sample data would represent the 100th percentile of the population distribution (Tobias & Trindade, 2011, p. 163). It is a common practice to neglect the last data point in the binomial estimate (Tobias & Trindade, 2011, p. 171). Column G, $x=\ln(t)$, where t is the interval end time. Then similar to the LS regression of the corrosion failure data, the values of Weibull parameters β and α can be calculated by the slope and intercept of the regression line.

Table 5 LS regression in Excel (RCF failure, interval data; assumed data)

	A	B	C	D	E	F	G	H	I
52	Failure mode 2 - RCF	Interval start (months)	Interval end (months)	Failures in interval	Cumulative failures	Binomial Estimate F(t)	$x=\ln(t)$	$y=\ln(-\ln(1-F(t)))$	
53		180	200	1	1	0,059	5,298317367	-2,803054168	
54		200	220	1	2	0,118	5,393627546	-2,078137249	
55		220	240	2	4	0,235	5,480638923	-1,315783759	
56		240	260	2	6	0,353	5,560681631	-0,831678317	
57		260	280	3	9	0,529	5,634789603	-0,282665606	
58		280	300	4	13	0,765	5,703782475	0,389436458	
59		300	320	2	15	0,882	5,768320996	0,760836746	
60		320	340	1	16	0,941	5,828945618	1,041411525	
61		340	360	1	17				
62									
63									
64									
65									
66									
67									
68					β	7,397043397	=slope		
69					$-\beta \ln(\alpha)$	-41,94486704	=intercept		
70					α (months)	290,1769384	=exp(-intercept/ β)		

The output of the regression analysis is:

- Linear regression equation: $y = 7.40x - 41.94$
- Weibull shape and scale parameters are $\beta = 7.40$ and $\alpha = 290.18$ months (approximately 24.18 years), respectively.

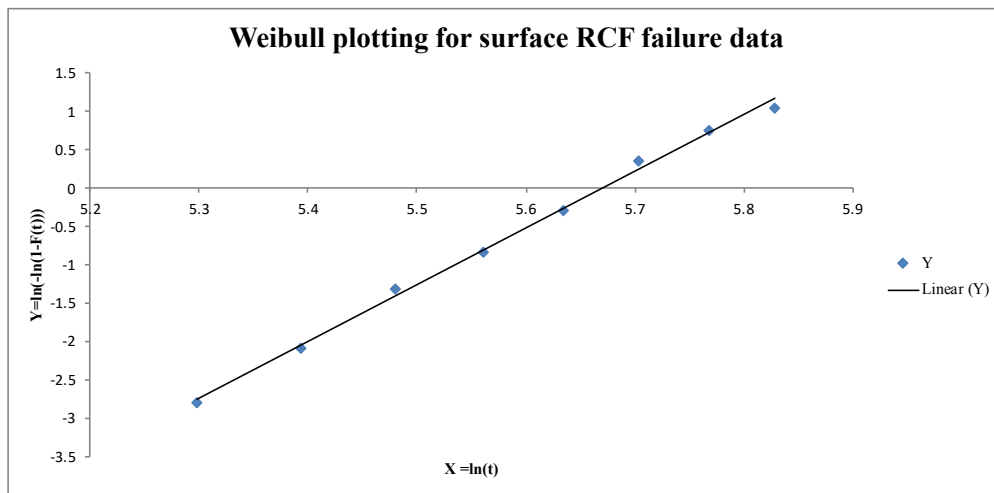


Figure 33 Weibull probability plotting (RCF failure data)

Use Excel 'regression analysis' tool the Weibull probability plotting for the assumed RCF failure data is given, as presented in Figure 33. The RCF failure data is fictitious so that the model fit will not be discussed here.

4.3 Maximum likelihood estimation (MLE) (step 3)

After testing the model fit and obtain the initial parameter values, MLE is executed in Excel to have more accurate Weibull parameter values for the given dataset. As shown in Table 6, put a starting guess in location C2 with $\ln(\alpha)$, where α is given by the LS estimate ($\alpha = 309.85$). Enter $\beta = 4.14$ in cell D2. Column E and F record the failure times, either exact times or interval estimates. Column G is used to distinguish the type of failure data. For corrosion-initiated failures, only the exact failure time data is available so that column F is left blank. Enter the exact times of failure (19 cases) in column E and zero in column G. The censor code in column G identifies the type of data in any row and the LIK functions in column I accordingly adapt to calculating the LIK function for each row of data, depending on the kind of data.

Recall the log LIK function for the exact failure time data, Eq.17, the function in Excel (column I) is expressed as (for data in row 2):

$$= \text{IF}(G2 = 0; H2 * \left(\text{LN}(\$D\$2) - \text{LN}(E2) + \$D\$2 * (\text{LN}(E2) - \$C\$2) - \left(\left(\frac{E2}{\text{EXP}(\$C\$2)} \right)^{\$D\$2} \right) \right); 0)$$

Sum all the log LIK values in column I and cell J2 returns the negative sum of the log LIK values.

Table 6 Weibull MLE for corrosion failure data (starting estimates from LS regression)

	A	B	C	D	E	F	G	H	I	J	K
1	MLE for corrosion failure data	Failure mode 1 - corrosion	$\ln(\alpha)$ put in guess to start with from least squares	β (Shape) put in guess to start with from least squares	Interval Start Time or Exact Time of Failure	Interval End Time	Censor Code 0 = exact, 1 = interval data	Count or Frequency	Log Likelihood	-Sum Log Lik use Solver to minimize this negative sum of the Likelihood column values by varying B2 and C2	α (scale: in months)
2			5,73607360	4,13686768	163		0	1	-6,40116208	108,41471110	309,84544
3					163		0	1	-6,40116208		
4					187		0	1	-6,02395722		
5					222		0	1	-5,61373038		
6					224		0	1	-5,59511374		
7					224		0	1	-5,59511374		
8					237		0	1	-5,48683317		
9					268		0	1	-5,31995184		
10					281		0	1	-5,29014309		
11					296		0	1	-5,28722659		
12					300		0	1	-5,29238156		
13					300		0	1	-5,29238156		
14					308		0	1	-5,31046374		
15					320		0	1	-5,35768954		
16					331		0	1	-5,42314833		
17					339		0	1	-5,48470052		
18					365		0	1	-5,77161814		
19					379		0	1	-5,98535800		
20					440		0	1	-7,48257576		

As shown in K2 and D2 (Table 6), the values are the same as LS estimates. Then open Excel Solver function. Solver is used to find an optimal value (maximum, minimum or an objective value) for a formula in one cell, subjected to the constraints in other cells (Microsoftoffice, 2018). The Solver entries are presented in Figure 34: set the Solver objective to be a minimized \$J\$2 by changing the values in cells \$C\$2 and \$D\$2. \$D\$2 is Weibull shape parameter, which ranges from 0.0001 to 100. Click on 'Solve'.

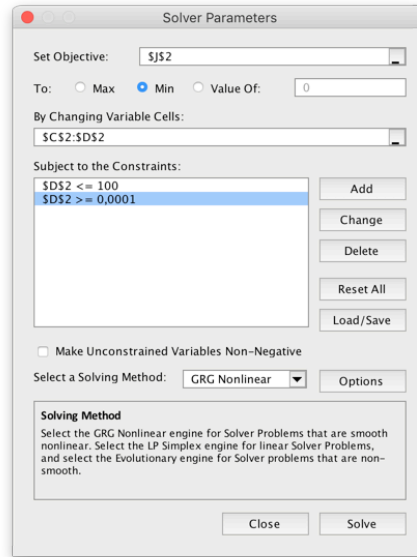


Figure 34 Solver entries for MLE

Then, as shown in Table 7, solver quickly converges to the Weibull parameter MLEs.

Table 7 Weibull MLE for corrosion failure data (after Solver)

	A	B	C	D	E	F	G	H	I	J	K
1	MLE for corrosion failure data	Failure mode 1 - corrosion	Ln(α) put in guess to start with from least squares	β (Shape) put in guess to start with from least squares	Interval Start Time or Exact Time of Failure	Interval End Time	Censor Code 0 = exact; 1 = interval data	Count or Frequency	Log Likelihood	-Sum Log Lik use Solver to minimize this negative sum of the Likelihood column values by varying B2 and C2	α (scale; in months)
2			5,73422100	4,28046453			0	1	-6,44567396	108,39149175	309,27195
3					163		0	1	-6,44567396		
4					187		0	1	-6,04667262		
5					222		0	1	-5,60969352		
6					224		0	1	-5,58973989		
7					224		0	1	-5,58973989		
8					237		0	1	-5,47333622		
9					268		0	1	-5,29169826		
10					281		0	1	-5,25806196		
11					296		0	1	-5,25286942		
12					300		0	1	-5,25785188		
13					300		0	1	-5,25785188		
14					308		0	1	-5,27619293		
15					320		0	1	-5,32544996		
16					331		0	1	-5,39469732		
17					339		0	1	-5,46028823		
18					365		0	1	-5,76897137		
19					379		0	1	-6,00077883		
20					440		0	1	-7,64624964		

In terms of the RCF failure mode, as the MLE calculation sheet has distinguished the type of failure data, it is easy to perform MLE for interval failure data. As presented in Table 8, enter the interval start time and end time in column E and F, respectively. Distinguish the data type by the censor code, 1, and enter the number of failures in each interval in column H.

According to Eq.18, the log LIK function for interval data in Excel can be expressed as:

$$\ln(\text{LIK}) = r \cdot [\ln [\text{Weibull}(t_{i-\text{end}}, \beta, \alpha, \text{True}) - \text{Weibull}(t_{i-\text{start}}, \beta, \alpha, \text{True})]]$$

where the Excel function Weibull($t, \beta, \alpha, \text{True}$) returns Weibull CDF at time t , given by parameters α and β .

As shown in Table 8, to distinguish the type of data, the function in column I is expressed as (take data in row 30 as an example):

$$= \text{IF}(G30 = 1; \text{IF}(E30 = 0; H30 * \text{LN}(\text{WEIBULL}(F30; \$D\$30; \text{EXP}(\$C\$30); \text{TRUE})); H30 * (\text{LN}(\text{WEIBULL}(F30; \$D\$30; \text{EXP}(\$C\$30); \text{TRUE}) - (\text{WEIBULL}(E30; \$D\$30; \text{EXP}(\$C\$30); \text{TRUE}))))); 0)$$

Use Solver to obtain the minimized negative sum of the log LIK function and obtain the MLEs.

Table 8 Weibull MLE for RCF failure data (after Solver)

	A	B	C	D	E	F	G	H	I	J	K
29	MLE for RCF failure data	Failure mode 2 - RCF (surface)	Ln (α) put in guess to start with from least squares	β (Shape) put in guess to start with from least squares	Interval Start Time or Exact Time of Failure	Interval End Time	Censor Code 0 = exact; 1 = interval data	Count or Frequency	Log Likelihood	-Sum Log Lik use Solver to minimize this negative sum of the Likelihood column values by varying B30 and C30	α (scale; in months)
30			5,668913368	7,619401169	180	200	1	1	-3,461023427	36,38178524	289,7195448
31					200	220	1	1	-2,849564652		
32					220	240	1	2	-4,677469912		
33					240	260	1	2	-3,890564846		
34					260	280	1	3	-5,10217822		
35					280	300	1	4	-6,618361768		
36					300	320	1	2	-3,756600005		
37					320	340	1	1	-2,469475824		
38					340	360	1	1	-3,556546591		

Table 9 presents the comparison of LS estimates and MLEs. It is observed they are very close. From the statistical point of view, MLE is usually a recommended approach³³ to estimate population parameters from large samples: the method is more precise as the sample size becomes large enough (especially when the failure times are larger than 10) (Tobias & Trindade, 2011, p. 99). Therefore, Weibull estimates provided by MLE will be used in the following steps.

Table 9 Comparison of LS estimates and MLEs

		Least squares		MLE (after Solver)	
Corrosion	α1=	309.85	months	309.27	months
	β1=	4.14		4.28	
Surface RCF	α2=	290.18	months	289.72	months
	β2=	7.40		7.62	

4.4 Reliability evaluation (step 4 & 5)

Follow step 4&5 in section 3.3.2, the overall reliability of the rails, considering the two failure modes, can be evaluated by the competing risk model. Substitute MLEs (Table 9) in Eq.26, the total hazard rate of the rail failures can be derived (where the current grinding interval T_0 is assumed to be 12 months). The cumulative hazard function is calculated by integrating the total hazard rate. And the other functions can be derived with their relations to the hazard rate and cumulative hazard function (Eq.7, Eq.8.1 and Eq.9).

³³ Further details about why MLE is the recommended estimation technique in most statistic books refer to Tobias & Trindade (2011, p. 98).

4.5 Cost optimization (step 6 & 7)

The last two steps in the model application is cost discounting in the extended age replacement model and obtain the optimized preventive replacement interval based on the minimized EMC or PV over infinity.

When estimating the cost, the research considers an 18-meter long Harmelen level crossing. The cost data regarding the activities to installing and maintaining the Harmelen LCS is collected from the interviews, by expert judgment, as shown in Table 10. As noted before, the activities for maintaining the assets are performed by both the asset owner (ProRail) and PGO contractors (e.g., Strukton and ASSET Rail). Grinding operations and ultrasonic inspection are within the national programme, where ProRail assigns contractors (not PGO) to be responsible for performing the specific maintenance activities for the whole national railway network in the Netherlands. As the expenses on these activities are always measured in one-time operation, depending on the scope (contract), a high level of uncertainty is involved in the cost data (i.e., *one-time grinding operation / ultrasonic inspection for one 18-m long LCS*). Point estimates are used in the cost optimization and it is expected to be verified by checking the related cost statements. In regard to the social cost, ‘how much does one passenger perceive per unit time train delay’ varies from person to person. This text presents an average condition in the Netherlands, provided by ProRail.

Table 10 Input cost data (ProRail)

Input values (monetary unit: €)										
Annual discount rate	r	5%				Preventive grinding cost	Cg	2000-5000 euros per time	2000	
Monthly discount rate	i	0,00407						ultrasonic inspection cost	200	
Initial investment	Cin	40000	*both rails (40000 euros in total)			Inspection cost	Ci	visual inspection	300	
Preventive replacement cost	Cp	36000	*30000 euros for single rail replacement; additional 20% for indirect cost (work preparation)			Grinding interval	Tpm	12	months	
			unit cost of track availability	17	/h/passenger	Ultrasonic inspection interval	Tui	6	months	
			average number passengers	128	passengers/train	Visual inspection interval	Tvi	12	months	
			average number of trains	4	trains/h					
Social cost	Cs	69632	unavailability duration	8	hours (*excl. free night possession period, i.e., 4 hours; fault duration 12 hours)					
Corrective replacement cost (w/ social cost)	Cc	108632	*30000 euros for single rail replacement; additional 30% for indirect cost (especially mobilization cost); social costs are included							

Moreover, various stakeholders, characterized by different norms and values, are involved in managing the railway assets. In such an institutional context, ‘who is telling the story’ may become a matter of great importance when evaluate the LCC of the railway assets. ProRail, as an asset owner, strives for providing a safe and on-time rail travel for passengers and freight in the Netherlands, and the track availability is of great interest. When it comes to the LCC of one rail asset, social costs should be included to account for the impact of train delay in case of unexpected failures. For the contractors however, typically the PGO contractors in the Netherlands, all issues (penalty or incentives) regarding the track safety and availability in the PGO contract period are monetized in the agreement, and they

may perceive the LCC of the railway assets differently. This research considers both ProRail and the PGO contractors are key stakeholders in managing the railway assets during their lifetime. It is necessary to consider the policy impact in LCC calculation and optimization. Firstly the LCC of the Harmelen LCS is calculated from the asset owner point of view (ProRail).

Define 12-month grinding interval (T_{pm}) as the reference case and follow the discounting procedures mentioned in section 3.4.2, the age replacement model yields an optimized preventive replacement interval, 179 months (approximately 15 years), in which both the EMC and PV over infinity are minimized, €556 and €136541, respectively.

As shown in Figure 35, the horizontal axis indicates the preventive replacement interval (in months) and the vertical axis represents the total EMC over infinity (€). Opting for different preventive replacement intervals will result in varied EMC. The teeth on the blue curve are caused by periodically incurred operating costs (grinding and inspection): the total LCC is measured in equivalent *monthly* cost while the operating costs occur per six months or longer. The minimized EMC is found when the preventive replacement interval is defined as 179 months. It is shown that at the later stage of the rail's lifecycle, the decisions on preventive replacement interval would not influence the cost criterion, total EMC, too much (EMC €556 at the 15th year versus EMC €669 at the 25th year).



Figure 35 Output of age replacement optimization (reference case: 12-month grinding interval)

The age replacement optimization is made by minimizing the total EMC or PV over infinity. The criteria are only useful for cost comparison, i.e., to find an economic optimum for preventive replacement interval, e.g., 15 years in this case, while they are not able to provide asset managers with the information about 'how much does it cost to own the asset in the optimized replacement cycle length', as the time span is infinity. In this case, PV of total LCC over infinity has to be converted to PV over the replacement cycle to inform the asset managers the exact amount of LCC.

- 1) Convert PV over infinity (€136541) to EAC by the capitalized equivalent worth factor (Eq.33)

$$EAC = PV_{\infty} \times r = €136541 \times 5\% = €6827$$

The EAC is a perpetual annuity so that it is a constant cash flow regardless of the time span, i.e., $EAC_{\infty} = EAC_{one\ cycle}$ (note 27).

2) Convert EAC to PV over 15 years by using the annuity factor (Eq.31.1)

$$PV_{15\text{ years}} = EAC \div (A/P, r, t) = €6827 \times \frac{(1 + 5\%)^{15} - 1}{5\% \times (1 + 5\%)^{15}} = €70862$$

The result can be interpreted as: given the rail degradation condition³⁴, current grinding interval as 12 months and cost data defined in Table 10, if one asset manager decides to set the preventive rail replacement interval (in Harmelen LCS) as 15 years, in which he can preventively replace the rail when the rail reaches the 15th year (in case no failure occurs in this period) or correctively replace the rail upon failure (and the next preventive replacement is scheduled after 15 years), probably he is able to own the asset at the minimized cost, €70862. Noted that the minimized cost here is not the minimized total cost over the life cycle but the minimized cost per unit time, i.e., the minimized EMC or total PV over infinity (which is the PV of EMC over infinity).

By contrast, given the modelling result that the total EMC at the 10th year is €628 (and total PV over infinity is €154123), follow the conversion procedure as presented above, the total PV over the life cycle (10 years) is €59505. It can be observed that, under the two scenarios, total EMC when preventive rail replacement is made at the 15th year is the minimum (EMC €556 at the 15th year versus EMC €628 at the 10th year), while, when it comes to the total PV over a lifecycle, the total PV in 10 years is the minimum (PV €59505 in 10 years versus PV €70862 in 15 years). It is not strange. As one rail under the 15-year age replacement policy stands 5 more years compared to the rails under the 10-year policy, the total PV in its lifecycle (15 years) should be larger than the latter. In sum, the total PV over a lifecycle has nothing to do with cost comparison and replacement optimization, and the EMC or total PV over infinity cannot provide an asset manager with the exact amount of money he has to save to own an asset.

³⁴ Corrosion-initiated failure is analyzed and validated by field data, while RCF-initiated failure is modelled by fictitious data.

5. Discussion

The preceding chapter demonstrates the application of the model and partly validate the model by field data. It presents the initial results of the age replacement optimization given the constraints (rail degradation, cost data, and maintenance intervals). This chapter is going to apply sensitivity analysis and facilitate better understandings about connections between model inputs and observations (i.e., optimized preventive replacement interval and LCC), in which the relevance of the policy study to different stakeholders is considered.

The sensitivity analysis is performed from two aspects, i.e., economic factors and policy (stakeholder and maintenance strategy), addressed in section 5.1 and 5.2, respectively.

5.1 Impact of economic factors

This section is going to vary the magnitude of operating cost, preventive replacement cost and discount rate to evaluate the impact of economic variables on the age replacement optimization and total LCC.

5.1.1 Operating cost

This research extends the age replacement model to incorporate the grinding and inspection cost in the age replacement optimization. The first task in the uncertainty analysis is to explore whether and how the inclusion of operating cost influences the optimization result.

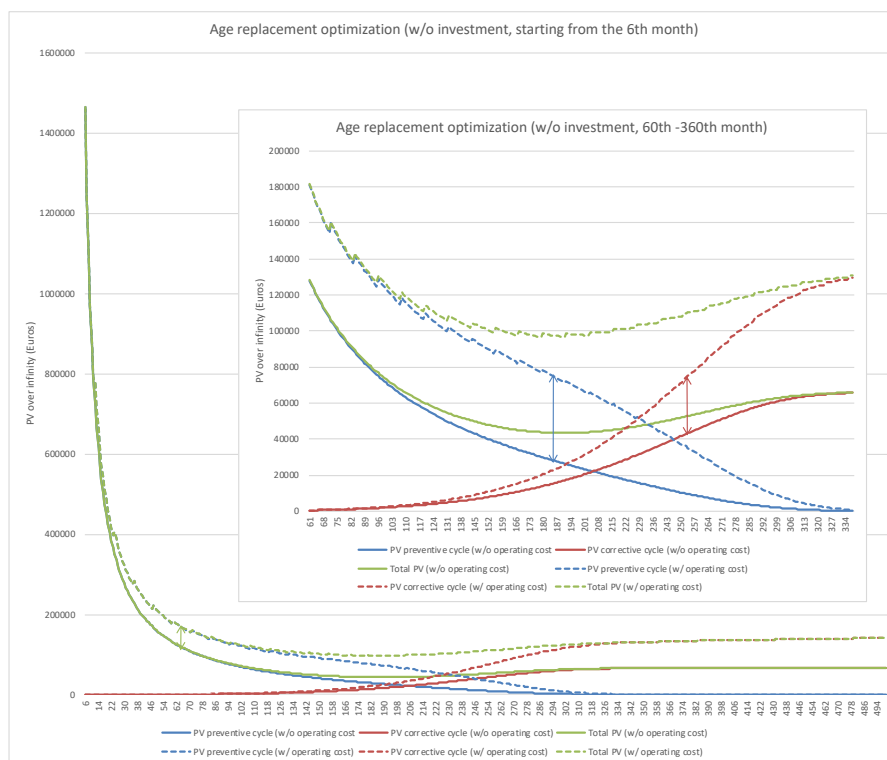


Figure 36 Impact of operating cost on age replacement optimization (excl. investment cost)

As shown in Figure 36, two situations are considered: the dotted curves represent the costs including the operating cost and the solid curves exclude the operating cost. Considering the initial investment is equally distributed over infinity and the constant value has no impact on the economic optimum for the preventive replacement interval, the investment cost is *excluded* here. The other cost elements, i.e., the preventive and corrective replacement cost remain the same in both scenarios, as defined in Table 10. The blue curves indicate the costs incurred in the preventive cycle and the red represent the costs in the corrective cycle. Their sum is total PV over infinity, indicated in green curves. The first observation is the difference (as shown in the green arrow) between the total PVs over infinity (with/without the

operating cost), which, indicating the contribution of the operating cost to the total PV over infinity, shows an obvious increase at the early stage of the asset's lifecycle and almost stays constant (but still a marginal increase) when they pass the optimization point, around 179 months (15 years).

The initial increase is caused by the cumulation of the operating cost, in which nearly all the operating costs are incurred in the preventive cycle (the blue and green dotted curves coincide at first, as presented in Figure 36), while, as time passes, the percentage of the operating costs in the corrective cycle gradually increases (as indicated in the red arrow) and, inversely, its percentage in the preventive cycle cost dramatically decreases (blue arrow), which is caused by the rail degradation. Combine Eq.35 and Eq.36, the equation for calculating the present value of maintenance costs (the sum of operating and replacement costs) over one replacement cycle is presented in Figure 37 (extended age replacement optimization), comparable to the equation for calculating the total expected replacement cost over a cycle as defined in the basic age replacement model (the numerator of Eq.1). The operating costs, denoted as $C_o(t)$, are split into two cycles in the extended age replacement model, governed by the reliability function $R(t)$ and CDF $F(t)$, respectively.

Extended age replacement optimization:

$$PV_m = \underbrace{C_p R(t_p) \alpha(t_p) + C_o(t_p) R(t_p)}_{\text{Preventive cycle cost}} + \underbrace{\sum_{t=1}^{t_p} C_c f(t) \alpha(t) + \sum_{t=1}^{t_p} C_o(t) F(t)}_{\text{Corrective cycle cost}}$$

Basic age replacement optimization:

$$PV_m = \underbrace{C_p R(t_p) \alpha(t_p)}_{\text{Preventive cycle cost}} + \underbrace{\sum_{t=1}^{t_p} C_c f(t) \alpha(t)}_{\text{Corrective cycle cost}}$$

Figure 37 The balance between preventive and corrective cycle cost in the age replacement optimization

It might be helpful to look into the curves of $R(t)$ and $F(t)$. As shown in Figure 38, the curve of reliability function $R(t)$ stays flat at first and begins to dramatically decrease after the 179th month (the optimum when the operating costs are included, as indicated in the solid arrow)/the 191st month (the optimum when excluding the operating costs, mentioned in the dotted arrow), and, the CDF curve, $F(t)$, shows an inverse trend, which leads to the percentage change of the operating costs as time passes.

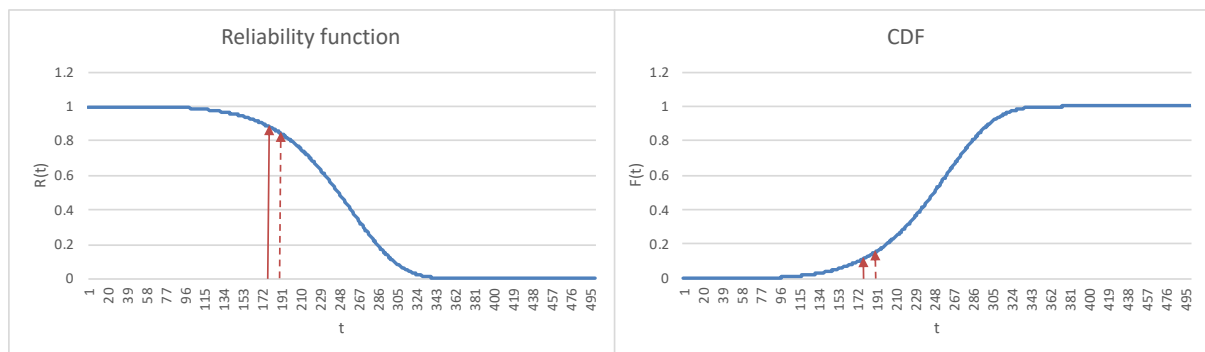


Figure 38 (Left) reliability $R(t)$; (right) CDF $F(t)$

As observed from Figure 37 and Figure 38, since the operating costs are split into two cycles and the age replacement optimization is made where the costs in the corrective and preventive cycles balance each other, the inclusion of the operating cost has limited impact on the optimization. Taking the grinding cost as an example, given the constant grinding interval as 12 months, let the one-time grinding cost range from €1700 to €5000, the age replacement model yields the same optimum, 179 months. If it varies from €100 to €1700, still, the model yields the same result, 191 months. For the inspection cost,

as it occupies a small percentage in the operating costs, their impact on the optimization can be neglected, based on the observation of the grinding cost.

However, the modelling shows a small deviation in the optimization results, i.e., 179 months (incl. operating cost) versus 191 months (excl. operating cost), which may be caused by the periodical incurrence of the operating costs. For instance, the grinding cost considered in the baseline scenario is €2000, incurred every 12 months. As presented in Table 11, the EMC (including the initial investment and operating cost) is €556.3³⁵ at the 179th month and shows an obvious increase at the 180th month, caused by the incurrence of the grinding cost, and gradually decreases until the 192nd month, when the next grinding cycle starts. By contrast, the EMC excluding the operating cost gradually decreases over the time and yield a minimum at the 191st month, €339.9. The model uses monthly discounting and the time unit is in months. The grinding cost is however not distributed over each month but depends on the intervention interval. The periodic incurrence of the costs results in the fluctuation of EMC over infinity and it can be observed that the EMC (including the operating costs) at the 179th and 191st month are very close.

Table 11 Comparison of total EMC (the 179th – 192nd month)

PR interval (months)	179	180	181	182	183	184	185	186	187	188	189	190	191	192
EMC (€; incl. investment & operating cost)	556.3	564.9	563.9	562.9	562.0	561.1	560.2	560.1	559.3	558.6	557.8	557.1	556.5	564.6
EMC (€; incl. investment)	341.5	341.2	341.0	340.8	340.6	340.4	340.3	340.2	340.1	340.0	340.0	339.9	339.9	340.0

The above observations are made based on the constant intervention intervals with the fixed one-time costs, as defined in Table 10. The reality may become more complicated, where the inspection interval, especially the visual inspection, would become more frequent at the later stage of one rail's lifecycle. The accumulation of the operating cost, in this case, will rise more quickly and may contribute more to the corrective cycle cost, as governed by $F(t)$, and the optimization time may move forward, i.e., the extended age replacement model advises to preventively replace the rail earlier, in order to avoid potentially higher accumulated operating cost and economic loss in case of rail failure.

This section only evaluates the magnitude of change in the operating cost, e.g., vary the one-time grinding cost in the range €100 - €5000. It can be drawn the variation in the magnitude of the operating cost can hardly influence the age replacement optimization, given the constant intervals and fixed costs (within the practical range) distributed over the lifecycle of the rails. Note excluding the operating costs implies the regular maintenance is not considered, in which the effectiveness of periodic grinding on reducing the risk of rail failures cannot be accounted for. In this case, the age replacement optimization result may deviate, which is addressed in section 5.2.1.

³⁵ The costs are rounded to 1 decimal place in order to observe the slight difference between the EMC at the 179th and 191st month, the same reason is applied in section 5.1.2. All other costs mentioned in the thesis are rounded to the integer.

5.1.2 Preventive replacement cost

Keep the basic grinding scenario (12 months) and the other cost data unchanged, this section considers 7 scenarios in regard to different preventive replacement (PR) costs, where both the initial investment and operating costs are included.

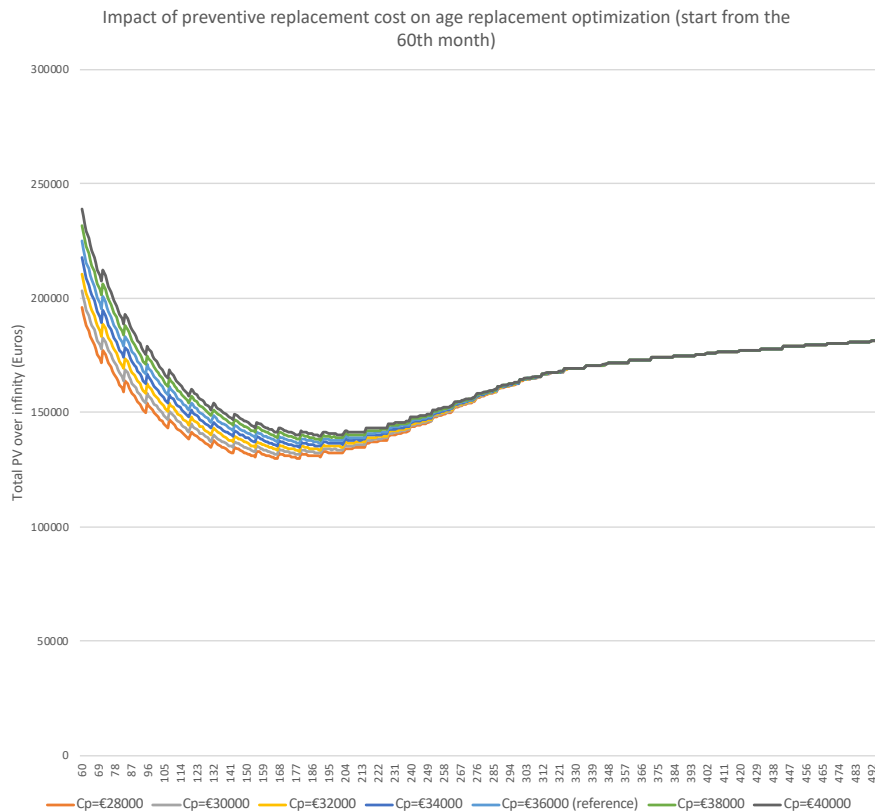


Figure 39 Impact of PR cost on age replacement optimization

As shown in Figure 39, the teeth on the curves are caused by the periodically incurred operating costs. Let the PR cost vary from €30,000 to €36,000, the optimization yields the same result, 179 months, as presented in Table 12. When the PR cost equals to €28,000, the economic optimums slightly change to 167 months. When the PR cost becomes larger, range from €38,000 to €40,000, the same result, 191 months, is found.

It can be observed that the difference in these optimized intervals is 12 months, which is, as stated in section 5.1.1, caused by the incurrance of grinding cost (every 12 months). In fact, with the PR cost = €28,000, the EMC when the PR interval is 167 and 179 months are very close, €528.6 and €529.0, respectively, which could create a policy window for the asset managers to make decisions on preventive rail replacement, i.e., one could look into the time frame around the optimized time advised by the age replacement model and take a decision³⁶ combined with the situation, e.g., resources (materials, labor), collaboration (with customers, contractors, and suppliers), etc. The thing is performing the preventive replacement before the next periodic grinding operation happens would be more cost efficient (it is the grinding operation that results in the fluctuation in total EMC). Another point is the delay of performing preventive replacement may lead to safety issues. The rails degrade

³⁶ Choose whether the 167 months or 179 months to be the preventive replacement interval in this case.

over time. It would be better in this case to look into $R(t)$ or $F(t)$, which mathematically measure the reliability condition of the rails, and define an acceptable reliability level to facilitate the decision making. Considering the rail degradation is a dynamic process and varies depending on the local conditions, it is also possible to carry out a thorough inspection around the optimized time and take decisions by combining the mathematical measures with the local conditions (e.g., bonding of Corkelast®, operating condition (MGT, speed), geometry condition in the transition zone, age of the rail, cracks in the rail, etc.).

It became clear from the interview that, for an 18-m long Harmelen LCS, the single-rail PR cost mostly varies from €30000 to €35000 (direct cost), with a few cases €27000 for direct cost and additional 20-25% for indirect cost. It was also understood that the total price of the PR (both rails) is €40000, which could be a ceiling price for the single-rail preventive replacement of an 18-m long Harmelen LCS, and €28000 - €40000 could be a reasonable range estimate for the PR cost (single rail). It therefore can be concluded that, from the practical point of view, the variation in PR cost only has a slight influence on the age replacement optimization.

In addition to the impact on the optimized PR interval, Table 12 presents the EMC, EAC and PV over the optimized replacement cycle under the different PR costs. The total PV over the cycle is calculated by following the conversion procedure presented in section 4.5. It can be observed that with an increase of €2000 in the PR cost, the difference in the PV over the optimized replacement cycle is not equal to €2000. Take €30000 and €32000 of the PR costs as an example (as they yield the same optimum), their total PV in 179 months are €68255 and €69124, respectively. The reason could be the impact of cost discounting and reliability condition of rails, $R(t)$, which is explained below.

Table 12 Impact of PR cost on age replacement optimization & total LCC over the optimized replacement cycle

Preventive replacement cost (€)	Optimized PR interval (months)	EMC (€)	EAC (€)	PV over the optimized replacement cycle (€)
28000	167	529	6487	64217
30000	179	536	6576	68255
32000	179	543	6660	69124
34000	179	549	6743	69993
36000 (reference)	179	556	6827	70862
38000	191	562	6903	74809
40000	191	568	6976	75601

According to the optimization result, the preventive rail replacement is made at the 179th month (around the 15th year), which means the PR cost is incurred at the end of the 15th year, so that the cost difference, €2000, is also incurred at that time. By using the present worth factor (Eq.30), the PV of the cost difference is calculated as $€2000 \times \frac{1}{(1+5\%)^{15}} = €962$. As addressed in section 3.1, two possible cycles of operation are involved under the age replacement policy, and one of which, preventive replacement cycle, is determined by the rail reaching a specified age t_p , with a probability $R(t_p)$. The PR cost, in

this sense, should be weighted by $R(t_p)$, so that $€962 \times R(179) = €850$ ³⁷. Convert €850 (PV) to EAC by the annuity factor (Eq.31.1), $€850 \times \frac{5\% \times (1+5\%)^{15}}{(1+5\%)^{15} - 1} = €83$. As observed from Table 12, the difference in EAC under the two scenarios (€30000 and €32000 of PR cost) is $€6660 - €6576 = €84$, close to the result directly derived from the cost difference in the PR cost, €83. The slight difference may be caused by the approximation of the numbers (round-off). When it comes to the total PV over a lifecycle, the cost difference under the two scenarios is $€69124 - €68255 = €869$, comparable to the results derived above, €850 (yearly discounting) and €854 (monthly discounting) (see note 37). The PV over the replacement cycle listed in Table 12 are calculated by EAC divided by the annuity factor (Eq.31.1). The deviation in EAC is amplified when considering the total PV over multiple years.

The above cost calculation is to illustrate how the PR cost contributes to the age replacement optimization. It also verifies the way of converting PV over infinity to PV over one lifecycle as presented in section 4.5. The proposed age replacement model supports the asset managers to find an optimized preventive rail replacement interval, based on the minimized total EMC or PV over infinity. Then the exact amount of money to be paid in the optimized interval can be found by calculating the PV over the optimized cycle, which might be useful in budget planning or possibly compare the cost at the same analysis period of similar rail assets³⁸.

5.1.3 Discount rate

The cost discounting accounts for the time value of money, as stated above. The discount rate plays a key role in cost discounting, which may significantly influence the present value of distant cash flows. For example, at a discount rate of 5%, a payment of €1000 in year 20 is worth €377 today. If the discount rate rises to 10%, the value of the future payment would drop about 61% to €149. The simple calculation reveals how small deviations in the discount rate can have a significant impact on the present value of the distant payment. As addressed in section 1.3, neglecting the cost discounting is the common problem in the related literature. The research takes the time value of money into account and it might be significant to investigate whether and how the discount rate influences the replacement optimization and total LCC under the age-based replacement policy. In most cases, the inclusion of cost discounting in the maintenance optimization models complicates the calculation. When it comes to the model applicability and practicability, there is always a tradeoff between the simplicity and accuracy. If it proves that the variation in the discount rate has limited impact on the age replacement optimization and total LCC, it would be wiser to neglect the time value of money when applying the model.

The research uses real discount rate and all the cash flows are indicated in real terms (implicitly include the impact of inflation/deflation) (note 23). Figure 40 presents the EMC curves with the varied discount rates, in which seven scenarios are considered: the discount rate varies from 1% to 13%, where 5% is the reference scenario. The economic optimums under the different scenarios are presented in Table 13, column 2. With the cost discounting, the variation in the annual discount rate slightly influences the age replacement optimization result, i.e., 1%, 3% and 5% yield the same optimum, 179 months; 7%, 9%

³⁷ $R(179) \approx 0.88385$. It is given by Excel calculation, governed by the 2-parameter Weibull distribution with parameters estimated by MLE.

If using monthly discounting, $€2000 \times \frac{1}{(1+0.004)^{179}} \times R(179) = €854$, slightly deviating from the yearly discounting result. 0.004 is the monthly discount rate when the annual discount rate is 5%. The deviation is caused by the approximation in time (179 months \approx 15 years) and round-off of the monthly discount rate.

³⁸ The ‘similar’ indicates the rail assets with similar failure mechanisms and maintenance interventions and can be modelled by life distributions (the *i.i.d* assumption holds).

and 11% have the same optimum, 191 months; 203-month interval is found for 13% discount rate. A trend could be observed in this case: discounting postpones the economic optimum. It makes the cash flows incurred at a later stage less valuable. The age replacement optimization is made based on a tradeoff between the costs in the preventive and corrective cycle. With the weight of $F(t)$, the corrective cycle cost only occupies a small portion of the total PV over infinity at first, and shows dramatic growth subsequently (Figure 38); however, its PV becomes less due to the discounting on the distant cash flows. The larger the discount rate, the less valuable the PV of the corrective cycle cost. The preventive cycle cost is the opposite: with the weight of $R(t)$, it is mostly incurred at the earlier stage. The larger the discount rate, the more weight the PV of the preventive cycle cost occupies in the total PV. Based on a tradeoff, the age replacement model advises to perform the preventive replacement later.

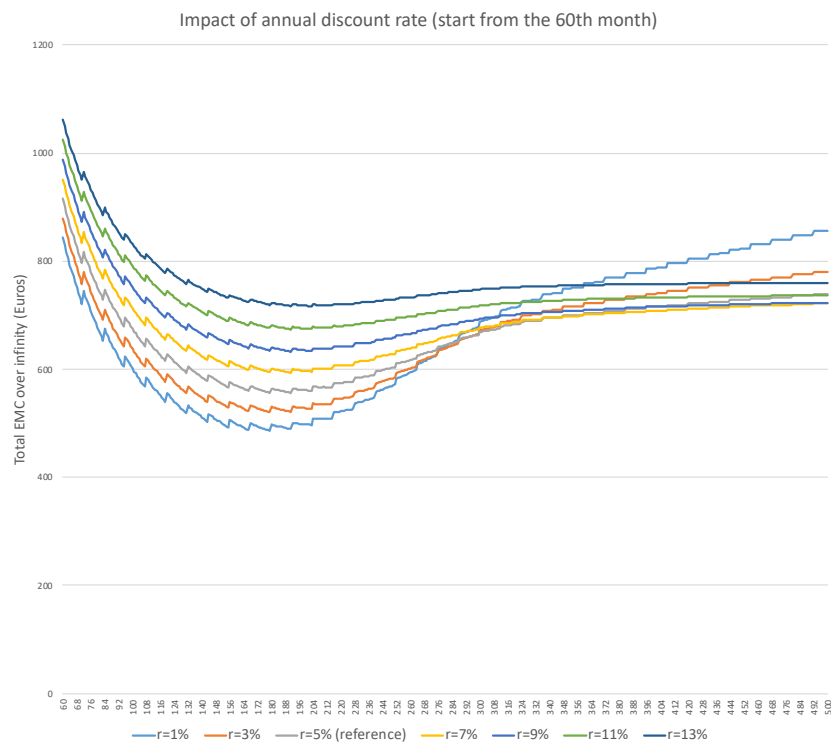


Figure 40 Impact of annual discount rate on age replacement optimization

When ignoring the time value of money, the optimum is consistent with the result of the lower annual discount rate, i.e., 1%, 3% and 5%, as indicated in Table 13, column 2. The optimization without cost discounting is found based on Eq.29, with the criterion ‘cost per month’, indicated in Table 13, column 5. Since the interest rate in this case is equal to zero, the cost discounting techniques, which derive the total EMC, EAC and PV, are not applicable. The figure indicated in Table 13 column 6, €82424, is the total expected cost over the cycle (the numerator of Eq.29), not measured in PV. Compare the result to the total PV over the same timespan with the cost discounting: when $r=1\%$, 3% and 5% , the total PV are €81263, €75512 and €70826, respectively. It is obvious that how small deviation in discount rate can significantly influence the total LCC with the same time span. Note that the LCC without discounting excludes the initial investment, while, with the cost discounting, the initial investment is equally distributed over infinity by discount rate. The fundamental age replacement model excludes the initial investment, as it has no impact on the replacement optimization. It however influences the calculation of total costs. When taking the initial investment into account, the cost per month (€560) and total cost in the optimized cycle (€82424) will become larger. And its deviation from the results (with cost discounting) will be amplified. It can be concluded that the discounting slightly influence the age replacement optimization, while it gains importance when calculating the total LCC and its impact cannot be ignored.

Then look into the total EMC and EAC as derived by the LCC techniques, as shown in Table 13 (column 3&4). With an increase in the annual discount rate, the total EMC and EAC at the optimums keep rising. It seems strange at first glance: a larger discount rate makes distant cash flows less valuable and the sum of the cash flows, total costs (here measured in EMC or EAC), should have become smaller. The modelling result however is the opposite.

Table 13 Impact of discount rate on age replacement optimization & total LCC over the optimized replacement cycle

1	2	3	4	5	6
Discount rate (%)	Optimized PR interval (months)	Total EMC (€)	Total EAC (€)	Cost per month (€)	PV over the optimized interval (€)
Without discounting	179	-	-	560	82424 (not PV)
r=1	179	486	5861	-	81263
r=3	179	520	6325	-	75512
r=5 (reference)	179	556	6824	-	70826
r=7	191	594	7354	-	69470
r=9	191	633	7904	-	65706
r=11	191	674	8491	-	62653
r=13	203	716	9099	-	61228

It becomes clear when splitting the total EMC into EMC of maintenance cost (the sum of replacement & operating cost) and EMC of initial investment, as presented in Table 14. With an increase in the annual discount rate, the EMC of the maintenance cost decreases, which is normal, while the EMC of initial investment shows a dramatic increase. The reason is the capitalized equivalent worth (Eq.38). The initial investment is considered as a perpetual annuity, i.e., equally distributed over infinity, in which its value of EMC is governed by the discount rate. The change in the discount rate has a significant impact on the EMC of investment. Sum the two EMC elements, the total EMC still shows a rising trend with the increased discount rates. The same is applied for the increased trend in the total EAC (Table 13, column 4). The difference of the EMC and EAC lies in the time units and discount rate (yearly or monthly).

Table 14 Cost components of total EMC under different annual discount rate

Discount rate (%)	Total EMC (€)	EMC maintenance cost (€)	EMC initial investment (€)
r=1	486	453	33
r=3	520	421	99
r=5 (reference)	556	393	163
r=7	594	368	226
r=9	633	345	288
r=11	674	325	349
r=13	716	307	409

5.2 Policy impact

This section looks into the policy impact and evaluate the model sensitivity from two perspectives, i.e., the maintenance policy (grinding frequency) and replacement optimization from the PGO contractors' point of view.

5.2.1 Grinding frequency

The extension of the age replacement model is aimed at incorporating the operating cost in the preventive replacement optimization. In section 5.1.1 it proves the magnitude change of the operating cost has limited impact on the economic optimum for the preventive replacement interval, while the observation is made with the fixed grinding interval, $T_{pm} = 12$ months. This section is going to vary the grinding interval to evaluate this maintenance decision variable on the rail degradation, preventive replacement optimization and total LCC.

Figure 41 presents the impact of grinding interval on the economic optimum for the preventive replacement interval, where 6 scenarios are considered and the 12-month interval is the reference case. The first observation is the change in grinding intervals leads to varied trends of EMC curves: they all keep decreasing at first but later they start to cross each other (approximately from the 150th month), which is caused by the assumption that the *current grinding interval (T_0) is 12 months*, which influences the rail reliability (represented by the adjusted hazard rate for modelling RCF-initiated failure, Eq.24 and Eq.26) and in turn causes the change in the EMC curves. Typically it is observed that the tails of the EMC curves are flatter when the grinding interval is below the 12 months, while with $T_{pm}=14$ or 16 months, there is an inflection on the curve.

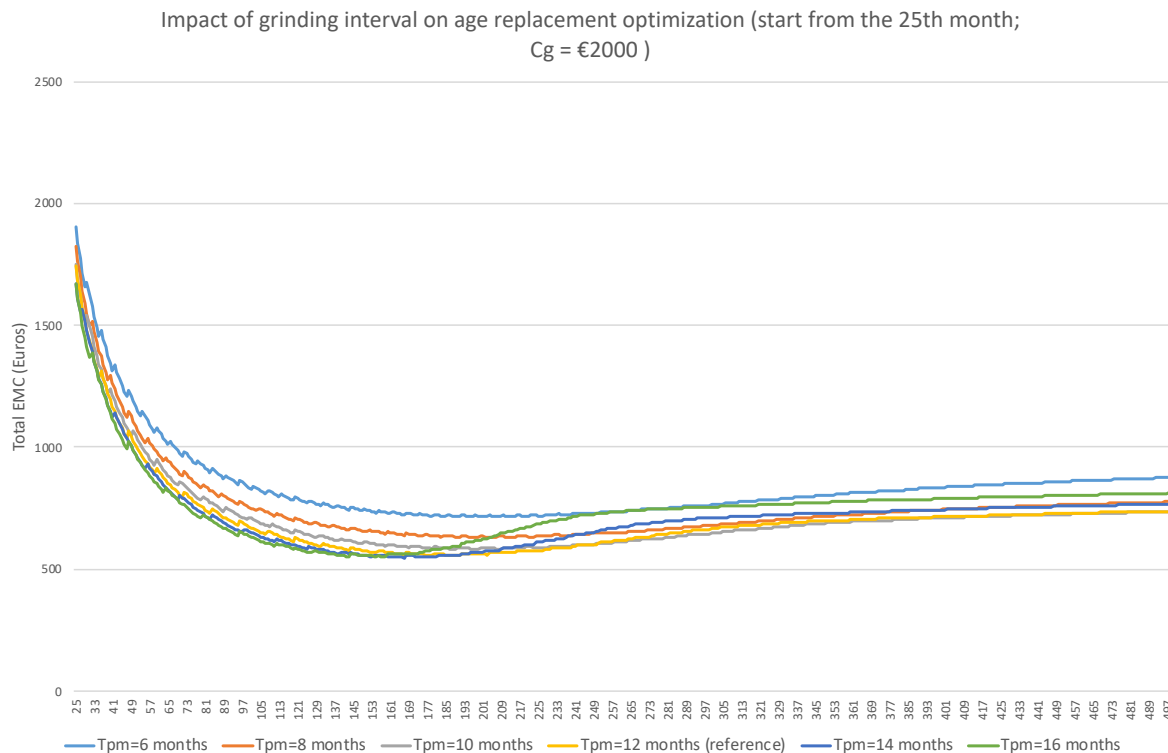


Figure 41 Impact of grinding interval on age replacement optimization (grinding cost €2000)

Recall Eq.24 for calculating the hazard rate of RCF surface defects, when both the current grinding interval T_0 and the grinding interval variable T_{pm} equal to 12 months, the equation is simplified to the basic formula of the Weibull hazard function (Eq.5), as the adjustment factor $\left(\frac{T_{pm}}{T_0}\right)^\beta$ (Eq.24) equals to 1. To capture the impact of grinding operations on the rail degradation, Figure 42 presents four graphs

of alternative reliability measures, namely CDF, PDF, reliability function and hazard rate, under the different scenarios regarding the grinding intervals, which are estimated based on MLEs (Table 9), Eq.5, Eq.7, Eq.8.1, Eq.9 and Eq.26, considering the two failure modes. It is obvious that in the total hazard rate graph (calculated by Eq.26), taking the curve where $T_{pm} = 12$ as a baseline, with more frequent grinding operations ($T_{pm} = 6, 8$ or 10), the total hazard rate shows a slight increase over time, as the adjustment factor lower the value of the RCF hazard rate. By contrast, $T_{pm} = 14$ or 16 , the adjustment factor is greater than 1 and leads to the larger RCF hazard rate, which in turn causes the dramatic increase in the total hazard rate curves over time.

Combining Figure 41 and Table 15 (column 2&3) it can be observed that the more frequent grinding operations postpone the economic optimums for preventive rail replacement interval. It is caused by the impact of grinding on retaining the rail reliability, i.e., the operations could to some extent control the incurrence and propagation of squats. The reliability modelling in Excel (two failure modes) shows when $T_{pm} = 6$, MTTF = 280 months (23 years); when $T_{pm} = 16$, MTTF = 195 months (16 years). The figures are not reliable as the RCF failure data is fictitious, while the comparison of MTTF under the two grinding policies is able to reveal the existing PM optimization model (see section 3.3.1) may overestimate the impact of PM on retaining the asset reliability. One assumption of the model is: the asset may degrade much slower under the current PM policy, compared to not performing any maintenance actions (see the derivation of Eq.22). Apparently, the effectiveness of PM varies and it seems like the model expects too much on the impact of PM, especially for minor maintenance actions.

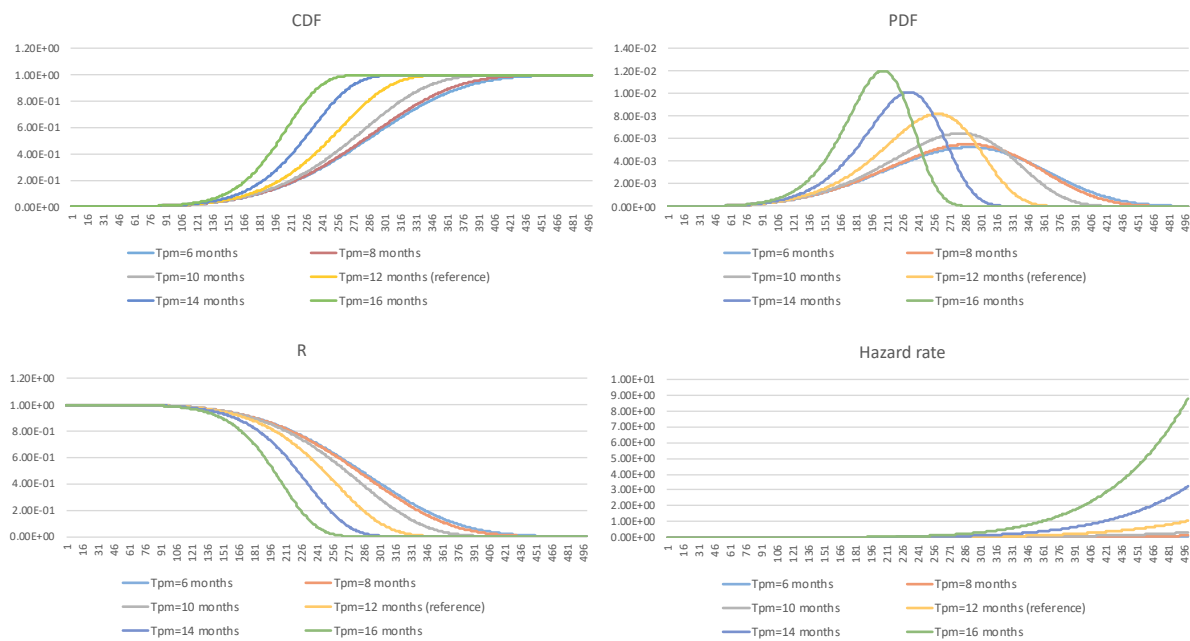


Figure 42 Impact of grinding operations on rail reliability (T_0 is assumed to be 12 months)

Then look into the influence of grinding intervals on the LCC. As presented in Table 15 (column 4), with less frequent grinding operations, there is a decreasing trend in the total EMC. An exception is the scenario where $T_{pm} = 16$. The PV over the optimized interval also shows the same tendency. It is considered that the decrease in the total PV may be caused by the reduced time horizons (column 2). Therefore the same analysis period (15 years, the optimum for the reference scenario) is created to calculate the PV over the same time span to explore whether it is cost efficient to perform the grinding operations more frequently during the lifecycle of the rails in the Harmelen LCS. The result is quite confusing. As indicated in column 6, the relation between the grinding interval and total PV over the same time horizon is non-monotonic, where the PV decreases at first but increases in the end. In this case, another cost scenario is considered, changing the one-time grinding cost to €500.

Table 15 Impact of grinding intervals on age replacement optimization & total LCC (when grinding cost is €2000)

1	2	3	4	5	6
Grinding interval (months)	Optimized PR interval (in months)	Optimized PR interval (in years)	Total EMC at the optimized time (€)	PV over the optimized interval (€)	PV over the same PR interval (e.g., 15 years) (€)
6	203	17	714	98794	91441
8	199	17	630	87186	81169
10	199/189	16/17	582.1/582.2	80542/77441	74407
12 (reference)	179	15	556	70862	70862
14	167	14	547	66475	70159
16	143	12	552	60024	73725

Figure 43 presents the comparison of the EMC curves when the one-time grinding cost is €500 and €2000. The EMC curves with $C_g = €500$ show a similar trend to the curves of the other: an inflection on the EMC curve with $T_{pm} = 14$ and 16; the tails of the other EMC curves look flatter. The difference lies in the magnitude of the total EMC. When $C_g = €500$, the more frequent grinding operations show an obvious cost advantage at a later stage, while if $C_g = €2000$, the advantage disappears. With such a high one-time cost, the more frequently the grinding activities being performed, the larger the total EMC.

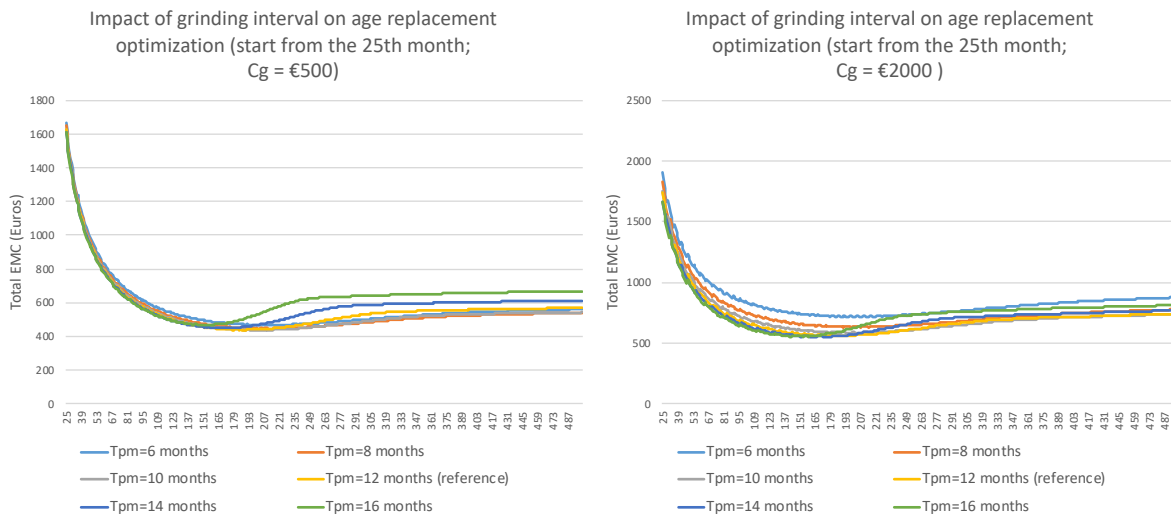


Figure 43 Impact of grinding interval on age replacement optimization (grinding cost €500 versus €2000)

Follow the same calculation procedures as performed in the scenario of $C_g = €2000$, Table 16 presents the optimized interval, the total EMC and PV in the optimized interval and PV over the same analysis period. As shown in column 2&3, the same conclusion can be made that the frequent grinding operations delay the optimums for preventive replacement interval. However, the variation tendency in the cost is complicated except column 5, where a decreasing trend is observed, influenced by the reduced timespans (column 2). The Total EMC (column 4) initially decreases but shows a slight increase afterward, so does the PV over 15 years (column 6). This observation is similar to the result in the scenario of $C_g = €2000$. It is considered that, in both scenarios, the initial decrease in the total EMC is caused by the reduced total grinding cost (with the longer grinding intervals) and the subsequent

growth is influenced by the rail degradation (less frequent grinding leads to the higher CDF and with the weight of CDF the corrective replacement cost weighs more in the total EMC).

Table 16 Impact of grinding intervals on age replacement optimization & total LCC (when grinding cost is €500)

1	2	3	4	5	6
Grinding interval (months)	Optimized PR interval (in months)	Optimized PR interval (in years)	Total EMC at the optimized time (€)	PV over the optimized interval (€)	PV over the same PR interval (e.g., 15 years) (€)
6	215	18	466	66783	60500
8	215	18	445	63842	57730
10	209	18	436	62611	56450
12 (reference)	191	16	437	58097	56158
14	167	14	447	54348	57441
16	155	13	466	53680	62329

Compared with the impact of financial variables on the model output, the grinding interval seems to have a significant influence on the proposed model, as the decision variable directly influences the rail degradation and in turn cause the variation in LCC and age replacement optimization. The more frequent grinding operations is effective in reducing the accumulated degradation of the rails and therefore postpone the optimized preventive replacement time.

However, the observations are not able to justify the cost efficiency of the grinding actions. It reveals the LCC over the same time horizon is not monotonically related to the grinding frequency. The fact is that the LCC is not only influenced by the grinding frequency, but other factors, e.g., the one-time grinding cost, rail degradation, preventive rail replacement interval, etc. The failure data regarding the RCF defect (squats) are fictitious and there is a high level of uncertainty in the cost data. It is recommended first collect reliable failure data with regard to the RCF failure modes and clearly define the one-time grinding cost specific to the Harmelen LCS. Then the one-time grinding cost and rail degradation can be somewhat fixed and the cost-effectiveness of grinding policy could be evaluated.

5.2.2 PGO contractors

The sensitivity analysis in the previous sections lays emphasis on the asset owner, ProRail. This section changes the problem setting and extends the model application to the PGO contractors. Characterized by different norms and values, the cost modelling result for the latter is expected to be different.

As stated in Chapter 2, the grinding operations and ultrasonic inspection are currently within the national programme so that the cost and interval regarding the grinding and ultrasonic inspection are set as zero in Table 17³⁹. The PGOs also do visual inspection⁴⁰ from time to time so that the cost for the

³⁹ The cost data presented in Table 17 refers to Appendix A, .

⁴⁰ Alternative inspection techniques are involved in detecting the rail defects in the Harmelen LCS, e.g., Strukton applies G-scan equipment after 15 years of rail installation. It is not extensively used by other PGOs. The information regarding its one-time cost and frequency is limited so that it is excluded. Besides, the frequency and cost of visual inspection depends on regions. Sometimes the visual inspection is for the whole network in their

visual inspection is retained. They are only responsible for maintaining the rail assets and thus the initial installation cost is zero. €30000 is defined for direct costs of the single rail replacement (both for the preventive and corrective). 20% addition accounts for the indirect cost in the preventive replacement and 30% addition for the corrective maintenance. A point of attention is the penalty cost, which would be of great importance to the PGOs. In case of preventive replacement, there is a penalty for unscheduled possession, which is around €10000-20000. This text takes an average, i.e., €15000. In case of an instant break, there is no penalty cost, but failure costs. Every failure leads to a negative bonus, which is around €6000 each plus €7500 for additional monetarized minutes, i.e., in total €13500.

Table 17 Input cost data (PGO contractors)

Input values (monetary unit: €)							
Annual discount rate	r	5%		Preventive grinding cost	Cg		0
Monthly discount rate	i	0,00407				ultrasonic inspection cost	0
Initial investment	Cin	0		Inspection cost	Ci	visual inspection	300
Preventive replacement cost	Cp	51000	*30000 euros for single rail replacement; additional 20% for indirect cost (work preparation); additional cost for unscheduled possession time	Grinding interval	Tpm	0	months
Unscheduled possession	Cun	15000	*10000-20000 euros (penalty for unseceduled possession in case of preventive replacement)	Ultrasonic inspection interval	Tui	0	months
Failure cost	Cf	13500	*6000 euros for negative bonus (in case of failure); 7500 euros for additional monetarized minutes	Visual inspection interval	Tvi	12	months
Corrective replacement cost	Cc	52500	*30000 euros for single rail replacement; additional 30% for indirect cost (especially mobilization cost); failure cost is included				

With the input cost data defined in Table 17, the modelling of preventive replacement optimization for the PGOs yields the economic optimum as 311 months (approximately 26 years), where the EMC is €158. As shown in Figure 44, approximately from the 240th month (20 years), the EMC curve stays almost flat to the end⁴¹: it fluctuates between €158-€170. In Chapter 4, the statistical analysis on the corrosion failure data has revealed that roughly 63.2% of the rails in the Harmelen LCS fails by 25.82 years due to the corrosion. It indicates there is a certain percentage of rails can survive after the 25th year, possibly extend to more than 30 years. Given the deterministic cost data and rail reliability condition, it can be drawn that, if the rails still survive at the 20th year, the cost influence of performing the preventive rail replacement from the 20th year to its failure does not differ too much. From the cost point of view, one would opt for a corrective replacement strategy. In case that rail fracture occurs in the Harmelen LCS, normally it does not have risks of derailment, and the option for the corrective replacement scenario is valid, from the cost point of view.

PGO regions, not specific to the Harmelen LCS. The rough estimate given from the interview is less than once a year so that the visual inspection here is assumed to be once a year and each costs €300.

⁴¹ The analysis period of the reliability analysis is 500 months (about 42 years).

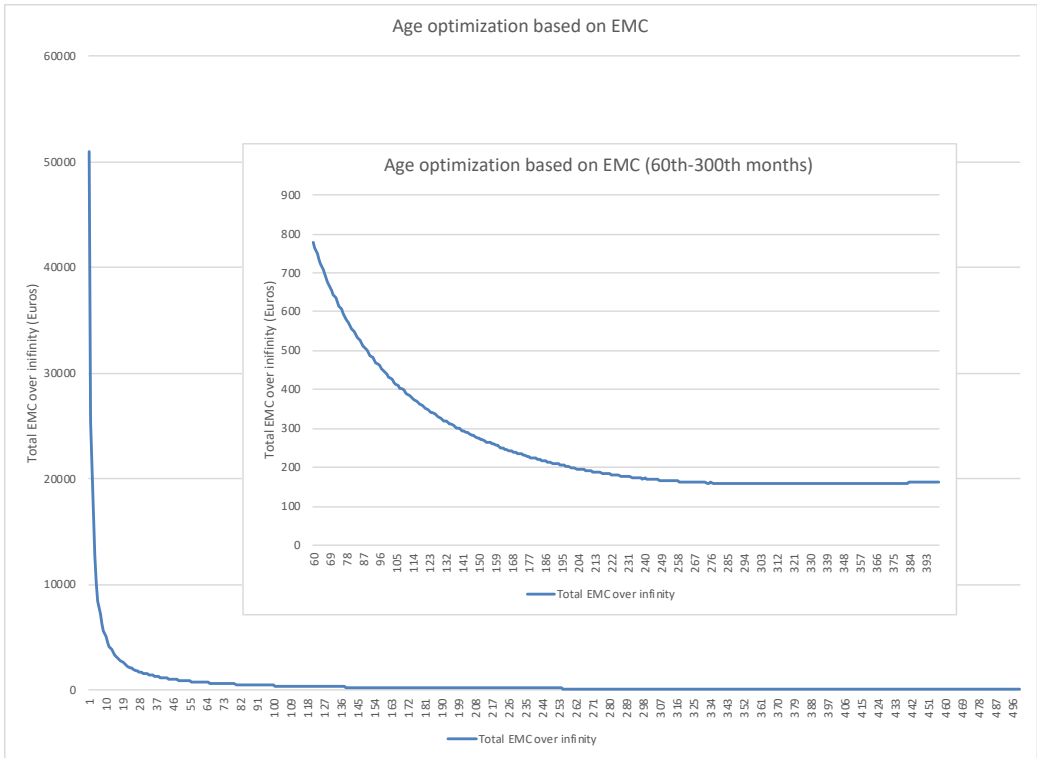


Figure 44 Age replacement optimization (PGOs)

6. Conclusions & Recommendations

6.1 Conclusions

In this thesis, a reliability-based LCC model is developed for the Harmelen LCS, in which the interaction between LCC and uncertainties involved in the rail degradation (corrosion and RCF failure modes) and maintenance strategies (preventive replacement interval, grinding interval, ultrasonic and visual inspection interval) are incorporated. The application of the model has been demonstrated and partly validated by the rail break data. With the cost data collected from the interviews, the model executed in Excel found an optimized time interval to inform the decision making on preventive rail replacement in the Harmelen LCS, in which the total LCC over the optimized life cycle has been calculated to provide one asset manager with the exact amount of money he has to save to own the asset.

6.1.1 Failure mode & failure data

Considering two competing failure modes exist in the rail degradation, it is proposed to separate the failure modes when collecting the life data of the rails in the Harmelen LCS. Normally the reliability analysis for the rail assets is performed based on the exact failure time data. Confronted with the practical issues where the potential rail failures caused by RCF defects can be prevented and the exact times of potential RCF-initiated rail breaks can hardly be observed, the research proposes to collect ultrasonic inspection reports and use interval data to infer and model the potential failures caused by RCF. Due to the inadequacy of the ultrasonic inspection reports, the intervals where the RCF-initiated rail failure may occur are assumed based on one ultrasonic inspection report and the 20-year expected lifespan of the rails in Harmelen LCS. The assumption is aimed at demonstrating how the proposed model can be applied, i.e., how to model the rail failure caused by the RCF failure mode; how to collect the data when exact failure times cannot be observed; how to process the data and calibrate the model; and, how to combine the two failure modes and evaluate the overall reliability of the rails.

In the model validation, it proves that the 2-parameter Weibull probability distribution is a reasonable fit to model the rail failures (by corrosion) in the Harmelen LCS. With the Weibull shape parameter, a conclusion can be drawn that, due to the corrosion, roughly 63.2% of the rails in the Harmelen LCS fails by 25.82 years.

6.1.2 Maintenance interventions & extension of age replacement model

The Harmelen LCS does not require much maintenance during their lifetime. Grinding operations and rail replacement are dominant maintenance activities. Both can be preventive and corrective. The replacement cost is perceived as the most important influencer in the LCC of the systems by many asset managers. It could be the first trial to apply the age replacement model in the railway industry to investigate the impact of preventive replacement decisions on LCC and seek an economic optimum for the preventive replacement interval. The optimum suggested by the age replacement model may ignore the safety issues. For most of the railway assets, the rail reliability may outweigh the cost optimization, while given the fact that in most cases there is no risk of derailment when a rail break occurs in the Harmelen LCS, the possible 'run-to-failure' strategy advised by the age replacement model would be effective.

The fundamental age replacement only considers a tradeoff between the preventive and corrective replacement cost. It is unknown whether the operating costs used for routine maintenance or perhaps extending the rails' lifespan influence the age replacement optimization. The research extends the age replacement model to incorporate the preventive grinding and inspection (ultrasonic & visual) cost in the replacement optimization. To investigate the impact of grinding policies on the optimization, a PM optimization model that was proposed in the scientific literature is included.

The research defines a reference case, as presented in Table 10, and the model advises to specify the preventive rail replacement interval as 179 months, in which the total EMC and PV over infinity are minimized, €556 and €136541, respectively. By converting the PV over infinity to the PV over the optimized replacement cycle, the exact amount of money that is needed to own the asset has been found,

which is €70862. Note the optimization result is based on the rail degradation modelling (influenced by the fictitious data in regard to the RCF failure mode) and point estimates of the cost data. The optimum could be unreliable, but the model application in this text is aimed at demonstrating the use of the model. It is expected to have more practical significance when more data is available, i.e., rail break data, ultrasonic inspection records, routine maintenance and replacement costs defined based on the cost statements.

6.1.3 Uncertainty exploration in age replacement optimization

- Economic factors

Due to the nature of the age replacement model, the operating cost is split into preventive and corrective cycles, governed by the rail reliability, so that the inclusion of the operating cost can hardly influence the age replacement optimization. As for the PR cost, although it is not split like the operating cost, its variation also has limited impact on the optimization, given the range estimation €28000-€40000. An interesting observation is the time difference in these optimums under the different PR cost scenarios are 12 months, which is caused by the predefined grinding interval. It is the grinding cycle that leads to the fluctuation in the cost criterion, total EMC. With the observations in the LCC under the different PR cost scenarios, it is concluded performing the PR before the next periodic grinding operation happens would be more cost efficient.

Compared to the magnitude of the costs, the discount rate seems to have a more significant impact on the optimization. Discounting, with an increase in the discount rate, postpones the economic optimum for the preventive replacement interval. Moreover, a small deviation in the discount rate significantly influences the total LCC over a lifecycle. This figure is of importance as it provides one asset manager with the exact money he has to pay to own or manage an asset in a certain time period, which could be used for budget planning and asset portfolio management. This research uses 5% annual discount rate as a reference scenario. To make the replacement optimization and total LCC calculation more robust, it is necessary to carefully define the discount rate in the model application. The recommended way is to use the weighted average cost of capital, calculated by checking a firm's balance sheet, as the discount rate.

- Policy

The grinding interval is influential in the age replacement optimization, as it is closely related to the rail degradation. The frequent grinding operations are effective in reducing the accumulated degradation of the rails and therefore postpone the optimized replacement age. The inclusion of grinding impact on the rail degradation is achieved by the existing PM optimization model. Opting for different grinding intervals result in distinct rail degradation patterns. The calculation of MTTF with different grinding policies reveals that this model may overestimate the impact of PM on the asset reliability. Moreover, the basic assumption in this model is the failure data has already been influenced by the current PM interval. This research assumes the current grinding interval to be 12 months, while there is no link between the current grinding interval and failure data (for RCF), as the data are fictitious. However, when collecting the field data regarding the RCF defects, it would reveal that the assumption of the constant PM interval is unrealistic. For instance, considering the expected lifecycle of the rails in the Harmelen LCS is 20 years, in such a long time period, the maintenance policies may change. The PGO contract period is 5 years, one Harmelen LCS could be maintained by different parties during its lifetime. In most cases, how and when to maintain railway assets are in the hand of asset managers. It is hard to have unchanged maintenance policies over the lifecycle of the railway assets.

Comparable to the reference case, the age replacement model provides the opposite suggestion for the PGO contractors, 'run-to-failure' strategy, which is caused by the penalty cost. Having a failure is actually cheaper than doing a preventive replacement if one only considers the penalty. Possibly it could be a point of attention for the asset owner to improve the outsourced maintenance management and drive better performance.

6.2 Recommendations

6.2.1 Model application in the Harmelen LCS

- *Include or exclude the RCF failure mode*

In practice 90% cases of rail replacement in the Harmelen LCS are preventive, while the research has not gained sufficient insight into this percentage. The first task of the model application is to verify the necessity for including the RCF failure mode. With more failure data, if it proves that the preventive cases are mostly corrosion related, it is possible to exclude the RCF failure mode from the reliability modelling and cost optimization. If not, the RCF is supposed to be incorporated and the expert judgment is proposed, otherwise the derived $R(t)$ and $F(t)$ would be highly unreliable. Follow the model step 1, 2, and 3, it is expected to determine a model being fitted to the RCF-initiated failure data, and, combining the proposed 2-parameter Weibull distribution (for modelling corrosion failure), it could be more accurate to represent the population characteristics (the variation in time to failures). With the estimated parameters, the characteristic life of the rails caused by each failure mode can be calculated; then the dominant failure mode would be clear.

This research assumes the independence between the corrosion and RCF failure modes, which is verified in the rail break record (failure mode analysis) provided by ProRail. If, in the future, with more information and data about the Harmelen LCS it proves that there is an interaction between the two, the more general competing risk model would be recommended. But it is very complicated as one has to know how the random failure times caused by the failure modes are correlated.

- *Time or MGT*

In most cases the statistical analysis about the rail failure is measured in traffic tonnage (MGT), with the focus on the RCF failure mode. The proposed model provides answers to the question ‘*when would be the most cost efficient to preventively replace the rails in the Harmelen LCS*’ and ‘*how much money does one asset manager have to save to own the asset in the optimized lifecycle*’. The optimum for the preventive replacement interval is time-based. Considering the corrosion failure mode is an important contributor to the rail failures in the Harmelen LCS, time is to some extent a good indicator. The question about ‘*whether to choose age-based or MGT-based replacement*’ depends on the dominant failure mode. In case the RCF damage contributes a lot in the preventive cases, it is proposed to use the unit MGT in the reliability analysis (for RCF-related failure), while, in this case, it seems like the cost discounting cannot be incorporated in the MGT-based model. The age replacement model could still be valid but it needs input about average annual tonnage, i.e., convert the accumulative MGT to time by average annual tonnage. The optimized PR (time) interval in this way is linked to the traffic condition and combine the reliability analysis of corrosion-initiated failure (governed by time), the total reliability of the rails in the Harmelen LCS can be more accurately evaluated.

- *Grinding interval*

The grinding frequency in ProRail is defined by traffic tonnage and curvatures. Follow the grinding practices in DB, the research sets 15 MGT equal to 12 months of train operations as an average to overcome the challenge of data gathering and investigate the grinding policies on the rail degradation. It is necessary to collect more information about the grinding practices in ProRail (like Figure 30) and possibly look into the grinding history to check whether the grinding operations have been performed with a fixed interval, 15 MGT or other. However, one step back, if the preventive cases are mostly corrosion-related, it seems like the grinding operations can hardly influence the rail degradation in the Harmelen LCS, as the grinding has nothing to do with rail corrosion. It would be wise in this case to leave out the grinding issues.

- *Inspection interval*

The modelling in this research defines the fixed visual inspection interval due to the inadequacy of data. The reality may become more complicated, where the inspection frequency would be constant in the first ten years of the rails but later increase over time. The recommended way is to define fixed (average)

inspection intervals with regard to small time spans. For instance, define a 30-year time horizon, in the first ten years, the frequency could be once per year. And in the 10th-15th year, it increases to be once per 10 months, and so on. The model is able to take changeable inspection intervals into account. The thing is the decision about it depends on the asset managers and local conditions. It is better to adapt the model according to their own standards.

- *Impact of technology development*

The age replacement model, life distribution (Weibull) and perpetual annuity (where $EMC_{cycle} = EMC_{\infty}$ in LCC techniques) share the common assumption: *i.i.d.* It may become problematic when it comes to the technology development; e.g., an improved manufacturing process or new materials lead to a more reliable component, and, the failure behavior of the rails in the Harmelen LCS would change. The potential failure times of new rails in this case and the broken rails that were recorded in the failure history is still independent (as every failure leads to a full replacement) but may not have a common distribution or they share a common distribution but with different parameter values. A point of attention is pre-coating measures are now being tested and applied in the rails of the Harmelen LCS. It is expected to effectively prevent the rail corrosion and possibly extend their lifespans. The output of the reliability analysis in this case may become useless after 10 years, i.e., the proposed distribution model cannot account for the variability in time to failure of the rails in the population of the Harmelen LCS. It is therefore recommended in case of the major technical evolution, like the introduction of new materials and new maintenance interventions, collect the updated field data and redo the reliability analysis, and possibly redefine the cost data with regard to the maintenance activities, to justify the LCC output and facilitate the replacement decisions.

- *Failure data*

The barrier confronted in the data gathering stresses the importance of field data record. It is proposed to link the inspection time (when significant rail defects are detected) and rail failure time to the traffic loading (accumulative MGT) in the ultrasonic inspection reports and rail break records, respectively. It is recognized in the literature that the RCF damage is mainly governed by the traffic tonnage. Making more complete inspection reports would be helpful for modelling the rail RCF degradation, and, linking the tonnage to the failure time in the rail break record is aimed at identifying whether the time or tonnage is the important contributor to the instant rail breaks in the Harmelen LCS, which could be supported by the correlation analysis. It would also be better to link the accurate information regarding the track installation to the rail failure records. After all, better practices in recording the failure data are able to support the failure analysis and facilitate better understanding about the failure behaviors of the rails in the Harmelen LCS, which could be adapted to improve the system development in R&D or manufacturing process (for system developers) and introduce new maintenance interventions (like the pre-coating does) to extend the system lifetime and strive for a more cost-efficient asset lifecycle management (for asset owners).

6.2.2 Applicability for other railway assets

- *The key role of the i.i.d. assumption*

When it comes to the model generalization, the first task is to verify whether the model assumptions are applicable to other types of railway assets. In a mathematical sense, the rails in the Harmelen LCS and other types of LCS are different. A full rail replacement is prompted in case of a break occurring in the Harmelen LCS, while the partial replacement is possible for the other LCS, as the rails are not restricted by the ‘no welding’ policy. The difference in the repair actions leads to the distinct system characteristics in the reliability analysis, i.e. non-repairable versus repairable. The premise of the proposed model is in line with the working assumption of the life distribution model (for modelling the non-repairable system), i.e., *i.i.d.* assumption. Whether the *i.i.d.* holds is the key to justify the use of the model for other assets.

In testing against the *i.i.d.*, as its name implies, it has two parts: one for checking the ‘identical distribution’; one for checking the ‘independence’. The former is aimed at checking whether the times

between failure follow a common distribution, which could be achieved by ‘trend test’: plotting the cumulative number of failures against the system age. The plotted points that approximately fall on a straight line imply no trend is present in the failure data (interarrival times of failures) and the data could be assumed to be identically distributed. To check for independence, test for serial correlation could be applied: plotting the interarrival times versus its earlier lag, i.e., the i^{th} time to failure versus the $(i-1)^{\text{th}}$ time to failure. Again, an approximately linear relation verifies the independence. But this method requires a large amount of failure data.

In the case of repairable systems, the i.i.d. assumption is retained in the renewal process model. As the renewal process and life distribution have the common premise, theoretical simplifications, as stated in section 3.2.2, are possible, where the life distributions and their analysis techniques are applicable. Then the failure data analysis can be connected to the proposed model: follow the procedures as proposed in Figure 29. The model could be used for seeking an optimized preventive replacement interval like the research has demonstrated. And, with the cost conversion method as mentioned at the end of Chapter 4, the total LCC over the optimized interval could be derived, which supports the asset managers to do budget planning or other asset management decisions.

If the i.i.d. assumption cannot be justified by the test for trend and serial correlation, NHPP model could be applied to model the trend in the failure data. However, the model generalization cannot go further, as the premise of the age replacement model is also i.i.d., so does the assumption made in the LCC discounting, $EMC_{cycle} = EMC_{\infty}$.

In case that the i.i.d. assumption is verified, it is recommended to consider the following aspects when applying the model.

- *Maintenance interventions*

Possibly the maintenance actions being performed for the other LCS differ from the actions involved in the Harmelen LCS. In addition to the replacement activity, the routine maintenance considered in this research is preventive grinding, ultrasonic inspection and visual inspection. The three are the common interventions that are applied to all. The cost used for additional interventions applied for the other LCS could be incorporated in the operating costs. Possibly the inclusion will not influence the age replacement optimization, while it may have a significant impact on the total LCC over the optimized interval, like the conclusion made in section 6.1.3.

- *Failure modes & dependence*

The railway assets are multi-component systems. The modelling focuses on the rail, in which its degradation is interactive with other components. The failure modes of the other LCS may differ from the rails in the Harmelen LCS and possibly multiple failure modes are involved. It is recommended to separate the failure modes in the data gathering and analyze their correlation to justify the competing risk model. If they are correlated, as stated in section 6.2.1, a more general competing risk model could be applied.

- *Safety constraints*

The limitation of the age replacement model is it only considers cost optimization and may compromise the track safety. The ‘run-to-failure’ strategy could be effective in the case of Harmelen LCS, while it is unknown about the safety issues in regard to the other railway assets. It is recommended when applying the age replacement model in the railway industry, be cautious about the reliability condition of the rails and take the safety constraints into account, i.e., include high risk costs in the optimization or predetermine an acceptable probability (e.g., 96% for the probability of rail break) and do cost optimization within the constraint. Considering the rail degradation is a dynamic process and it may vary depending on the local conditions, it is also possible to carry out a thorough inspection around the optimized time and take decisions by combining the mathematical measures ($R(t)$ or $F(t)$) with the local conditions (e.g., bonding of Corkelast®, operating condition (MGT, speed), geometry condition in the transition zone, age of the rail, cracks in the rail, etc.).

6.2.3 *Future improvement*

- *Reliability model*

The model validation is made by visual test and regression statistic R^2 criterion, where in addition to the Weibull distribution, exponential distribution is tried as a reference. It is however noted that the failure to rejection (by visual test and R^2 criterion) does not necessarily lead to the absolute model fit, which could only be considered as a reasonable model fit, as the non-rejection only means there is no strong statement to reject the preconceived model, given the sample data. The list of possible models for reliability analysis is endless and finding a model that best fits the data is often difficult. One basic principle in model validation is replicability of the results, which implies additional experimentation is generally required for model validation. More formal approaches, i.e., statistical hypothesis testing methods, would be recommended, like the *chi-square* (χ^2) *goodness-of-fit test* for deciding whether the specified model (with parameter estimates) is consistent with the sample data. The research does not perform the test as it requires a large sample data. Note that the validation by the hypothesis testing methods does not result in the absolute model fit, either. It just provides more evidence to test the model fit.

- *Global sensitivity analysis*

The research performs the sensitivity analysis to observe connections between the input variables and model outcomes. The results can tell how changes in one variable affect the outcome; however, it is insufficient to judge which input variable is the most influential one in a mathematical sense. The global sensitivity analysis could be applied to apportion output uncertainty to different sources of uncertainty in model input and evaluate the relative influence of input parameters.

Bibliography

- Ahmad, R., & Kamaruddin, S. (2012). An overview of time-based and condition-based maintenance in industrial application. *Computers & Industrial Engineering*, 63(1), 135-149.
- Ammar, M., Zayed, T., & Moselhi, O. (2012). Fuzzy-based life-cycle cost model for decision making under subjectivity. *Journal of Construction Engineering and Management*, 139(5), 556-563.
- ASSETRail. (2018). *Rapport Ultrasoon Spoorstaven*.
- Benard, A., & Bos-Levenbach, E. (1955). *The Plotting of Observations on Probability-paper*: Stichting Mathematisch Centrum. Statistische Afdeling.
- Blischke, W. R., & Murthy, D. P. (2000). *Reliability: Modeling, Prediction, and Optimization* (Vol. 335): John Wiley & Sons.
- Brealey, R. A., Myers, S. C., Allen, F., & Mohanty, P. (2012). *Principles of corporate finance*: Tata McGraw-Hill Education.
- Caetano, L. F., & Teixeira, P. F. (2015). Optimisation model to schedule railway track renewal operations: a life-cycle cost approach. *Structure and infrastructure engineering*, 11(11), 1524-1536.
- Campos, J. (2009). Development in the application of ICT in condition monitoring and maintenance. *Computers in industry*, 60(1), 1-20.
- Cannon, D., Edel, K. O., Grassie, S., & Sawley, K. (2003). Rail defects: an overview. *Fatigue & Fracture of Engineering Materials & Structures*, 26(10), 865-886.
- Christophi, C., & Mazarrasa, L. (2015). Vertical Hyper-Speed Train Hub Literally Flips High Speed Rail on its Head.
- Cleves, M., Gould, W., Gould, W. W., Gutierrez, R., & Marchenko, Y. (2008). *An introduction to survival analysis using Stata*: Stata press.
- Coria, V., Maximov, S., Rivas-Dávalos, F., Melchor, C., & Guardado, J. (2015). Analytical method for optimization of maintenance policy based on available system failure data. *Reliability Engineering & System Safety*, 135, 55-63.
- Draper, N. R., & Smith, H. (1998). *Applied regression analysis* (3rd ed. ed.). New York: Wiley.
- Ebeling, C. E. (2005). *An introduction to reliability and maintainability engineering*. Long Grove :: Waveland.
- edilon)(sedra. (2018a). EDILON Level Crossing Systems (LC).
- edilon)(sedra. (2018b). (ERS-HR) Rail Fastening System for High-Speed and Heavy Rail. *edilon)(sedra ERS*.
- Elmahdy, E. E. (2015). A new approach for Weibull modeling for reliability life data analysis. *Applied Mathematics and Computation*, 250, 708-720.
- Esveld, C. (2001). *Modern railway track*.
- Fernández, J. F. G., & Márquez, A. C. (2012). *Maintenance management in network utilities: framework and practical implementation*: Springer Science & Business Media.
- Gailienė, I., & Laurinavičius, A. (2017). The need and benefit of slab track: case of Lithuania. *Gradevinar*, 387-396.
- Gautier, P.-E. (2015). Slab track: Review of existing systems and optimization potentials including very high speed. *Construction and Building Materials*, 92, 9-15.

- Jardine, A. K., & Tsang, A. H. (2013). *Maintenance, replacement, and reliability: theory and applications*: CRC press.
- Kumar, S. (2006). *Study of rail breaks: associated risks and maintenance strategies*: Luleå tekniska universitet.
- Lindholm, A., & Suomala, P. (2007). Learning by costing: Sharpening cost image through life cycle costing? *International journal of productivity and performance management*, 56(8), 651-672.
- Liu, X., Lovett, A., Dick, T., Rapik Saat, M., & Barkan, C. P. (2014). Optimization of ultrasonic rail-defect inspection for improving railway transportation safety and efficiency. *Journal of Transportation Engineering*, 140(10), 04014048.
- Meeker, W. Q., & Escobar, L. A. (2014). *Statistical methods for reliability data*: John Wiley & Sons.
- Microsoftoffice. (2018). Define and solve a problem by using Solver.
- NeTIRail. (2015). *Practices and Track Technology Tailored to Particular Lines (Deliverable 2.2)*. Retrieved from <https://ec.europa.eu/research/participants/documents/downloadPublic?documentIds=080166e5adbffc9d&appId=PPGMS>
- Olofsson, U., & Nilsson, R. (2002). Surface cracks and wear of rail: A full-scale test on a commuter train track. *Proceedings of the Institution of Mechanical Engineers, Part F: Journal of Rail and Rapid Transit*, 216(4), 249-264. doi:10.1243/095440902321029208
- Patra, A. P., Söderholm, P., & Kumar, U. (2009). Uncertainty estimation in railway track life-cycle cost: a case study from Swedish National Rail Administration. *Proceedings of the Institution of Mechanical Engineers, Part F: Journal of Rail and Rapid Transit*, 223(3), 285-293.
- Popović, Z., Radović, V., Lazarević, L., Vukadinović, V., & Tepić, G. (2013). Rail inspection of RCF defects. *Metalurgija*, 52(4), 537-540.
- Overweg met zware overwegplaten type Harmelen, (2010).
- ProRail. (2012). *Spoorstaafgebreken*. ProRail.
- ProRail. (2018a). *Breuken Harmelen 2015-2018*.
- ProRail. (2018b). *Spooronderhoud / PGO*.
- Rahman, A., & Chattopadhyay, G. (2010). *Modelling cost of maintenance contract for rail infrastructure*. Paper presented at the International Conference on Industrial Engineering and Operations Management.
- Rajamäki, J., Vippola, M., Nurmikolu, A., & Viitala, T. (2018). Limitations of eddy current inspection in railway rail evaluation. *Proceedings of the Institution of Mechanical Engineers, Part F: Journal of Rail and Rapid Transit*, 232(1), 121-129.
- Sánchez-Silva, M., & Klutke, G.-A. (2016). *Reliability and life-cycle analysis of deteriorating systems* (Vol. 182): Springer.
- Stapelberg, R. F. (2009). *Handbook of reliability, availability, maintainability and safety in engineering design*: Springer Science & Business Media.
- Strukton. (2018). *Rapport Ultrason Spoorstaven*.
- Sullivan, W. G., Wicks, E. M., Koelling, C. P., Kumar, P., & Kumar, N. (2012). *Engineering Economy*: Pearson/Prentice Hall/Pearson Education International.
- Tobias, P. A., & Trindade, D. (2011). *Applied reliability*: CRC Press.
- UIC. (2002). *UIC code 712R - Rail defects*. France: International Union of Railways (UIC).

- Valkenburg, C. (2015). Technisch onderzoek en LCM-analyse conserveringsmethoden - ProRail gaat spoorstaven conserveren. *Civiele Techniek*, nummer 7 2015.
- van den Boomen, M., Schoenmaker, R., Verlaan, J., & Wolfert, A. (2017). *Common misunderstandings in life cycle costing analyses and how to avoid them*. Paper presented at the Proceedings of the 5th International Symposium on Life-Cycle Civil Engineering.
- van den Boomen, M., Schoenmaker, R., & Wolfert, A. (2018). A life cycle costing approach for discounting in age and interval replacement optimisation models for civil infrastructure assets. *Structure and infrastructure engineering*, 14(1), 1-13.
- Van der Weide, J., & van Noortwijk, J. (2008). Renewal theory with exponential and hyperbolic discounting. *Probability in the Engineering and Informational Sciences*, 22(1), 53-74.
- Van der Weide, J. A., Pandey, M. D., & van Noortwijk, J. M. (2010). Discounted cost model for condition-based maintenance optimization. *Reliability Engineering & System Safety*, 95(3), 236-246.
- van Noortwijk, J. M. (2003). Explicit formulas for the variance of discounted life-cycle cost. *Reliability Engineering & System Safety*, 80(2), 185-195.
- Vandoorne, R., & Gräbe, P. J. (2018). Stochastic modelling for the maintenance of life cycle cost of rails using Monte Carlo simulation. *Proceedings of the Institution of Mechanical Engineers, Part F: Journal of Rail and Rapid Transit*, 232(4), 1240-1251.
- Wang, W. (2012). An overview of the recent advances in delay-time-based maintenance modelling. *Reliability Engineering & System Safety*, 106, 165-178.
- Wilson, J. H., Keating, B. P., Beal-Hodges, M., & Business Expert, P. (2012). *Regression analysis : understanding and building business and economic models using Excel* Quantitative approaches to decision making collection, 2163-9582; Quantitative approaches to decision making collection. 2163-9582; 2012 digital library.; Business Expert Press digital library.,
- Wu, S., & Zuo, M. J. (2010). Linear and nonlinear preventive maintenance models. *IEEE Transactions on Reliability*, 59(1), 242-249.
- Zhao, J., Chan, A., Roberts, C., & Madelin, K. (2007). Reliability evaluation and optimisation of imperfect inspections for a component with multi-defects. *Reliability Engineering & System Safety*, 92(1), 65-73.
- Zhao, J., Chan, A. H. C., Roberts, C., & Stirling, A. B. (2006). Assessing the Economic Life of Rail Using a Stochastic Analysis of Failures. *Proceedings of the Institution of Mechanical Engineers, Part F: Journal of Rail and Rapid Transit*, 220(2), 103-111. doi:10.1243/09544097jrtr30
- Zhao, J., Chan, A. H. C., & Stirling, A. B. (2006). Risk analysis of derailment induced by rail breaks-a probabilistic approach. *RAMS'06. Annual (pp. 486-491)*.
- Zhi, S., Li, J., & Zaremski, A. (2014). Modelling of dynamic contact length in rail grinding process. *Frontiers of Mechanical Engineering*, 9(3), 242-248.
- Zoeteman, A., Dollevoet, R., & Li, Z. (2014). Dutch research results on wheel/rail interface management: 2001–2013 and beyond. *Proceedings of the Institution of Mechanical Engineers, Part F: Journal of Rail and Rapid Transit*, 228(6), 642-651.
- Zoeteman, A., & Esveld, C. (1999). *Evaluating track structures: life cycle cost analysis as a structured approach*. Paper presented at the World Congress on Railway Research, Tokyo.

Appendices

Appendix A Interview transcript

Interview I

Q&A

1) Failure modes & maintenance

Q1. What failure modes are most likely to occur in the Harmelen LCS?

A: The RCF failure mode in the Harmelen LCS does not differ too much from the conventional ballasted tracks. The problem is corrosion. It could be a dominant failure mode in the rails of the embedded rail system. We always see the rail corrosion is associated with the debonding of the elastic compound. Bonding of Corkelast® materials is a serious problem in the embedded rail LCS. It is more likely to suffer from dirt and moisture once the debonding occurs.

Geometric degradation of ballast in the transition zone is another issue. It is not allowed to use tamping machines in the transition zone so that when severe track settlement occurs, we have to exchange the ballast.

Q2. What does maintenance of the Harmelen LCS include (related to dominant failure modes)?

A: The Harmelen LCS does not require much maintenance. Usually we do rail replacement. Preventive rail grinding is carried out by ProRail once a year, but it is not specific to the Harmelen LCS.

The probability of the rail replacement is low in the Harmelen LCS, but once it is needed, it costs a lot compared to the tradition LCS.

Q3. Are they preventive maintenance or corrective maintenance?

A: The replacement can be preventive or corrective. Once a rail break occurs, we perform immediate replacement within 24 hours. The preventive replacement is conducted based on inspections.

Q4. If maintenance tasks are preventive, are they condition-based or time-based?

A: It depends on conditions. We make replacement decisions after we carry out inspections. When the defects are small, we leave it and keep monitoring. If the defects are significant, we decide to do replacement.

Q5. How frequently does preventive maintenance normally take? How long does it take?

A: Preventive maintenance is performed once we identify rail defects.

2) Inspection

Q6. What inspection and measurement techniques are used for defect detection?

A: Visual inspection is performed to check bonding of Corkelast® materials, quality of ERS, and corrosion problem. The rails sticking out of the LCS are more likely to suffer from dirt and we also check it. Ultrasonic inspection is performed for checking internal defects of the rails and additional hand-held equipment is used to verify the weak points that are detected by ultrasonic inspection trains. G-scan II is used for detecting rail corrosion and it is more reliable than the ultrasonic inspection. Geometry measurement inspection is to check the track geometry, but not specific to the Harmelen LCS.

Q7. How often does inspection need to be performed?

A: Once a year for normal track inspection, but it is not specific to the Harmelen LCS. Ultrasonic inspection is performed twice a year. G-scan II is used after 15 years of installation. The frequency is once for five years; if defects are detected, once a year for the following inspections.

Q8. What is the possibility that defects cannot be detected by inspection, e.g., non-destructive cars fail to detect internal cracks of rail?

A: Ultrasonic inspection is not reliable. It is possible that the internal defects are not detected.

Interview II

Q&A

Q1. Except rail replacement, how about the other major cost contributors in LCC of Harmelen level crossings?

A: The expected lifecycle of concrete slabs in the Harmelen level crossings is 40 years. After 30 or 31 years or so, the replacement of slab is decided based on the inspection.

Based on the past experience, the expected lifecycle of embedded rail system (including Corkelast® bonding material and rail) is reconsidered and set as 20 years. After 15 years of installation, inspections will be conducted more frequently to detect possible failures. The lifecycle of ERS is largely dependent on rail. Since new technical solutions (different types of coating) are introduced, it is expected to have the longer life of rail.

Tamping of ballast tracks in the transition zone is also a cost contributor. Tamping frequency depends on situations.

Q2. What are main factors that influence the rail life? Or what are dominant types of rail defects that lead to rail break?

A: Rail corrosion is an important influencer on rail break. Rail degradation is a very complex process and its replacement depends greatly on the specific conditions so that it is hard to predict how many years it has left. Rail break mostly occurs in the gaps between concrete plates but it can also occur in the middle of a plate. In the past years we have faced four or five times of rail breaks in the Harmelen level crossings. It is very unpredictable.

Q3. If rail corrosion is an important failure mode in Harmelen LCS, which indicators can be used to measure the condition of corrosion?

A: G-scan is used to measure the condition of rail corrosion, but it is not successful yet. The indicator is like the amount of lost materials in rail (how much of the rail you have lost on the surface). But the inspection is more like an indication and not accurate enough as it cannot detect the exact location of rail corrosion, like foot, web or head of the rails. The percentage of lost materials that is used to trigger rail replacement is not clear. It is not easy to through Corkelast® materials to see how much of rail has left.

Possibly it is not necessary to use G-scan in the hotspot area, where rail corrosion is intense and severe, manual inspection is followed to check out if rail break occurs.

Q4. Which areas are vulnerable to rail corrosion?

A: Rail corrosion can occur anywhere in the rail, more likely to occur between the gaps of concrete plates. It can occur in the rail head, rail web or rail foot.

If through the detection the rail corrosion is severe, perhaps more things we can do, but we consider the rail replacement is the quickest way to solve the problem. For preventive maintenance, we are trying to use different types of coating.

Q5. Any interaction among rail fatigue, rail corrosion and rail break? Does rail corrosion influence rail break?

A: Both rail fatigue and corrosion can lead to rail break, but I don't observe the interaction between rail fatigue and rail corrosion. In the Harmelen level crossings, the main cause of rail break is corrosion.

Q6. What inspection measures are used to detect rail defects and break?

A: Eddy-current inspection is used to detect the fatigue defects, but it has limited depth of penetration. Ultrasonic inspection can only detect cracks with more than 4mm depth. When a crack is over 4mm, the lifetime of rail ends and some calculation should be done and the replacement decision should be made within one year.

It is very hard to do spot maintenance after detecting rail defects through inspection, as the problem with rail defects is that when you discover the rail defects, most of the time, they have already been deep, over 4mm, and the replacement decision should be made within one year.

Q7. What does rail maintenance include? Is rail maintenance time-based or condition-based?

A: The Harmelen LCS do not require much maintenance during its lifespan. We do not do any maintenance in level crossing itself, except rail replacement. It is a very robust structure. Rail replacement is an important cost contributor.

We do rail grinding as routine maintenance. We tend to shift the preventive maintenance, rail grinding, to rail milling, with low running costs.

Q8. Except for rail defects and break, are there other failure modes in the Harmelen LCS that make substantial distributions in LCC?

A: Settlement of ballast track in the transition zone. When a train moves from the level crossing to transition zone (concrete slabs to ballast), there is a bump causing the vertical settlement of track.

Interview III

Q&A

1) Rail defects

Q1. What types of rail defects are most likely to occur / may lead to rail breakage or cause preventive rail replacement in the Harmelen level crossings?

A: Rail foot corrosion at the end of rails (connected to the ballasted track): dirt flows into LCS with water. 50% of the rail foot corrosion causes rail breaks. Considering the period of PGO contract (5 years), there are no maintenance needs (only regular inspection) at the first contract period. While normally at the third contract period (10-15 years after new installation or rail replacement), the corrosion becomes severe and depending on the situation we decide to replace the rails. The rail breaks caused by rail corrosion are very unpredictable; we do not want to take a risk so that we decide to replace it (no repairs). Rail ends are more susceptible to corrosion. As for the LCS (level crossing zone), rail corrosion only occurs if debonding of Corkelast happens but normally it doesn't occur.

Small cracks in the rail web: it is not a direct safety issue. Ultrasonic inspection can detect the cracks and if the crack is greater than 4 cm (regulation), replace the rail within 24 hours.

Debonding of Corkelast: it is not a direct safety issue but it is related to rail foot corrosion. When some of Corkelast does not stick to the channels and rails, dirt combined with water will flow into the gaps and rail corrosion starts. The debonding of Corkelast is mainly caused by train movement (from the ballast tracks onto the LCS or from LCS to the ballast tracks - geometry condition in the transition zone).

Q2. I consider the rail fatigue is the main cause of rail breaks, do you agree? Is the rail fatigue degradation mainly governed by traffic loading?

A: Refer to the answer Q1, rail foot corrosion and small cracks in the web of rails are dominant rail defects in the Harmelen LCS. The rail degradation is not governed by traffic loading. It is caused by other factors like time, water, winter services (in the main road water comes in faster from the sideway of railways).

Q3. Is there any severity category for the rail defects? Like 'keep it under observation', 'repair it in a certain period', 'repair it without delay'?

A: It depends on the situation. If the corrosion is severe, replace the rail without delay; if Corkelast® gets loose and water flows in, replace the rail within 2-4 years; if there are cracks, depends on the severity, replace the rail in 24h (cracks larger than 4cm; in this case it is corrective rail replacement) or 6 months.

2) Inspection

Q4. How do you inspect rail defects in the Harmelen LCS?

A: Ultrasonic inspection, eddy-current inspection, visual inspection;

Visual inspection: especially the rail ends, inspect the condition of rail corrosion. Sometimes only visual inspection and sometimes check the corrosion with a contrast (measure the difference in profiles between the corroded and standard rails);

Eddy-current inspection: has better accuracy than the ultrasonic inspection but the former can only detect 4 mm in the rail (from the top of the rail);

Ultrasonic inspection: can inspect more about the rail condition; in addition to RCF cracks, it can give an indication about the rail foot corrosion by measuring the difference in height. The result of the ultrasonic inspection is not reliable as the accuracy of this technique is 'bad' but it provides information and supports repair and replacement decisions. There is no repair action for rail corrosion, but for surface RCF defects like head checks (curve issue) and squats (break issue), it is possible to use corrective grinding to remove them;

Depending on the rail condition from inspection reports around the 10th year, we decide whether we can go another 5 years (replace it or not). There is a form of the inspection report for embedded rail level crossings, in which 5 aspects should be clearly recorded, namely track geometry, geometry of LCS, quality LCS, quality Corkelast, condition transition zone (sleepers, etc.).

Q5. In practice which technique is the dominant one used for detecting the rail fatigue defects? How about its accuracy (probability of defect detection)?

A: Ultrasonic inspection both for RCF cracks and corrosion; visual inspection for rail foot corrosion at the end of the rails. The accuracy of ultrasonic inspection is 'bad' – just an indication

Q6. Is the inspection carried out in a fixed interval or depending on the situation?

A: Ultrasonic inspection: twice a year with ultrasonic cars. The inspection results of ultrasonic cars are not reliable and weak points detected by cars need to be verified by inspectors (with hand-held ultrasonic equipment) – spot inspection;

Visual inspection at the rail ends (corrosion) specifically for the Harmelen LCS is performed every four years. Once a year for the general visual inspection in ProRail (the person carries out the visual inspection in a typical region he is responsible for).

3) Maintenance

Q7. What activities are involved in maintaining the rails of Harmelen level crossings?

A: Rail replacement (corrective, preventive), grinding/milling (preventive, corrective)

Q8. Is there any repair action carried out to remove the defects after inspections, like heavy/corrective grinding?

A: Only corrective grinding/milling exists for removing the surface RCF defects like head checks and squats. These surface defects are not related to the embedded rail system. Squats may cause safety issues (rail breaks). Corrective grinding can remove 1-3 mm top materials. It is only performed once or twice in the lifetime of the rails in the Harmelen level crossings, depending on the situation.

Q9. During the lifecycle of the rail in the Harmelen LCS, does it have multiple defects and can they be removed by repairs? Does the rail continue working after the repairs, without replacing it? Or is it too late to carry out repair actions once a rail defect is identified by an inspection? Is every detection of defect automatically lead to rail replacement?

A: Only some defects on the top of rail (surface RCF defects) can be removed by grinding or milling. In case of rail corrosion and internal cracks, it is not possible to perform repair actions. To reduce the risk of rail breaks, replace the rail when these defects occur.

Q10. How do you make decisions on preventive rail replacement for the Harmelen LCS, based on the usage level (amount of traffic loading), the number of rail defects or the severity of a local defect? Or other indicators? If on the severity of the local defect, what is the severity category?

A: Some IMs make decisions on preventive rail replacement for the Harmelen LCS according to the regulation. The expected lifespan of the rails in the Harmelen level crossings is 20 years, so they preventively replace the rail when its age is 20 years.

I make decisions based on the situation. Some indicators are related to the severity of rail corrosion at the rail ends, bonding of Corkelast materials, cracks (how bad the rail is in the LCS) and the age of the rail.

Q11. From the past experience, what is the expected preventive rail replacement interval of the Harmelen level crossings (expressed in time or MGT)? And expected corrective rail replacement interval?

A: If the quality of Corkelast installation is poor, the expected preventive rail replacement is around 15-25 years. It is also influenced by operating conditions, e.g., for the freight line (5-10 trains per day), rails can stay for a longer time, say, 35-40 years.

For corrective replacement interval: normally no rail break occurs; we see the corrosion and we decide to replace the rail before it breaks.

Q12. In most cases, the rail replacement in the Harmelen LCS is single rail replacement or both? How about the percentages of these two cases?

A: Mostly both by planned maintenance; in case of an instant break a single rail. 10% for single rail replacement and 90% for both.

Q13. Is the rail grinding a cyclical preventive maintenance? How often do you perform the rail grinding?

A: Grinding can be cyclical or corrective. For preventive grinding, perform it every 15 MGT for straight lines and 50 MGT in the curves.

Q14. Does rail grinding have the different impact on the occurrence and propagation of different types of fatigue defects?

A: Grinding only has an impact on surface defects.

Q15. What is the expected number of corrective grinding in the lifecycle of rails in the Harmelen level crossings? What are the factors that influence the number of corrective grinding?

A: Approximately once or twice over the lifecycle of the rail in the Harmelen LCS. Normally if the preventive grinding can control the RCF defects, it is not necessary to perform the corrective grinding.

4) Cost

The information is not available due to confidentiality reasons.

Interview IV

Q&A

1) Rail defects

Q1. What types of rail defects are most likely to occur / may lead to rail breakage or cause preventive rail replacement in the Harmelen level crossings?

A: a few different types.

Rail cracks (instant breaks) caused by rotation of the rail is one of the urgent failure mechanisms: in the transition zone, sleepers are loaded differently compared to the concrete slabs. Due to the settlement and dynamic loading we are seeing rail cracks in this region 1-2 meters from the end of the plate.

RCF-related defects, not instant breaks, but like squats, head checks, especially the squats. If there is an indication that a crack is growing, we do replacement before the defect become a real break. The only variable is how urgent it is: replace it within 4 weeks, 3 months or 6 months.

Q2. I consider the rail fatigue is the main cause of rail breaks, do you agree? If not, what are the dominant failure modes of rails in the Harmelen level crossings?

A: most of the fatigue defects (90%) are squats (not sure if it is the case for Harmelen LCS).

Q3. Is the rail degradation mainly governed by traffic loading? What are factors that influence the rail failure in the Harmelen level crossings?

A: yes, the train load in combination with the bonding between the rails and slabs. There are many factors influence the rail degradation but I think MGT is a useful indicator. (Personal opinion) it is very important to have a good change (gradual change of elasticity) from the ballasted tracks to the Harmelen LC (a rigid structure). Have seen a lot of dynamic impact in the transition zone. Road traffic deposit lots of dirt in the rail, like small stones, trains will take them away into small defects in the rail head, developing into squats or other defects.

Q4. There are four categories which classify the severity of rail defects after one inspection: category 1 – replace the rail within 24 hours; category 2 – replace the rail within 4 weeks; category 3 – replace the rail within 6 months and category 4 – continue monitoring. What do you think of the time from an initial point that the rail condition is defined to category 2 in an inspection to the point where a rail break occurs, without performing any preventive action? How about the time of other categories?

A: the time frames are written in the regulations and we cannot change them. I am not sure why it is 24 hours or 4 weeks... one point is in the new contract, category 4 means replacing the rail within 6 months and category 3 is replacing the rail within 3 months. In the most cases, if it is not in urgency we shift the category 2 to 3 to organize the replacement within 6 months in order to have more time to mobilize.

2) Inspection

Q5. How do you inspect rail defects in the Harmelen LCS? What inspection techniques are used in practice?

A: Most of the inspections are performed by ProRail in national programmes.

Ultrasonic inspection: once every three to six months. Ultrasonic cars give a first indication of the possible defects. If a certain spot is suspicious, we (ASSET Rail) will send manual crews and will do validation of the weak points. The crews classify the numbers of defects and severity levels, based on RLN00036 catalogue, and write the ultrasonic report.

Visual inspection: check the condition of the bonding of Corkelast®, signs of growing defects, dirt, water... Not sure about the frequency as it depends on PGO contractors. ASSET Rail carried out the visual inspection at least once a year. It is for the whole railway network not specific to the Harmelen level crossings. The visual inspection specific to Harmelen is less than once a year. Every contractor has its own standard of visual inspection report.

We are not convinced by the result of G-scan. There is no evidence whether it is reliable, also the ultrasonic inspection. It is not completely reliable because of the reflection of the signal. Inspection is still a difficult part (we are always surprised by the defects).

If we do rail replacement in the Harmelen LCS, it will take 12 hours. We have to work with traffic management companies to deal with the road traffic – deviation of routes (give access to the part of the villages), put signs and barriers.

The scheduled possession is for free; however, there is no 12-hour scheduled possession time. We can book the possession within 24 hours, but there is a penalty involved, depending on the contracts (PGO region), e.g., the maximum amount per year, first 10-20/year (scheduled possession times) for free.

Q6. In practice which technique is the dominant one used for detecting the rail defects? How about its accuracy (probability of detecting the defects)?

A: ultrasonic inspection. It is not completely reliable because of the reflection of the signal. Inspection is still a difficult part (we are always surprised by the defects).

Q7. Is the inspection carried out in a fixed interval or depending on the situation?

A: Ultrasonic inspection: once every three to six months.

3) Maintenance

Q8. What activities are involved in maintaining the rails of Harmelen level crossings?

A: cleaning the area between the rail head and concrete slab grooves; cleaning of the first concrete plates; visual inspection.

PGO contractors do not do much inspection & maintenance on the Harmelen LCS, both ultrasonic inspection and grinding are within national programmes. As a PGO contractor, we have to solve the problem caused by ProRail (some of the grinding actions were skipped) – one of the most criticized points in the PGO contract. We've seen many failures caused by the grinding programme - around 2013-2014, a lot of grinding were not performed or performed well and we saw some extra defects caused by this.

Currently both preventive and corrective grinding are within the national programme (while there is hardly any corrective grinding that was performed – we have more than 200 issues of preventive grinding but I see 5 issues of corrective grinding in the past and it is almost zero), while in the new PGO contract (starting this year), corrective grinding is in the scope of contractors (we can choose grinding or milling).

Difference between grinding and milling: preventive grinding 0.5 mm of steel – do a little bit of reprofiling; for corrective grinding, 1-1.5 mm of steel; milling – take away of more steel, like 3 mm in one pass and it is also possible to do multiple passes – really take away of the core of the defects (cracks) – reprofiling. Preventive grinding is not sufficient to remove the cracks. Corrective grinding can take away of small cracks, while if there are deeper cracks, grinding will not help. Milling will be a better solution.

Q9. Is there any repair action carried out to remove the defects after inspections, like heavy/corrective grinding?

A: corrective grinding.

Q10. How do you make decisions on preventive rail replacement for the Harmelen level crossings, based on the usage level (amount of traffic loading), the number of rail defects or the severity of a local defect? Or other indicators?

A: I do not think there is preventive rail replacement because the preventive replacement is conducted based on a schedule. The replacement is performed either after the ultrasonic inspection (identifying the defects) or the instant breaks. I think both the cases are corrective rail replacement. I feel it would be a better choice to have a predefined preventive replacement interval because every time when we do replacement, it is always at the bad moment – organize everything within 24 hours or a few weeks to prepare, but the better one is planning the replacement a few months ahead, based on the preventive replacement regime. From asset managers' point of view, 20 year-interval or whatever years based on train loads could be useful. It can also be read in the new contract – usage-based (amount of MGT, actual train loads).

Q11. From the past experience, what is the expected preventive rail replacement interval of the Harmelen level crossings? And expected corrective rail replacement interval?

A: we have the initial point of reference 10 years ago and we don't have experience on the second rail replacement in the Harmelen LC.

Q12. Is the rail grinding a cyclical preventive maintenance? How often do you perform the rail grinding?

A: see Q8.

Q13. Does rail grinding only have an impact on the occurrence and propagation of surface defects, e.g., squats?

A: we don't have much experience in corrective grinding; from the personal expectation, corrective grinding is not enough to remove the defects. If preventive grinding performs well, most of the defects are under control and there is no need to do the corrective grinding.

4) Cost

The information is not available for confidentiality reasons.

Appendix B Overview inspection & maintenance for Harmelen LCS

The overview of inspection practices and maintenance interventions that are applied for Harmelen LCS is made based on the interviews (Appendix A).

Failure modes	Inspection			Maintenance		
	Techniques	Features	Frequency	Preventive		Corrective
				Activity	Frequency	
Corrosion	Visual inspection	Especially the rail foot at the end of Harmelen LCS (connecting to the ballasted tracks)	Every four years specially for Harmelen (ProRail); Once a year for general inspection (ProRail; Strukton)	Replacement (both rail & ERS)	1) Depending on local conditions (criteria: severity of rail corrosion at the rail ends; bonding of Corkelast; cracks in the level crossings; age of the rail); 2) or when the age of the rail is 20 years (the expected lifecycle of the rails in Harmelen LCS defined by ProRail)	Replacement (both rail & ERS)
	Ultrasonic inspection (trains)	Both for corrosion and RCF defects; just an indication of condition of the rail - not accurate	Twice a year (ProRail; Strukton); Once every three to six months (ASSET Rail)			no repair for corrosion
	G-scan	More accurate than ultrasonic inspection; but the inspection about corrosion still in development (Strukton; Prorail)	Start after 15 years of installation; once for five years; if defects are detected, once a year for the following inspections (Strukton)			
RCF cracks	Ultrasonic inspection (trains)	Both for corrosion and RCF defects; just an indication of condition of the rail - not accurate	Twice a year (ProRail; Strukton); Once every three to six months (ASSET Rail)	Grinding	15 MGT for LCS	Grinding (in average one/two times in the lifecycle of rails) depending on local conditions; if preventive grinding is enough to control RCF, no need to do corrective (ProRail)
	Visual inspection (hand-held equipment)	Verification of weak points	Being performed after ultrasonic inspection trains have detected defects (ProRail; Strukton; ASSET Rail)	Replacement (both rail & ERS)	Depending on ultrasonic inspection report	Replacement (both rail & ERS)
	Eddy-current inspection	Better accuracy than the ultrasonic inspection but it can only detect 4 mm in the rail (from the top of the rail)				

Appendix C Rail break record in Harmelen LCS (2015-2018) (ProRail, 2018a)

This appendix is not attached for confidentiality reasons.

Appendix D Ultrasonic inspection reports

This appendix is not attached for confidentiality reasons.

Appendix E Exponential distribution & probability plotting

Basics of the exponential distribution are presented (Tobias & Trindade, 2011, p. 47). The linear transformed formula of the exponential distribution is formulated and like the Weibull probability plotting, the exponential probability plotting is executed in Microsoft Excel based on the linear rectification formula. The results of exponential probability plotting (LS) is presented in Figure 32.

$$\text{CDF: } F(t) = 1 - e^{-\lambda t}$$

$$\text{Reliability function: } R(t) = e^{-\lambda t}$$

$$\text{PDF: } f(t) = \lambda e^{-\lambda t}$$

$$\text{Hazard function: } h(t) = \frac{f(t)}{R(t)} = \lambda$$

λ is the single parameter that defines one exponential distribution.

Transform the CDF of the exponential distribution to obtain the linear rectification formula (Tobias & Trindade, 2011, p. 162):

$$-\ln[1 - F(t)] = \lambda t$$

Test the exponential distribution via probability plotting: if the exponential distribution fits the dataset, plotting $-\ln[1 - F(t)]$ on the linear y-axis versus time t on the linear x-axis should result in an approximately straight line, where the parameter λ is estimated by the slope of the regression line.